

Hydrological drought characteristics*

Hege Hisdal¹, Lena M. Tallaksen², Tobias Gauster³, John P. Bloomfield⁴, Simon Parry⁵,
Christel Prudhomme^{5,6,7} and Niko Wanders⁸

¹Hydrology Department, Norwegian Water Resources and Energy Directorate (NVE), Oslo, Norway; ²Department of Geosciences, University of Oslo, Oslo, Norway; ³Institute of Statistics, University of Natural Resources and Life Sciences, Vienna (BOKU), Vienna, Austria; ⁴Groundwater Science, British Geological Survey, Wallingford, Oxfordshire, United Kingdom; ⁵UK Centre for Ecology & Hydrology (UKCEH), Wallingford, Oxfordshire, United Kingdom; ⁶Forecast Department, European Centre for Medium-Range Weather Forecasts (ECMWF), Reading, United Kingdom; ⁷Geography Department, Loughborough University, Loughborough, United Kingdom; ⁸Physical Geography, Utrecht University, Utrecht, Netherlands

Chapter outline

5.1 Introduction	158
5.2 Drought terminology	160
5.3 Low flow characteristics	162
5.3.1 Percentiles from the flow duration curve	162
5.3.2 Mean annual minimum flow	167
5.3.3 Base flow indices	170
5.3.3.1 <i>The Base Flow Index</i>	170
5.3.4 Recession indices	174
5.3.4.1 <i>Analytical expression</i>	176
5.3.4.2 <i>Derivation of a characteristic recession</i>	177
5.4 Drought deficit characteristics	179
5.4.1 Threshold level method	179
5.4.1.1 <i>Threshold selection</i>	181
5.4.1.2 <i>Time resolution</i>	185
5.4.2 Indices for intermittent and ephemeral rivers	192
5.4.3 The sequent peak algorithm	195
5.5 Standardised indices	198
5.5.1 Empirical quantiles	198
5.5.2 Standardised (to the normal distribution) indices	198
5.6 Multivariate indices	205

*This chapter builds upon: Hisdal, H., Tallaksen, L.M., Clausen, B., Peters, E., Gustard, A., 2004. Hydrological Drought Characteristics, Chapter 5. In: Tallaksen, L.M., Van Lanen, H.A.J. (Eds.), *Hydrological Drought. Processes and Estimation Methods for Streamflow and Groundwater*. Developments in Water Science, 48, Elsevier Science B.V., 139–198.

5.6.1 Modelled indices	205
5.6.2 Combined indices.....	207
5.7 Spatial drought characteristics	208
5.7.1 Examples of non-contiguous drought area approach.....	210
5.7.2 Examples of contiguous drought area approach	212
5.7.3 Drought tracking.....	214
5.8 Application at large scale.....	214
5.9 Relationship between indices.....	215
5.9.1 Ranks and correlation coefficients.....	216
5.10 Summary.....	222
5.11 Further reading	224
References	224
Web references	231

5.1 Introduction

One of the first steps in a drought analysis is to decide on the hydrological drought characteristics to be studied. Drought affects a wide range of sectors in society, and there is a need for different ways of defining or characterising drought. The problem under study will influence the choice. Drought indices are, for example, applied in analyses of trends and non-stationarity, for monitoring and forecasting, to estimate design values and in analyses of drought impacts ([Chapters 10, 12 and 13](#)). Data availability and the hydrological regime will also influence the choice. Therefore, no single hydrological drought characteristic is suitable to assess and describe droughts for any type of analyses in any region. It is important, however, to be aware of how various ways of characterising a drought may lead to different conclusions regarding the drought hazard and its impacts. For example, even in a wet year, when the mean annual river flow indicates no drought, one may have a dry growing season, and the mean seasonal river flow does indicate a drought. Furthermore, a drought in terms of a river flow deficit may not coincide in time or space with a drought in terms of a groundwater deficit (i.e., a low groundwater level, discharge or recharge). [Tallaksen et al. \(2009\)](#) illustrate how the drought signal is modified at the catchment scale in both time and space as drought propagates from a lack of rainfall to manifest itself as a drought in the hydrological system. Another example is a study of spatial patterns of drought frequency and duration in the United States, where [Soulé \(1992\)](#) showed that the type of drought indices analysed had a major impact on the spatial patterns found. As concluded by the World Meteorological Organization ([WMO and GWP, 2016](#)) and several authors (e.g., [Lloyd-Hughes, 2014](#)), there is no single drought index that is suited for all types of droughts, climate regimes and sectors affected by drought.

When calculating hydrological drought characteristics, often separated into low flow and drought deficit characteristics, it is important to be aware of the seasonality of the time series in the region under study ([Section 2.2](#)). The magnitude and timing of the low flow period is primarily related to climate ([Section 8.2.1](#)), commonly reflecting a pronounced seasonality in precipitation (e.g., a monsoon type of climate) or precipitation falling as snow during the winter season. Various seasonality indices have been developed for the purpose of grouping catchments with similar low flow behaviour

(Sections 8.2.1 and 8.2.2). Thus, it is necessary to separate droughts caused by different processes to characterise hydrological drought in a consistent way. A separation between seasons experiencing summer drought caused by lack of precipitation and/or high evaporation, and winter drought caused by frost, can be carried out by including information, such as air temperature and river flow (Section 3.6). For example, one can let the summer season begin at the end of the spring flood period and end when the mean monthly temperature falls below 0°C (Hisdal et al., 2001). In very cold climates, snow and glaciers may contribute melt water during the summer season, and hence, summer drought in the traditional sense does not exist.

General drought definitions are presented in Section 1.2, whereas in this chapter, we introduce the drought terminology used throughout the textbook (see Glossary) and focus on how to quantify low flow and drought characteristics. The main objective of Chapter 5 is to present a range of quantitative low flow and hydrological drought indices and their pros and cons. Methods to derive single and multivariate drought indices at a single site, as well as over a region are presented, including spatial (or areal) drought indices. Furthermore, the relationship between indices is described. Worked examples are given based on time series from the International Dataset (Section 4.5.1). It is assumed that the time series are stationary and undisturbed by human influence unless explicitly stated. Non-stationarity and human influences are specifically addressed in Section 7.2.5 and Chapter 10, respectively.

Time series commonly have gaps, and infilling methods are often required, such as those described in Section 4.3.7. If infilling is not possible, hydrological drought indices can still be estimated from the available data, however, with caution. The presence of natural long-term variability in hydrological time series requires that hydrological observations for a sufficiently long period are needed for robust calculations. The hydrological regime under study and the type of hydrological drought characteristics to be determined influence the number of years required. Often a 20–30-year period is recommended (Section 2.4.2). If not available, shorter periods can be accepted, but the shorter the period, the higher the uncertainty. In the era of climate change, trends have commonly emerged in more recent decades, and this requires awareness when interpreting the results from both short- (<20–30 years) and long-term (>50 years) records.

Following this introduction, Section 5.2 describes the drought terminology introduced. Section 5.3 introduces common low flow characteristics for river flow and groundwater that characterise specific features of the low flow regime. The derivation of low flow indices based on a single variable is outlined, including indices derived from the flow duration curve, mean annual minimum values and indices based on base flow and recession analyses. Section 5.4 introduces methods to derive drought deficit characteristics based on the threshold level method (perennial as well as intermittent and ephemeral rivers) and the sequent peak algorithm (SPA). Section 5.5 describes standardised indices, for example, the Standardised Streamflow Index (SSI) and Standardised Groundwater Index (SGI). Indices describing drought behaviour can also be based on several variables, for example, indices based on simulated hydrological variables often in combination with meteorological variables (modelled indices) or combined drought indices that merge stand alone indices and, in some cases, also qualitative information. Such modelled or combined multivariate indices are covered in Section 5.6. How to quantify the spatial or areal aspect of drought is addressed in Section 5.7, and considerations to be made in global or continental scale studies discussed in Section 5.8. Many indices refer to similar drought characteristics, and Section 5.9 describes the relationship between indices. Finally, the chapter is summarised in Section 5.10.

This chapter presents several worked examples that in a stepwise manner demonstrate the calculation of indices, including indices based on the flow duration curve, annual minimum series, the base flow separation method, the threshold level method, time series with zero flow (no-flow indices), the sequent peak algorithm and standardised groundwater time series. A worked example to illustrate the relationship between indices is also included.

5.2 Drought terminology

How can a hydrological drought be characterised in a quantitative manner? In a drought situation, river flows are low or even zero. Hence, indices characterising the low flow regime, or a time series of low flow values, such as the annual minimum flow, can be said to characterise the drought behaviour of a river and used to derive streamflow drought indices. Similarly, time series of low groundwater level, recharge and discharge can be said to characterise the drought behaviour of groundwater and used to derive groundwater drought indices. These time series or indices characterise droughts by considering fluxes (e.g., flows) or states (e.g., groundwater or lake levels) at a given time. They do not provide a complete characterisation of the drought. For example, questions, such as what was the start, end, total duration and the severity of the drought are not addressed. To be able to quantify the latter aspects for a river or a groundwater system, it is necessary to define a threshold level below which the flow or groundwater is regarded as being in a drought situation or not.

Hydrological drought characteristics, including low flow and deficit characteristics can be illustrated by considering a time series of daily river flow (Fig. 5.1). From the original time series, low flow indices can be derived. These describe the low flow regime of a river. They can be an index obtained using the whole time series of flow directly in its derivation, a percentile from the flow duration curve (e.g., Q_{90} , Section 5.3.1) being one example (Fig. 5.1, column I). Another low flow characteristic would be the lowest flow in a specific period. Hence, a time series of, for example, the lowest daily river flow value each year can be obtained, that is the Annual Minimum (AM) series. Based on this time series, a low flow index, for example, the ‘mean annual minimum flow (MAM)’ (e.g., $MAM(1\text{-day})$, Section 5.3.2), can be derived (Fig. 5.1, column II).

Drought events can be defined by introducing a threshold below which the flow is regarded as being in a deficit. Each event has a beginning and an end. The drought deficits can be described by a variety of characteristics, such as duration, severity, time of occurrence and spatial extent. Once the threshold has been selected, a time series of deficit characteristics, for example, the drought deficit duration, can be derived. Finally, a drought deficit index, for example, the ‘mean drought deficit duration’, can be estimated (Fig. 5.1, column III).

To summarise, an (single or multivariate) index is seen as a single number characterising an aspect of the drought or low flow behaviour at a site or in a region. A drought event definition implies the use of a method to select drought events from a time series. By introducing a threshold level, it quantitatively defines whether the site can be regarded as being in a deficit situation (drought) or not. Whether or not the drought, as a natural hazard, will have adverse impacts will depend on the vulnerability of the region under study (Box 12.1).

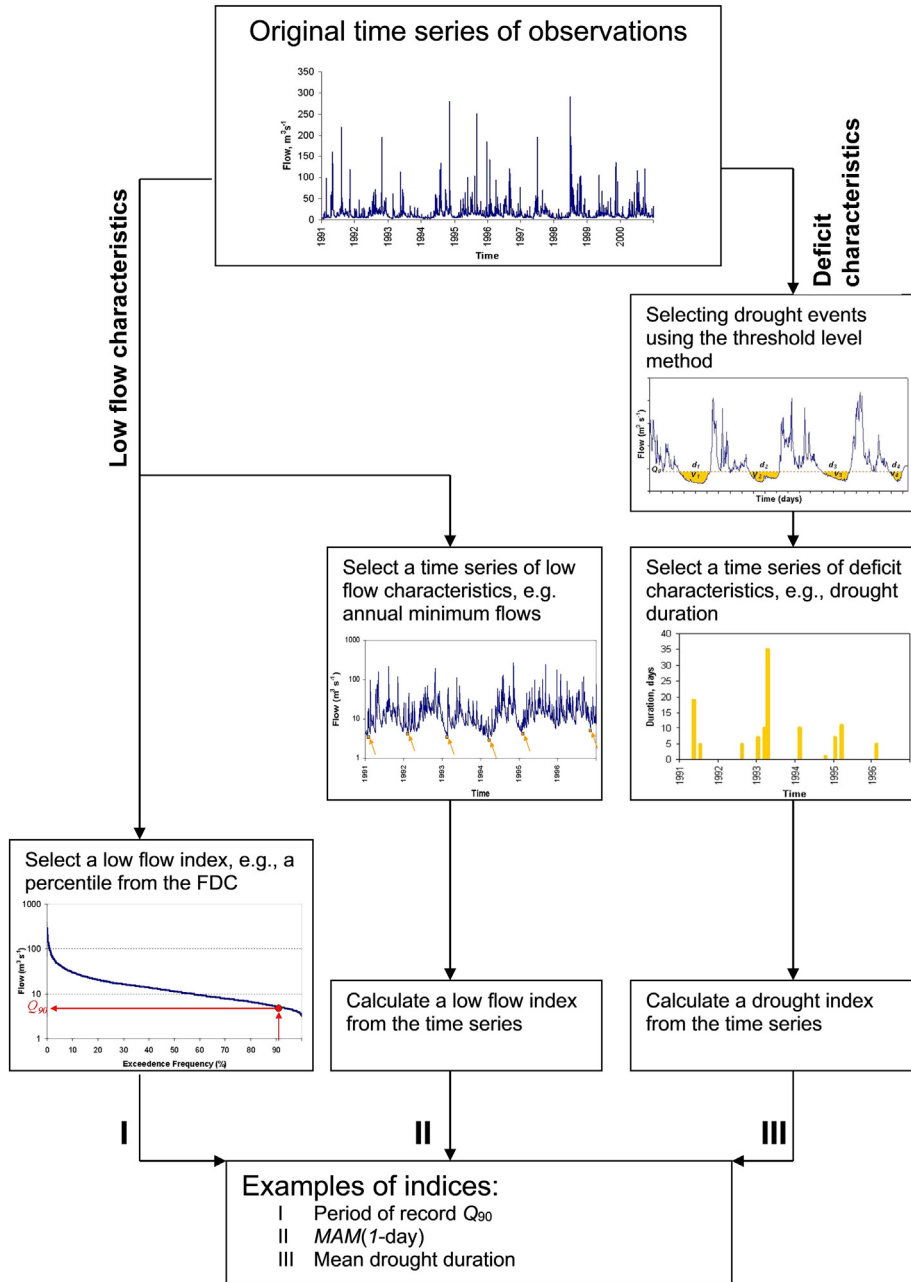


FIGURE 5.1

Work chart showing how low flow and hydrological drought characteristics are derived, exemplified for river flow.

5.3 Low flow characteristics

This section describes different ways of quantifying low flow characteristics in terms of time series and indices derived from series of river flow or groundwater recharge or discharge (water fluxes). Some methods can also be applied to time series of state variables, such as lake or groundwater levels. Estimation methods for ungauged sites are treated in [Chapter 8](#). The term low flow statistic is used equivalent to low flow index in this book. In the literature, the terms low flow measure, metric, parameter, and variable are also used for low flow index.

The calculation procedures are applied to data from different climatic regions as represented by the International Dataset ([Section 4.5.1](#)). Variability in climate combined with differences in physiographic catchment characteristics, result in a wide variety of river flow regimes ([Section 2.2.2](#)). Accordingly, the approach and index recommended for a given river or region of interest may vary. Most approaches have been developed for perennial rivers and applying them to intermittent and ephemeral streams should be done with caution. For example, the mean annual minimum flow will be zero if the river runs dry every year ([Section 5.3.2](#)). Instead, methods targeted specifically for rivers experiencing shorter or longer periods with zero flow can be applied ([Sections 5.4.2 and 5.8](#)).

It should be noted that many indices are derived based on procedures that involve the whole spectrum of flows, from high flow to low flow. This includes:

- (a) the flow duration curve, from which low flow percentiles are selected ([Section 5.3.1](#))
- (b) the base flow separation techniques aimed at identifying different flow components, from which base flow indices are derived ([Section 5.3.3](#))
- (c) recession analysis aimed at characterising the falling limb of the hydrograph, from which recession indices are derived ([Section 5.3.4](#)).

5.3.1 Percentiles from the flow duration curve

The flow duration curve (FDC) plots the empirical cumulative frequency of river flow as a function of the percentage of time that the river flow is exceeded, commonly termed an empirical distribution function ([Section 6.2.2](#)). The same approach is applicable for any other hydrological variable. As such, the curve is constructed by ranking the data in ascending (or descending) order, and for each value, the non-exceedance (or exceedance) frequency of the i th largest (or smallest) value is computed ([Eq. WE5.1.1](#)). The empirical FDC for the River Ngaruroro at Kuripapango in New Zealand (NZ) is shown in [Fig. 5.2](#) (see also [Worked Example 5.1](#)).

FDCs represent the overall river flow variability of a catchment, and both high- and low flow values are included. To improve the readability of the curve in the low flow end, river flow is often plotted on a logarithmic scale. It is also common to let the cumulative frequency (x-axis) be based on the normal probability distribution. The transformation from exceedance frequencies to the standard normal distribution is described in [Section 6.5](#). Low flow percentiles from the FDC are used in various water management applications, such as water supply, hydropower and irrigation planning and design, discharge permits, river and reservoir operational measures and water transfer and withdrawals. The use of percentiles as drought indices is also applicable for groundwater, for example, groundwater level percentiles ([Bachmair et al., 2016](#)).

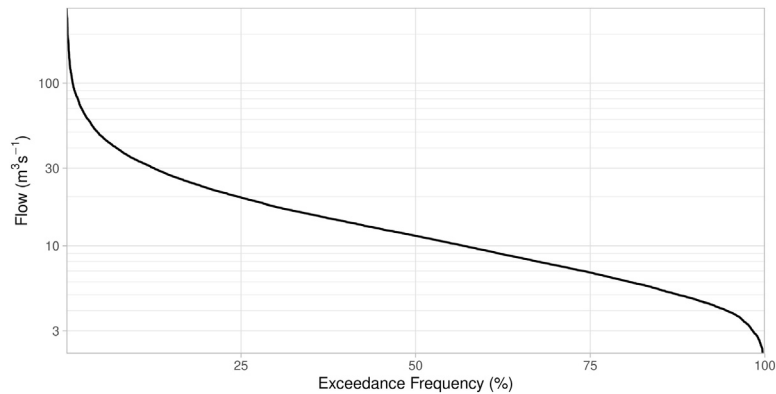


FIGURE 5.2

Flow duration curve based on daily river flow for River Ngaruroro at Kuripapango, NZ. The y-axis is plotted in logarithmic scale.

Box 5.1 Exceedance (non-exceedance)

Low flow indices are often derived directly from the flow duration curve as low flow exceedances (or non-exceedances). A flow exceedance is an index that expresses the proportion of time that a specified daily flow is exceeded during the period of record. The flow exceedance (or non-exceedance) is often given in terms of percentiles. For example, in hydrology the 90th percentile flow, or Q_{90} , is commonly referred to as the flow that is exceeded for 90% of the period of record. However, within statistics, a percentile refers to the non-exceedance, that is, the value below which a given percentage of the sample falls. In this case, the 10th percentile (Q_{10}), that is, the value below which 10% of the values fall, is used as a low flow index, equivalent to Q_{90} above. The statistical terminology is also used within hydrology (e.g., Gudmundsson et al., 2011) and thus, it is important to communicate clearly your choice of terminology to avoid confusion. In this chapter, the hydrology terminology is used, if not stated otherwise.

Traditionally, percentiles are obtained from FDCs based on the total period of record. Alternatively, it is possible to obtain percentiles for a particular period of the year, for example, the summer period only or, if the record is sufficiently long, even for a particular month or day of the year (Figs. 5.8 and 5.9, Section 5.4.1). Vogel and Fennessey (1994) discuss how the FDC depends on the period of record on which it is based. They suggest calculating separate FDCs for each individual year, which allows assigning confidence intervals and recurrence intervals to the FDC.

The FDC can be based on daily, monthly or some other temporal resolution of the river flow series. If daily data are analysed, the FDC shows the relationship between the daily flow values and their corresponding exceedance frequencies. As the river flow between successive time steps generally is correlated (i.e., the values are autocorrelated), notable for daily and monthly resolution, the flow duration curve cannot be viewed as a probability curve, which would require independent data (Section 6.2.2).

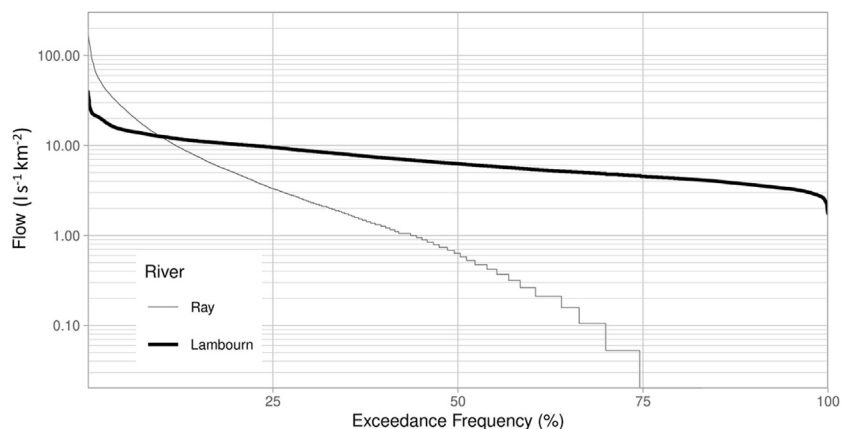


FIGURE 5.3

Flow duration curves based on daily river flow for two contrasting flow regimes; Lambourn: permeable catchment, Ray: impermeable catchment. The y-axis is plotted in logarithmic scale.

Expressing flows as percentiles allows flow conditions in different rivers to be compared provided that the flow duration curves are standardised. This can be achieved by dividing the original river flow value by the mean or median flow (e.g., [Gustard et al., 1992](#)) or the catchment area. In the first case, the river flow will be dimensionless, and in the second case, it will have the unit $\text{l s}^{-1} \text{km}^{-2}$ and is indexed q rather than Q . Flow duration curves for two contrasting British catchments are shown in [Fig. 5.3](#) (see also [Worked Example 5.1](#), Step 6). The original time series of daily river flow are here standardised (divided) by the catchment area.

Lambourn is a permeable, groundwater-fed catchment located in a chalk area. The low variability of flows in this type of regime is reflected in a relative flat flow duration curve. Ray, on the other hand, is a typical impermeable catchment with a flashy flow regime characterised by a high variability in daily flow and thus a steep flow duration curve. This particular catchment also has a high proportion of zero values (intermittent river). Accordingly, many of the low flow percentiles usually applied as low flow indices are zero (e.g., q_{80} , q_{90}). The fraction of zero flows (slightly more than 25%) is shown in the figure. An even larger percentage of zero values can be found in ephemeral streams in semi-arid (e.g., Pecos River, [Section 4.5.1](#)) or in polar regions, leading to q_{50} and even lower percentiles being zero.

Worked Example 5.1 Flow duration curve (FDC)

<https://github.com/HydroDrought/hydrodroughtBook>

1. Loading the data

In this example, we use river flow data from the River Ngaruroro at Kuripapango (NZ), which is part of the International Dataset (Section 4.5.1). The complete record (20 September 1963 to 8 October 2019) of daily data are used to construct a FDC based on a daily time step, $\Delta t = 1$ day. The total number of Δt intervals is $N = 20473$ days. Table 5.1 lists the first seven flow values. The first three columns show the row number, the date and the corresponding river flow value, Q ($\text{m}^3 \text{s}^{-1}$), respectively.

2. Calculating the FDC

The flow duration curve is constructed as follows:

- (a) the rank, i , of each value (column 4 in Table 5.1) is calculated (using the $\text{rank}()$ function), which means that if the list is sorted, the rank will be its position. Here, the series is sorted in descending order, and the i^{th} largest value has rank i (i.e., the largest value has rank 1)
- (b) the exceedance frequency (column 5 in Table 5.1), EF_{Q_i} is calculated as:

$$EF_{Q_i} = \frac{i}{N} \quad (\text{WE5.1.1})$$

which gives an estimate of the empirical exceedance frequency of the i^{th} largest flow value. EF_{Q_i} designates here the observed frequency when the flow, Q , is larger than the flow value with rank i , Q_i .

Table 5.1 First steps in the calculation of the daily flow duration curve for River Ngaruroro at Kuripapango, NZ (derivation of Rank and Exceedance frequency).

No.	Date	River flow, Q ($\text{m}^3 \text{s}^{-1}$)	Rank, i	Exceedance frequency, EF_{Q_i}
1	1963-09-20	30.5	2501	0.124
2	1963-09-21	52.8	827	0.0409
3	1963-09-22	43.6	1228	0.0607
4	1963-09-23	37.3	1686	0.0834
5	1963-09-24	32.3	2240	0.111
6	1963-09-25	29.0	2736	0.135
7	1963-09-26	25.3	3482	0.172

With 20,466 more rows

3. Plotting the FDC

The sorted table columns (river flow and exceedance frequency) are then plotted (Fig. 5.2). The ordinate axis is here logarithmic.

4. Selecting exceedance values

Flow values for a particular exceedance frequency, for example, the 90th percentile (Q_{90}), equal the value of Q corresponding to the largest value of EF_{Q_i} that is less than or equal to the value of EF_{Q_i} sought for. The set of flow values in the range corresponding to the 90th percentile is shown in Table 5.2, and the 90th percentile flow value is taken as $4.94 \text{ m}^3 \text{ s}^{-1}$. Alternatively, in the case of large differences between successive values, a linear interpolation can be used.

No.	Date	River flow, Q ($\text{m}^3 \text{ s}^{-1}$)	Rank, i	Exceedance frequency, EF_{Q_i}
1	2001-03-03	4.94	18,202	0.900
2	1999-01-16	4.94	18,203	0.900
3	2005-11-24	4.94	18,203	0.900
4	2013-01-18	4.94	18,203	0.900
5	1990-12-29	4.93	18,206	0.900
6	1968-02-17	4.93	18,207	0.900
7	1994-03-28	4.93	18,207	0.900
8	1998-03-29	4.93	18,207	0.900
9	2002-03-26	4.93	18,207	0.900

5. Using fast track

The function `lfquantile()` calculates percentiles (or quantiles, Section 6.2.2) directly. The (interpolated) values for Q_{95} , Q_{90} and Q_{70} are 4.10925 , 4.93600 and $8.07550 \text{ m}^3 \text{ s}^{-1}$, respectively, which for Q_{90} is rounded off to $4.94 \text{ m}^3 \text{ s}^{-1}$.

6. Standardising the FDC

Comparing FDCs from different catchments requires standardisation, for example, dividing the discharges by the catchment area, or the median or mean discharge. Here, we provide an example where the river flows for two contrasting British catchments, Lambourne and Ray, are standardised by catchment area. The corresponding FDCs are calculated and plotted in Fig. 5.3.

Table 5.3 displays q_{95} , q_{90} and q_{70} for daily river flow series from stations in the International Dataset (Section 4.5.1). Göta älv in Sweden and Upper Guadiana in Spain are not included as these are heavily human influenced catchments. The River Rhine, the two Norwegian rivers Lågen and Breelvi, River Hurunui in New Zealand, River Pecos in the United States and the two Russian rivers Chusovaya and Unzha, all have a distinct winter low flow period influenced by frost. Therefore, a summer season, caused by lack of precipitation and high evaporation losses, has been defined to calculate indices characterising the summer low flow. For the remaining catchments, percentiles are derived based on observed river flow

Table 5.3 Corresponding flow values for particular percentiles ($1 \text{ s}^{-1} \text{ km}^{-2}$) for selected rivers (see text) from the International Dataset. The summer season refers to the season without influence of frost.

River, country	Summer season	q_{95}	q_{90}	q_{70}
Lindenberg, Denmark	—	7.47	7.99	9.35
Dawib, Namibia	—	0.00	0.00	0.00
Bagamati, Nepal	—	8.88	10.9	17.7
Rhine, the Netherlands	1 Mar–30 Nov	6.19	7.08	9.58
Hurunui, NZ	1 Nov–30 Jun	14.3	17.3	25.1
Ngaruroro, NZ	—	11.1	13.3	21.9
Breelvi, Norway	15 Jun–30 Sep	81.7	110	190
Lågen, Norway	15 Jun–30 Sep	7.97	9.61	15.2
Chusovaya, Russia	1 May–15 Oct	2.45	3.08	4.57
Unzha, Russia	1 May–15 Oct	1.68	1.93	3.24
Elands, South Africa	—	0.05	0.12	0.38
Sabar, Spain	—	0.00	0.00	0.00
Lambourn, UK	—	3.29	3.64	4.87
Ray, UK	—	0.00	0.00	0.11
Arroyo Secco, US	—	0.00	0.00	0.40
Honokohau, US	—	30.6	33.5	43.8
Pecos, US	1 Mar–30 Nov	0.00	0.00	0.01

for the whole year (standardised with catchment area). If the difference between Q_{95} , Q_{90} and Q_{70} is small, this indicates a flat FDC resulting from a river with low variability in river flow. For the Norwegian River Breelvi, snow and glacier melt contribute to the river flow during the whole summer season, and high percentile values can be seen. For the ephemeral rivers, Dawib in Namibia and Sabar in Spain, even q_{70} is zero. For the intermittent rivers, Ray in the UK and Arroyo Secco in the US, q_{90} is zero and q_{70} is very small. The fraction of zero-flow values specifies whether the river is perennial, intermittent or ephemeral. Croker et al. (2003) combine a model for estimating the percentage of time the river is dry with a model for estimating the FDC for the non-zero period to determine a transformed FDC.

5.3.2 Mean annual minimum flow

One of the most frequently applied low flow index is derived from a time series of the annual minimum (AM) of the n -day average flow, $AM(n\text{-day})$. In its simplest form, this would be the mean annual 1-day flow, hence, the average of the annual minimum values. For $n > 1$, the daily flows are replaced by average flows over the previous n -days, or alternatively the previous $n/2$ days and the coming $n/2$ days. For example, if $n = 7$, the entry on 1 January 2003 is the average flow over the period 26 December 2002 to 1 January 2003 inclusive (backward smoothing) or alternatively, the average flow over the period 29 December 2002 to 4 January (mid-day smoothing). The derived data can thus be regarded as the outcome of passing a moving average smoothing filter of n -day duration through the daily time series. Based on the ‘filtered’ or ‘smoothed’ hydrographs mean annual minimum n -day indices, $MAM(n\text{-day})$, can be derived (Worked Example 5.2). It is recommended to select the annual minimum flow from a period of 12 months that avoid splitting the low flow period between hydrological years. Annual minimum series often contain years with zero values. How to deal with zero values in frequency analysis is discussed in Sections 6.3.2.1 and 6.3.3.

Worked Example 5.2 Mean annual minimum n -day flow ($MAM(n\text{-day})$)

<https://github.com/HydroDrought/hydrodroughtBook>

1. Loading the data

In this example, we again use river flow data from the River Ngaruroro at Kuripapango (NZ) of the International Dataset (Section 4.5.1). Here, 10 years of daily data (1990–99) are used to estimate the mean annual minimum of the n -day average flow ($MAM(n\text{-day})$), for n equal to 1, 7 and 30 days. The lowest flows are observed around the turn of the calendar year. Therefore, the annual minima are selected from hydrological (or water) years starting 1 September and ending 31 August. Table 5.4 lists a subset of flow values for January 1990. The first three columns show the row number, the date and the corresponding flow value, Q ($\text{m}^3 \text{s}^{-1}$), respectively.

In order to calculate the mean annual minimum n -day flow, each observation is attributed to a year according to the date of observation using the function `water_year()`, which appends an additional column named ‘Year’ to the dataset.

2. Calculating mean annual minimum values

We start by extracting the annual minimum (AM) values from the three flow series, and then we calculate the mean annual minimum values, $MAM(1\text{-day})$, $MAM(7\text{-day})$ and $MAM(30\text{-day})$ by averaging the annual minimum time series. The $MAM(1\text{-day})$, $MAM(7\text{-day})$ and $MAM(30\text{-day})$ are 4.13, 4.39 and $5.43 \text{ m}^3 \text{ s}^{-1}$, respectively.

Table 5.4 Daily river flow and n -day average flow ($\text{m}^3 \text{s}^{-1}$) for selected averaging windows (1, 7 and 30-days), for River Ngaruroro at Kuripapango, NZ. A moving average with a window length n implies $n-1$ not available (NA) values at the start of the series (corresponding to 0, 6 and 29 days for the three averaging intervals using backward smoothing).

No.	Date	River flow Q ($\text{m}^3 \text{s}^{-1}$)	Year	MA (1-day)	MA (7-day)	MA (30-day)
1	1990–09–01	19.5	1990	19.5	NA	NA
2	1990–09–02	17.9	1990	17.9	NA	NA
3	1990–09–03	16.7	1990	16.7	NA	NA
4	1990–09–04	17.5	1990	17.5	NA	NA
5	1990–09–05	21.2	1990	21.2	NA	NA
6	1990–09–06	30.8	1990	30.8	NA	NA
7	1990–09–07	24.5	1990	24.5	21.1	NA
.						
.						
.						
27	1990–09–27	7.62	1990	7.62	8.23	NA
28	1990–09–28	7.42	1990	7.42	8.03	NA
29	1990–09–29	7.34	1990	7.34	7.86	NA
30	1990–09–30	8.67	1990	8.67	7.91	13.5
31	1990–10–01	17.4	1990	17.4	9.24	13.4

With 3622 more rows

Table 5.5 displays the $MAM(n\text{-day})$ results for averaging periods of 1, 7 and 30 days for stations in the International Dataset (Section 4.5.1) (same stations as in Table 5.3). These indices are often highly correlated with low flow percentiles obtained from the flow duration curve (Section 5.3.1) and have the same areas of application. The relationship between indices is explored in Section 5.9.

It is possible to perform a low flow frequency analysis by fitting a probability distribution to the annual minimum n -day series (Worked Example 6.1). The distribution portrays the annual minimum n -day average flow not lower than a given value with a specific probability. These curves allow the estimation of return periods or so-called T -year events (Box 6.2), an event that *on average* will occur every T year. Such T -year events can in turn be applied as low flow indices. For example, in the United States, a widely used low flow index is the 10-year 7-day minimum flow, $AM(7\text{-day})_{10}$ (Riggs et al., 1980) and Feyen and Dankers (2009) used the 7-day minimum flow for several return levels to study the impact of global warming on streamflow drought in Europe.

A similar approach as for low river flows can be applied for time series of groundwater levels, which commonly have a lower measurement frequency than river flow, because of the lower temporal variability. The n lowest groundwater levels can be identified in a hydrological year, and subsequently averaged over several years to obtain the mean lowest groundwater level (Van der Sluijs and De Gruijter, 1985). Caution is required to ensure that the sample data of low groundwater levels are independent.

Table 5.5 Mean annual minimum values ($1 \text{ s}^{-1} \text{ km}^{-2}$) for selected rivers (see text) from the International Dataset.

River, country	Summer season	$MAM(1\text{-day})$	$MAM(7\text{-day})$	$MAM(30\text{-day})$
Lindenberg, Denmark	—	7.58	7.79	8.20
Dawib, Namibia	—	0.00	0.00	0.00
Bagamati, Nepal	—	10.7	11.1	12.6
Rhine, the Netherlands	1 Mar–30 Nov	6.78	6.93	7.73
Hurunui, NZ	1 Nov–30 Jun	15.1	16.0	20.0
Ngaruroro, NZ	—	10.5	11.0	13.6
Breelvi, Norway	15 Jun–30 Sep	69.2	87.6	97.3
Lågen, Norway	15 Jun–30 Sep	9.40	10.2	13.5
Chusovaya, Russia	1 May–15 Oct	2.87	3.32	3.88
Unzha	1 May–15 Oct	2.72	2.80	3.22
Elands, South Africa	—	0.11	0.14	0.15
Sabar, Spain	—	0.00	0.00	0.00
Lambourn, UK	—	3.98	4.13	4.18
Ray, UK	—	0.01	0.01	0.05
Arroyo Secco, US	—	0.13	0.14	0.17
Honokohau, US	—	32.1	33.9	43.5
Pecos, US	1 Mar–30 Nov	0.00	0.00	0.01

5.3.3 Base flow indices

Base flow is a term used to describe the flow that is sustained during extended dry periods, that is, between precipitation events in perennial rivers. Accordingly, it is closely related to the low flow behaviour of the river. Many hydrograph separation techniques have been developed for identification of the different flow components of the total river flow, including the base flow. The components are thought to represent different flow paths in the catchment, each characterised by different residence or response times, the outflow rate of groundwater being the slowest. In their review, [Nathan and McMahon \(1990\)](#) distinguish between methods aimed at deriving the response for a given event and automated methods for a continuous separation of the flow hydrograph. Methods for continuous separation generally divide the flow into two components, one quick and one delayed, using an automated time-based separation. The relative slowly varying component of river flow as quantified by the delayed component is commonly referred to as the base flow (Q_{base}). It can be seen as representing the catchment's ability to store and release water during dry weather. A high index of base flow would imply that the catchment has a rather stable flow regime and is able to sustain flow during extensive dry periods.

Base flow indices are generally highly correlated with hydrological properties of soils and geology and other storage-related catchment descriptors, such as the percentage of lake or wetlands ([Table 4.2](#)). Accordingly, such flow-derived base flow indices ([Supporting Document 3.2, <https://github.com/HydroDrought/hydrodroughtBook>](#)) have performed satisfactorily as catchment descriptors in many low flow and drought studies because even a rough estimate of storage properties greatly increases the performance of the estimation model ([Section 8.4](#)). Although valuable as measures of the storage property of a catchment, response factors derived based on hydrograph separation techniques are of limited use as characteristics of the flow processes operating as emphasised by [Hewlett and Hibbert \(1967\)](#).

A well-known flow-derived index, the Base Flow Index (BFI), is based on a continuous separation of the hydrograph. The BFI is frequently included in low flow and drought studies, and although useful as a predictor (of e.g., low flow), it should not be considered a low flow or drought index as such. The BFI is presented below, and details of the calculation procedure are given in [Worked Example 5.3](#). Alternative approaches to identify the base flow component by a continuous separation, include physically based methods ([Chapman, 1999](#); [Furey and Gupta, 2001](#)) and the use of observed groundwater heads ([Peters and Van Lanen, 2005](#)).

5.3.3.1 The Base Flow Index

The Base Flow Index (BFI) was originally developed during a low flow study in the UK ([Institute of Hydrology, 1980](#)) for characterising the hydrological response of soils and geology. Later applications commonly refer to it as the UKIH method for the calculation of base flow. The index gives the ratio of the volume of base flow to the volume of total river flow calculated from a hydrograph smoothing and separation procedure using daily discharges. The separation cannot start on the first day of the record and similarly cannot finish on the last day. Accordingly, it is recommended to compute the base flow separation and the BFI for the entire period of record rather than breaking it into a series of shorter periods (e.g., years) to avoid the loss of some days at the start and end of each year. Nevertheless, an

assessment of the annual variability in the index can be of value, in which case, annual BFIs are derived by summing up the base flow and total flow volume separately for each year. Note also that BFI is sensitive to missing data — one missing day may result in several days of data being omitted from the base flow separation — and thus, it is recommended that missing periods are filled in prior to its derivation (Section 4.3.7.4).

Values of the index range from 0.15–0.2 for an impermeable catchment with a flashy flow regime to more than 0.95 for catchments with high storage capacity and a stable flow regime. Fig. 5.4 compares the daily hydrograph and base flow separation line for the year 1996 for two UK rivers of contrasting geology; the Lambourn at Shaw located in a chalk area (BFI = 0.96) and the Ray at Grendon Underwood, located in an area dominated by glacial clay and mudstone (BFI = 0.20).

The BFI has found many areas of application, including low flow estimation, groundwater recharge assessment and classification of catchment response time. As the BFI is closely related to other low flow indices, relationships between the index and catchment descriptors have been derived for different hydrogeological regimes and used to estimate BFI and hence flow indices, at the ungauged site. In a revision of the UK low flow study (Gustard et al., 1992), the necessity to estimate BFI at an ungauged site was replaced by information on soil types, and different low flow soil groups were identified based on the HOST soil classification system (Section 8.3.2). The BFI is not only a result of catchment characteristics, such as soil and geology, but also climate variability plays a role, as the procedure is sensitive to the frequency and duration of rainfall events (Tallaksen, 1987; Longobardi and Van Loon, 2018).

The BFI procedure was originally developed for rainfall regimes with a typical river flow response in hours or days. This guided the choice of model parameters in the base flow separation procedure (i.e., block length, N (in days), and turning point factor, TP). The two parameters govern the identification of turning points in the time series of daily flow, points that are later connected to obtain the separation line (base flow hydrograph). The parameter values were determined by calibration and visual inspection of the estimated base flow hydrograph from over 100 catchments in the UK. In the original procedure (Institute of Hydrology, 1980), a 5-day (non-overlapping) minimum was identified as a turning point if it reads 0.9 ‘less than’ the neighbouring minimum. However, the latter test did not behave properly when river discharge was zero (Tallaksen, 1987). Hence, it was later recommended to apply the test ‘less than or equal to’ instead, along with the constrain that the estimated base flow is set equal to the observed river flow on any day when the base flow exceeds the observed flow. This ensures that the BFI does not exceed one and is thus limited to the range $[0, 1]$.

In regions with long high flow periods (e.g., snow-dominated catchments) or slowly responding catchments with large storage capacity (Section 3.4.2), a turning point may be identified in the high-flow period, and the separation procedure fails to provide reliable results. In this case, as well as for catchments in other hydrological regimes, alternative parameter values can be sought or the BFI can be calculated for each season separately. Seasonal calculations imply shorter period of observations, and the calculation must be performed for each year separately. Accordingly, longer records are necessary to obtain stable values. Alternative parameters were first suggested by Tallaksen (1987) and later tested for shorter block length ($N = 1–4$ days) in Piggot et al. (2005) and for a wide range of block length ($N = 1–180$ days) in Stoelzle et al. (2020). Interpretation of the BFI should always be made with care, and a visual inspection of the base flow hydrograph plotted along with the total river flow is recommended to ensure that appropriate and robust parameter values are chosen.

Worked Example 5.3 Base Flow Index (BFI)

<https://github.com/HydroDrought/hydrodroughtBook>

1. Loading the data

Three years of daily flow (1995–97) from the River Ray at Grendon Underwood (UK) from the International Dataset (Section 4.5.1) are used. The base flow separation is done for the whole 3-year period, whereas the BFI is calculated for the mid-year 1996. This ensures that days at the start and end of the calculation year are included. In Table 5.6, the calculation steps are illustrated using data from the start of the period, that is, 1995.

Table 5.6 Steps in the calculation of the base flow separation line from time series of daily flow; non-overlapping 5-day blocks are indicated by dotted lines and turning points in the sequence of $0.9 Q_{\min}$ values are marked bold. Daily base flow is obtained by linear interpolating between turning points.

Date	Daily flow, Q ($\text{m}^3 \text{s}^{-1}$)	Q_{\min} ($\text{m}^3 \text{s}^{-1}$)	$0.9 Q_{\min}$ ($\text{m}^3 \text{s}^{-1}$)	Base flow, Q_b ($\text{m}^3 \text{s}^{-1}$)
1-Jan-1995	0.109			
2-Jan-1995	0.063			
3-Jan-1995	0.043			
4-Jan-1995	0.039	0.039	0.0387	
5-Jan-1995	0.229			
6-Jan-1995	0.186			
7-Jan-1995	0.116			
8-Jan-1995	0.111			
9-Jan-1995	0.095	0.095	0.0855	
10-Jan-1995	0.123			
11-Jan-1995	0.178			
12-Jan-1995	0.091			
13-Jan-1995	0.076			
14-Jan-1995	0.073			
15-Jan-1995	0.062	0.062	0.0558	
16-Jan-1995	0.054	0.054	0.0486	0.054
17-Jan-1995	1.06			0.056
18-Jan-1995	0.856			0.058
19-Jan-1995	1.05			0.060
20-Jan-1995	1.34			0.062
21-Jan-1995	1.64			0.064
22-Jan-1995	1.35			0.067
23-Jan-1995	0.559			0.069
24-Jan-1995	0.255	0.255	0.2295	0.071
25-Jan-1995	0.644			0.073
26-Jan-1995	0.793			0.075
27-Jan-1995	0.896			0.077

Table 5.6 Steps in the calculation of the base flow separation line from time series of daily flow; non-overlapping 5-day blocks are indicated by dotted lines and turning points in the sequence of $0.9 Q_{\min}$ values are marked bold. Daily base flow is obtained by linear interpolating between turning points. — cont'd

Date	Daily flow, Q ($\text{m}^3 \text{s}^{-1}$)	Q_{\min} ($\text{m}^3 \text{s}^{-1}$)	$0.9 Q_{\min}$ ($\text{m}^3 \text{s}^{-1}$)	Base flow, Q_b ($\text{m}^3 \text{s}^{-1}$)
28-Jan-1995	0.631			0.079
29-Jan-1995	1			0.081
30-Jan-1995	0.492	0.492	0.4428	0.083
31-Jan-1995	0.377			0.085
1-Feb-1995	1.67			0.087
2-Feb-1995	0.448			0.090
3-Feb-1995	0.237			0.092
4-Feb-1995	0.163	0.163	0.1467	0.094
5-Feb-1995	0.123			0.096
6-Feb-1995	0.102			0.098
7-Feb-1995	0.1	0.1	0.09	0.100
8-Feb-1995	0.151			0.107
9-Feb-1995	0.178			0.115

2. Calculating the BFI

- Divide the daily flows, Q ($\text{m}^3 \text{s}^{-1}$) into non-overlapping blocks of 5 days (Columns 1 and 2, Table 5.6)
- mark the minima of each of these blocks and let them be called $Q_{\min_1}, \dots, Q_{\min_n}$ (Column 3, Table 5.6). Consider in turn $(Q_{\min_1}, Q_{\min_2}, Q_{\min_3}), \dots, (Q_{\min_{n-1}}, Q_{\min_n}, Q_{\min_{n+1}})$. In each case, if $0.9 \cdot \text{central value} \leq \text{outer values}$, then the central value is identified as a turning point (bold numbers in Table 5.6). Continue this procedure until the whole time series has been analysed
- join the turning points by straight lines to form the base flow separation line and assign to each day a base flow value Q_b , by linear interpolation between the turning points. If, on any day, the base flow estimated by this line exceeds the total flow, the base flow is set equal to the total flow Q , on that day
- calculate the volume of water (V_{base}) beneath the base flow hydrograph between the first and last date of interest. The volume (m^3) is simply derived as the sum of the daily base flow values multiplied by 86,400 (the number of seconds per day)
- calculate the corresponding volume of water beneath the recorded hydrograph (V_{total}). The volume (m^3) is obtained by summing the daily flow values between the first and the last dates inclusive
- the BFI is then $V_{\text{base}}/V_{\text{total}}$.

3. Results

- (a) The first and second turning points (marked bold) are found on 16 January 1995 and 7 February 1995 (Column 4, Table 5.6), respectively, and a linear interpolation is used to estimate the base flow at time steps (days) between these dates (Column 5, Table 5.6). The daily base flow separation line is subsequently calculated for the whole period by linear interpolation between all turning points
- (b) the volume beneath the base flow line, V_{base} , for 1996 is found to be 348,494.5 m³, whereas the volume of the total flow, V_{total} , is 1,721,693 m³. The resultant BFI is 0.20. The base flow separation line for the two rivers is shown in Fig. 5.4.

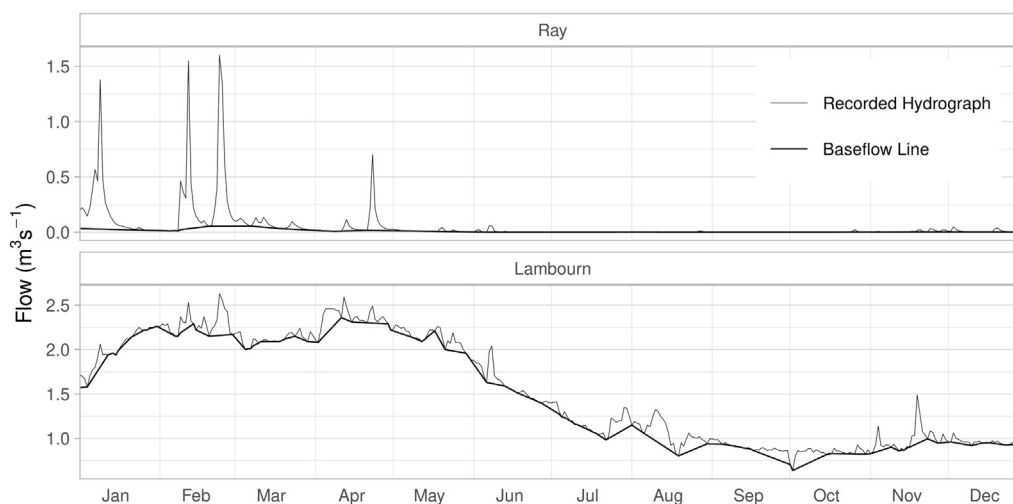


FIGURE 5.4

Daily recorded hydrograph and calculated continuous base flow line for two UK rivers (Ray and Lambourn) for the year 1996, based on the BFI separation procedure (Worked Example 5.3).

5.3.4 Recession indices

The gradual depletion of water stored in a catchment during periods with little or no precipitation is reflected in the shape of the recession curve, that is, the falling limb of the hydrograph (Fig. 5.5a). A recession period starts following a peak flow and lasts as long as the flow declines, whereas a recession segment is a selected part of the recession curve (Fig. 5.5b). The recession curve describes in an integrated way how various catchment storages and subsurface processes control the river outflow (Section 3.4.2). Catchments with a slow recession rate are typically groundwater or lake dominated catchments, whereas a fast recession rate is characteristic of flashy, impermeable catchments with limited storage. The most important catchment characteristics found to affect the recession rate are hydrogeology, topography and climate (Tallaksen, 1995). Catchments with a fast recession rate typically show lower minimum flow as compared to catchments with a slow recession rate, and a trend towards faster recessions has been shown to coincide with decreasing annual minimum flows (Sawaske and Freyberg, 2014). An assessment (quantification) of the shape of the recession curve has proved

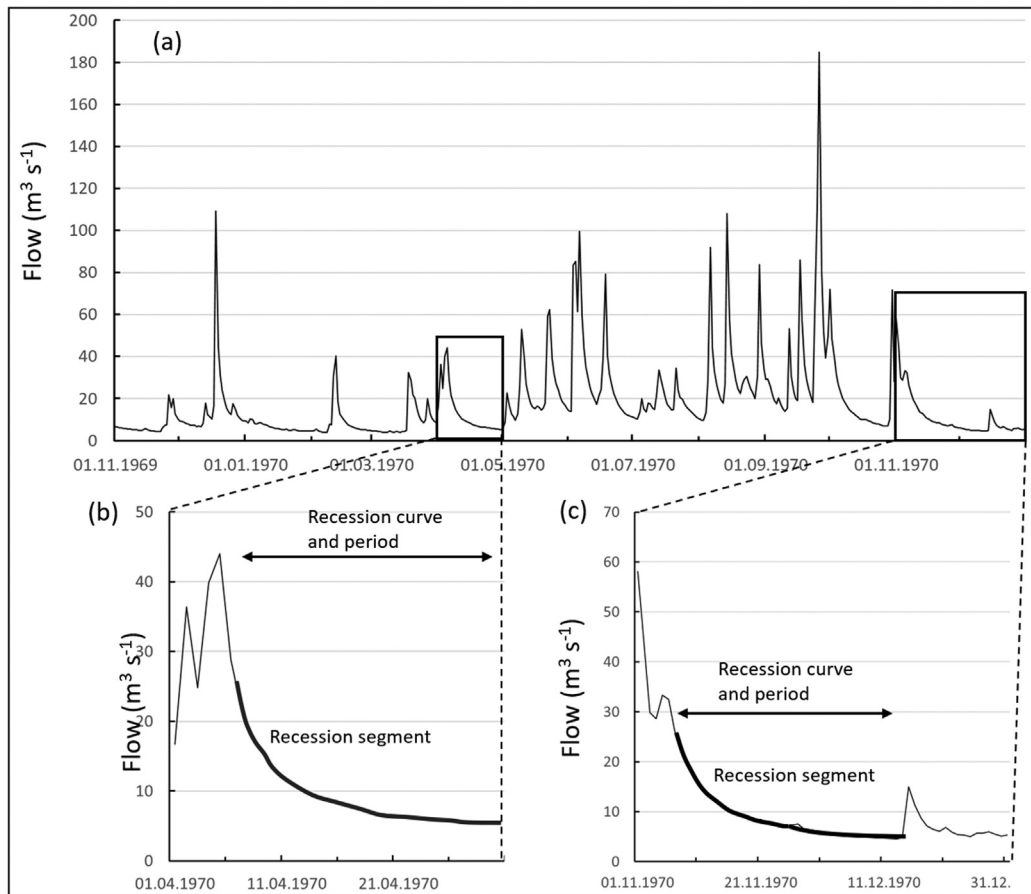


FIGURE 5.5

Identification of a characteristic recession curve, period and segment (*bold line*): (a) daily discharge data from River Ngaruroro at Kuripapango, NZ (Section 4.5.1), (b) smooth recession, and (c) interrupted recession.

useful in many hydrological applications; in hydrograph analysis for separation of different flow components (Section 5.3.3), in frequency analysis for estimating low flow indices (Section 6.6.1), as an index of catchment storage in regional regression models (Section 8.4), as a measure of discharge rate in rainfall-runoff models (Staudinger et al., 2011), and in low flow forecasting of gauged rivers (Section 13.4).

In a humid climate, rainfall frequently interrupts the recession period by creating short ‘bumps’ or increases in the flow and a series of recession segments of varying duration results (Fig. 5.5c). The segments represent different stages in the outflow process, and the recession rate changes from steeper to slower rates as the initial flow decreases. Transmission loss, including evaporation losses from the river and evapotranspiration from riparian areas, as well as seepage from the river to groundwater during dry weather (McMahon and Nathan, 2021), further adds to the variability in the recession rate.

Overall, steeper recession curves are found during the growing season along with a reduction in base flow and drying up of the catchment (Tallaksen, 1989). In drier regions and in flashy catchments experiencing zero flow, the recessions often lack the slowly declining flow typically of groundwater flow. This may also be the case in regions with frequent rainfall events that interrupt the declining flow. Thus, it is important to keep in mind that climate – not only physiographic characteristics – influences the recession rate.

Quantification of the recession curve or segment involves the selection of an analytical expression, derivation of a characteristic recession and optimisation of the recession parameters. Optimisation of recession parameters is commonly done using a simple or weighted least-squares regression (Section 8.4.2) and not dealt with further here. There are many choices to be made as part of these calculation steps, and this section introduces some common approaches. A comprehensive review of recession analysis (and transmission loss) is provided by McMahon and Nathan (2021) building on previous reviews by Hall (1968) and Tallaksen (1995).

5.3.4.1 Analytical expression

The starting point of a recession analysis is to select an analytical expression to fit to the outflow function Q_t , where Q is the rate of flow and t the time. Often an upper threshold is imposed, for example, the mean flow, below which a recession segment would start. The time interval Δt , is normally in the order of days. The theoretical decay of the aquifer outflow rate (groundwater discharge) can be modelled as a function of aquifer characteristics (Sections 3.4.2.2 and 9.3.1). Such a process-based modelling approach has proved successful at the catchment scale for relatively homogeneous conditions (Brutsaert and Nieber, 1977). However, applications in a heterogeneous catchment and at a regional scale are limited.

If Q_t is modelled as the outflow from a first order linear storage with no inflow, the recession rate will follow the simple exponential equation, written here in the three alternative forms:

$$Q_t = Q_0 \cdot e^{\left(-\frac{t}{C}\right)} \quad (5.1a)$$

$$Q_t = Q_0 \cdot e^{(-\alpha t)} \quad (5.1b)$$

$$Q_t = Q_0 \cdot k^t \quad (5.1c)$$

where Q_t is the flow at time t , and Q_0 the flow at the start of the recession period ($t = 0$). C , α and k are recession constants characterising the slope of the recession curve, that is, how fast low flow is reached (the recession rate). Hence, they can be regarded as low flow indices.

The equation plots as a straight line of slope $-1/C$ (or alternatively $-\alpha$ or $\ln k$) on a semi-logarithmic plot of t against $\ln Q_t$ (Eq. 5.1a) and is commonly thought of as the base flow or groundwater flow. The lack of fit of Eq. 5.1 for individual recession segments has led to the separation of the curve into distinct flow components representing different transit times in the catchment (e.g., overland flow, unsaturated and saturated flow). Each component has been modelled as the outflow from a linear reservoir representing an exponential decay and combined into a series of linear reservoirs to yield the resultant catchment recession (e.g., Klaassen and Pilgrim, 1975). Alternatively,

nonlinear relationships have been sought (e.g., Brutsaert and Nieber, 1977; Santos et al., 2019; McMahan and Nathan, 2021). In either case, more than one recession parameter is needed to describe the recession rate. Other modelling approaches include modelling the recession as an autoregressive process, from a simple first-order autoregressive process to more complex autoregressive moving average models. Additionally, empirical expressions have been sought (Tallaksen, 1995).

5.3.4.2 Derivation of a characteristic recession

The high time variability experienced in the recession rate has made it difficult to select recession segments from a continuous flow record in a consistent way. As a result, various procedures have developed to identify and parameterise a catchment characteristic recession behaviour. These can be classified into two main approaches; those based on constructing a master recession curve (MRC) and those performing a separate calculation for individual recession segments (IRS). In either case, the first step is to define a set of criteria for selecting recession segments from a continuous record. A fixed or constant starting value restricts the recession to flows below a predefined discharge, whereas a variable starting value can be defined as the flow at a given time after rainfall or peak discharge to exclude the influence of overland flow. Similar, the length of the recession period can be a constant or a varying number of time steps. Normally, a minimum length is imposed (commonly in the order of 5–7 days).

The MRC approach tries to overcome the problem of time variability in individual segments by constructing a mean or master recession curve (e.g., Duncan, 2019). In the correlation method, discharge at one time interval (Q_t) is plotted against discharge one time interval later (Q_{t+1}) during the recession period. By plotting all pairs of discharge from a series of recession segments in one diagram, a master recession curve can be fitted to the data points (WMO, 2008). If the recession rate follows an exponential decay, a straight line results, and the recession parameter can be estimated from the slope k provided that the line is forced to intercept at (0,0) (Eq. 5.1c for a time step equal to one):

$$k = \frac{Q_{t+1}}{Q_t} \quad (5.2)$$

The recession constant C in Eq. 5.1a can then be expressed as:

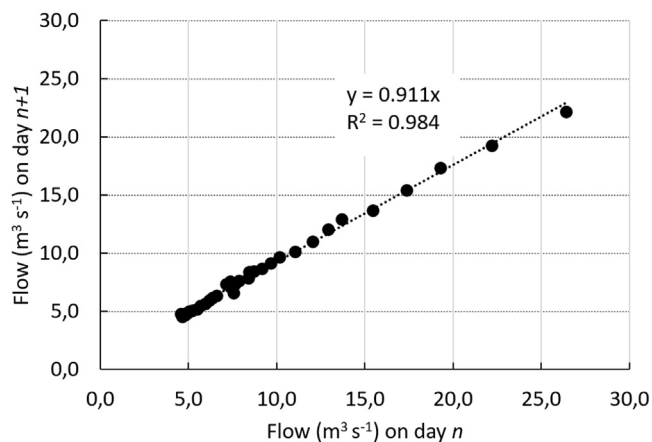
$$C = \frac{-1}{\ln(k)} \quad (5.3)$$

In Fig. 5.6, the method is demonstrated using data from the same recession period as depicted in Fig. 5.5c (i.e., 1 November to 14 December 1970). Starting at the peak (1 Nov.) gives a slope k of 0.86 ($R^2 = 0.94$). By starting 4 days later at the peak of the minor bump (5 Nov.) or 2 days after the bump (7 Nov.), only leads to a slightly slower recession rate of 0.906 ($R^2 = 0.94$), respectively, 0.911 ($R^2 = 0.98$). The latter is equivalent to a C of 10.6. The value of k in this example approaches one (as the flow decreases), indicating an exponential decay.

Other applications of the correlation method rather plot the rate of change of flow, $\Delta Q/\Delta t$, against Q . The graphical analysis of the relationship is often performed by means of the upper and lower envelope of points, representing the maxima and minima observed recession rates, respectively (Brutsaert and Nieber, 1977; Jachens et al., 2020). The correlation plot requires high accuracy in the low flow measurements, and the quality of the low flow data (Section 4.3.7) is often a limiting factor for the analysis. An overview of methods used to estimate a master recession curve is provided by Brodie and Hostetler (2005).

FIGURE 5.6

Recession rate determined by the correlation method. Flow data (daily) from River Ngaruroro at Kuripapango, NZ.



In the IRS method, the variability in individual recession segments is explicitly accounted for by fitting a recession model to each segment. Sample statistics of the model parameters, for example, mean and variance of the recession constant, can subsequently be used to characterise the overall recession behaviour of the catchment. If a separate model is fitted to each recession segment by the least squares method, the average slope equals the arithmetic mean of the individual slopes provided the segments are of equal length; otherwise, a weighted average must be calculated to obtain an unbiased estimate of the average slope (Tallaksen, 1995).

The high-time variability found in recession segments argues against the use of a master recession curve except, as an overall approximation that may be applicable for comparative studies at the regional scale (Tallaksen, 1995; Jachens et al., 2020). Overall, variability owing to model limitations and the calculation procedure should be minimised, whereas physically based short-term or seasonal variation should be accounted for.

The choice of recession model and calculation procedure depends on the nature of the region under study and the purpose of the study (e.g., which part of the recession curve is most important). In a regional study where recession indices are thought to represent storage properties, it is the time required to reach low flow that is most important. Accordingly, a simple, one parameter, expression is preferable as the recession behaviour generally varies considerably between sites. Only one parameter also facilitates mapping regional differences, and both the IRS and MRC method are suited. On the other hand, low flow forecasting strives towards high precision in the lower end of the recession curve (Section 13.4), and it is important to fit a model capable of representing the lower end of the recession curve satisfactory. Accordingly, more complex models may be sought, also providing an estimate of the uncertainty in the forecasted low flow by accounting for the variability in the recession rate in the extreme lower range. Web-based tools, such as the Matlab toolbox HYDRORECESSION (Arciniega-Esparza et al., 2017) or MRCPtool (Carlotto and Chaffe, 2019), allow the user to choose among automated approaches for streamflow recession analysis.

5.4 Drought deficit characteristics

As opposed to low flow characteristics presented in the previous sections, drought deficit characteristics are based on introducing a threshold below which the flow is regarded as being in a drought situation. Each deficit or drought event can be characterised among others by its duration and deficit volume. This section describes two methods, the threshold level method and the sequent peak algorithm (SPA), which are used to select and characterise drought events.

5.4.1 Threshold level method

In the following, a detailed description of the threshold level method for defining drought events is given. The method is based on defining a threshold, Q_0 , below which the river flow – in this case – is considered to be in a drought (also referred to as a low flow spell). The threshold level can be constant or vary over the year, following the seasonal flow pattern.

The threshold level method is often applied to time series of river flow or groundwater discharge, but can also be applied to time series of water levels – it being lake levels or groundwater levels (or heads), as demonstrated by Peters et al. (2006). Tallaksen et al. (2009) applied the method to rainfall, groundwater (recharge, level and discharge) and river flow in a study of drought propagation at the catchment scale. If applied to a state variable, such as groundwater level, it is important to be aware that these represent a measure of storage and not a flux. Accordingly, they need to be treated differently in the derivation of drought deficit characteristics.

The threshold level method, which generally studies runs below or above a given threshold, was originally named ‘method of crossing theory’ (Box 7.1), also referred to as run-sum analysis, and commonly applied to annual or monthly time series. Early application of crossing theory in hydrology includes Yevjevich (1967), who applied the statistical theory of runs for analysing continental scale drought. Based on a sequential time series of run-sum above or below a threshold, also referred to as a Partial Duration Series (PDS, Section 6.3.2.2) of surpluses or deficits, several drought indices were proposed. The theory of runs is among other relevant for storage and yield analysis, which is associated with hydrological design and operation of reservoir storage systems (Section 5.4.3). Important areas of application are hydropower and water management, water supply systems and irrigation schemes.

Fig. 5.7 illustrates how drought events in a time series of daily river flow are identified using the threshold level method and a constant threshold, Q_0 . When the flow falls below or equals the threshold value, a drought event starts to develop, and when the flow rises above the threshold again, the drought event ends. Hence, both the beginning and the end of the drought can be identified. Statistical properties of the distribution of drought deficit, drought deficit duration (run-length, d_i , Fig. 5.7) and volume or severity (run-sum, v_i , Fig. 5.7), are used as characteristics for at-site drought. Often another drought deficit characteristic, the drought intensity (sometimes also referred to as drought magnitude, m_i), is introduced as the ratio between drought deficit volume and drought duration. It is also possible to define the minimum flow of each drought event, $Q_{\min,i}$ (Fig. 5.7), which can then be regarded as a deficit characteristic. The time of drought occurrence has been given different definitions, including the starting date of the drought, the mean of the onset and the termination date or the date of the minimum flow. Based on the time series of drought deficit characteristics (e.g., duration), it is possible to derive drought deficit indices (e.g., mean drought duration, mean deficit volume) as described in Fig. 5.1, column III.

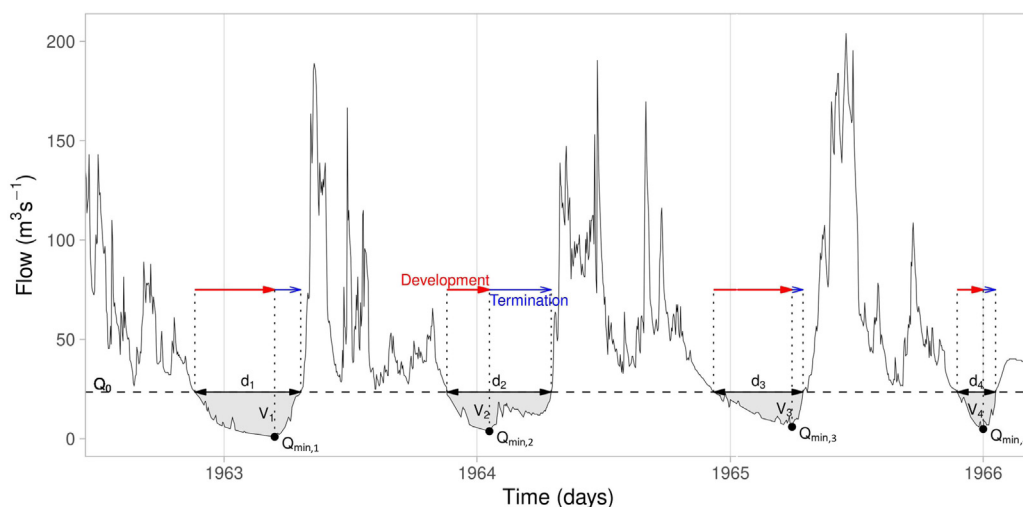


FIGURE 5.7

Definition of drought deficit characteristics for a daily time series of river flow comprising four drought events.

If state variables, such as hydraulic head or lake level, are considered, the drought deficit as defined by the threshold level approach will have a unit of length and time ($L T$) rather than volume (L^3), if derived for a time series of discharge or recharge (flux). Instead of summing up the deficit at each time step (run-sum), the average deficit over the drought duration can be calculated for state variables, then in units of (L) (Tallaksen et al., 2009). This average deviation from the threshold also characterises the drought intensity (Van Lanen and Peters, 2000).

Traditional applications of the threshold level method rarely focus on characterising the recovery from drought, although for many applications this may be the drought phase of interest (Parry et al., 2016a). The rate of drought termination (i.e., the rate of change from the minimum value to full recovery) has been found to vary widely among catchments (e.g., Schwalm et al., 2017) due to a range of natural (e.g., hydrometeorological drivers, hydrogeological processes) and human-influenced drivers (e.g., augmentation of low flow, reservoir releases). The termination date is a specific point in time at which the drought is considered to have recovered (Fig. 5.7), whereas the post-drought recovery is considered a period (e.g., Bonsal et al., 2011). Hence, the drought deficit duration can be sub-divided into two phases: the drought development (red arrow, Fig. 5.7) and the drought recovery (blue arrow Fig. 5.7). The drought development phase starts when the flow falls below the threshold level and lasts until the flow reaches Q_{\min} . The drought recovery starts at the time of Q_{\min} and ends when the flow crosses the threshold level again (termination date). By sub-dividing the drought deficit period, the recovery phase can be quantified by its duration and rate. The rate can be defined as the average increase in flow per unit of time in the recovery phase. Despite being developed for — and found to be successful in — analysing river flows and groundwater levels in the United Kingdom (Parry et al., 2016a, 2016b), there has been steady uptake of the approach across a diverse range of regions and applications within hydrology (e.g., Iñiguez et al., 2016; Margariti et al., 2019).

5.4.1.1 Threshold selection

The threshold may be chosen in several ways and the choice is, among other, a function of the type of water deficit to be studied. In some applications, the threshold is a well-defined flow quantity (absolute value), for example, a reservoir specific yield or a minimum ecological flow. It is also common to apply low flow indices themselves as thresholds (Sections 5.3.1 and 5.3.2), for example, a percentage of the mean flow or a percentile from the flow duration curve (Box 5.1).

Two main types of threshold level selections can be distinguished, the constant and the variable threshold level. In case of the constant threshold level, a constant value is used for the whole series. If the threshold is derived from the flow duration curve it implies that the whole river flow record (or a predefined period or season) is used in its derivation. This is illustrated in Fig. 5.8a-d, where the threshold is the Q_{90} for the period of record. If summer and winter droughts are studied separately, the threshold can also be constant as for the whole year (Fig. 5.8a), but is then based only on flow data from the respective season (Fig. 5.8b). A variable threshold is a threshold that varies over the year, for example, using a monthly (Fig. 5.8c) or daily (Fig. 5.8d, here smoothed with a centred moving average)

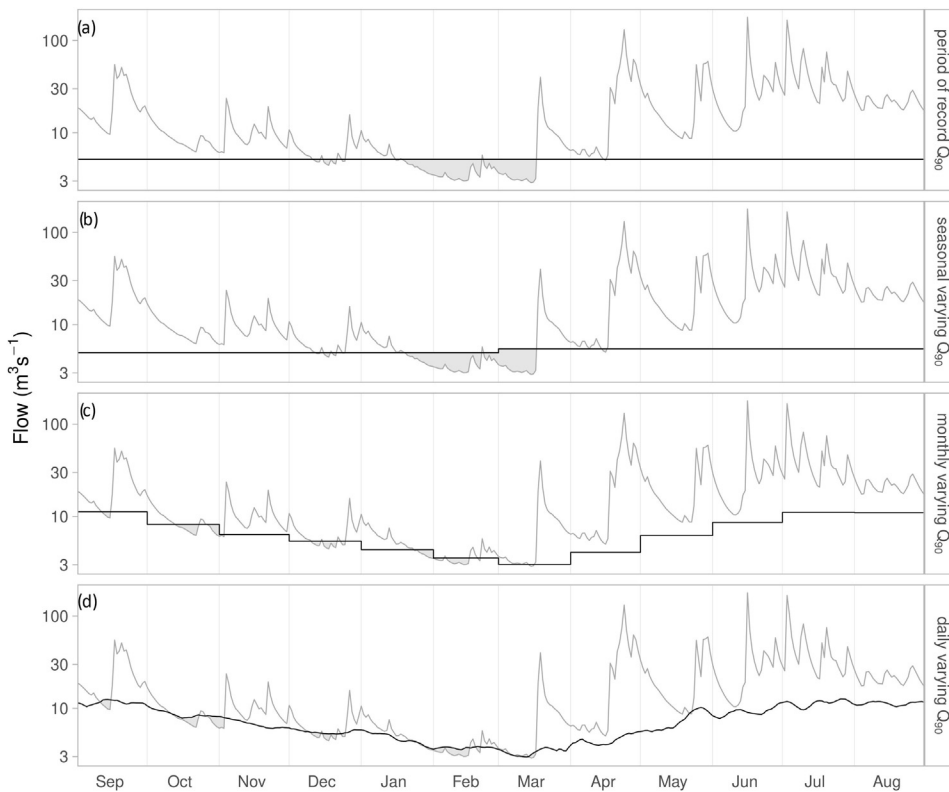


FIGURE 5.8

Illustration of different types of threshold levels: (a) constant threshold, (b) seasonal threshold level, (c) monthly varying threshold, and (d) daily varying (7-day smoothed) threshold.

7-day filter) varying threshold level. When applying the seasonal or monthly varying threshold to a time series of daily river flow (Fig. 5.8c), abrupt onsets or terminations of drought events at the beginning of a new season or month may occur. This can be avoided by smoothing the monthly threshold values using a centred moving average 30-day filter (e.g., Van Loon and Van Lanen, 2012).

The variable threshold approach can be adopted to detect river flow deviations (higher or lower than normal) during both high and low flow seasons, or low groundwater levels during the wet and dry season. Below normal precipitation or recharge, shorter than normal duration of the rainy season, an early start of the cold season or a delayed onset of snowmelt, are all possible causes for such deviations. Below normal river flow in the high flow season is normally not considered a drought, rather it is viewed as a deviation from normal (i.e., an anomaly) that potentially may affect the water availability later in the season (or year). Deviations less than normal are known as river flow deficiencies or river flow anomalies rather than streamflow droughts. The same terminology applies to groundwater, where such events are referred to as groundwater anomalies. However, if negative impacts are felt at the time of occurrence or the anomaly is expected to cause negative impacts later in the year, anomalies in the wet season are referred to as droughts by some end users.

The use of the variable threshold approach, similar to standardised indices (such as the SRI, Section 5.5.2), implies a shift towards the use of anomalies in drought research and hydrology in general. This paradigm adopted from climatology has facilitated collaboration between the climate community and large-scale hydrological modellers (Stahl et al., 2020). However, care is needed in the interpretation of the results across regions with diverse hydrological regimes, notable if the term ‘drought’ rather than ‘anomaly’ is used.

A variable threshold is used to define periods of river flow (or groundwater) deficits as departures from the ‘normal’ seasonal or daily range. A daily varying threshold level can, for example, be defined as a daily exceedance frequency based on the 365 daily flow duration curves, one for each day in the year. Exceedances derived on a daily basis may be highly uncertain if the data series are short. To increase the sampling range and smooth the threshold, daily exceedances can be calculated from flow duration curves based on all flow values within an n -day window. For example, if applying a 31-day window, the flow exceedance on 1 June would be calculated from all discharges recorded between 17 May and 16 June each year in the record.

Using a period of record of N years, and provided there are no gaps in the daily flow record, the empirical flow exceedance (or i^{th} percentile flow, $Q_{i,d}$) on any given day d of the year is given by:

$$EF_{Q_{i,d}}(n\text{-day}) = \frac{((nN + 1) - i_d)}{nN} \quad (5.4)$$

where $EF_{Q_{i,d}}(n\text{-day})$ is the empirical flow exceedance of the i^{th} largest value on day d , n is the length of the window in days, N is the number of record years and i_d is the rank of the daily flow on day d (flows are ranked in descending order) in the set of nN values.

A stepwise illustration of the threshold calculation for different time resolutions using the same period of record is seen in Fig. 5.9. Derivation of daily, monthly, seasonal and period of record flow duration curves are illustrated in Fig. 5.9a and the derivation of daily flow duration curves calculated from an n -day moving window demonstrated in Fig. 5.9b. Subsequently, a given value from one of the FDCs (e.g., Q_{90}) can be applied as a varying threshold (Fig. 5.8d). A streamflow drought or anomaly is said to occur when the river flow on a given day is lower than (or equal) the threshold for that particular day.

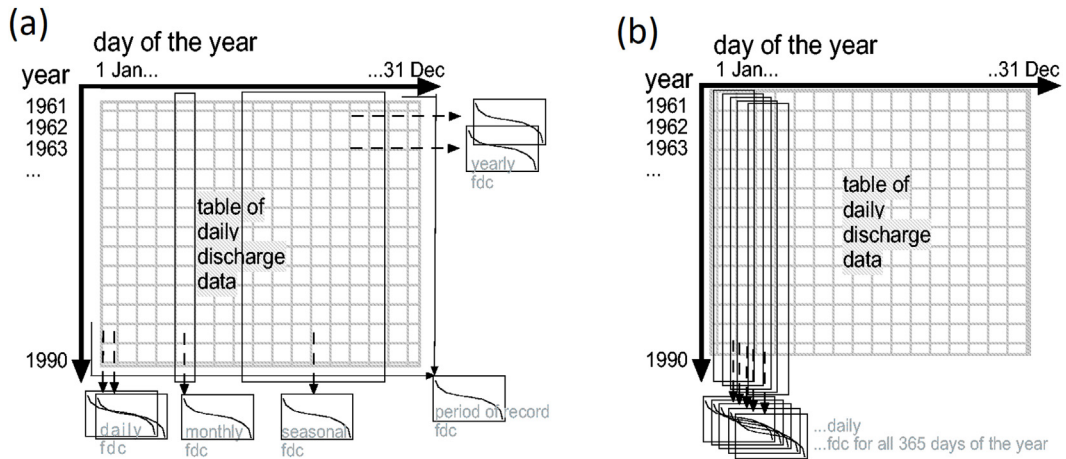


FIGURE 5.9

Scheme for determination of different flow duration curves (FDCs) to define possible threshold levels: (a) daily FDC, for example, the 1 January FDC is derived from all daily flows on 1 January in the period 1961–90; monthly FDC, for example, the FDC for March is derived from all daily flows in March (1–31 March) in the period 1961–90; seasonal FDC, for example, the FDC for April–September is derived from all daily flows in that 6 month period (1 April–30 September) in the period 1961–90; yearly FDC, for example, the 1963 FDC is derived from all daily flows in 1963 (1 January–31 December); period of record FDC is derived from all daily flows in the period 1961–90, and (b) daily FDC derived from n-day moving window, for example, the 1 June FDC with a centered 31-day moving window is derived from all daily river flows recorded between 17 May and 16 June each year in the period 1961–90.

Modified from Stahl (2001).

Heudorfer and Stahl (2017) compared the constant and variable threshold approach in a drought propagation study. They analysed precipitation, river flow and groundwater drought duration in four German catchments. For river flow and groundwater, they found that choosing a variable versus a constant threshold gave a large increase in short duration droughts, a moderate decrease in droughts of medium duration and a minor increase in long duration droughts. Sarailidis et al. (2019) concluded for a station in Cyprus that monthly and daily variable thresholds capture abnormal drought events during the whole year, whereas a constant (seasonal and whole period of record) threshold only selected the most severe ones. This illustrates a risk of diverging conclusions about drought characteristics depending on the threshold. The choice of threshold should be tailored to the hydrological regime and purpose of the study.

Knowledge about the hydrological regime is also important when selecting a specific percentile from the FDC as threshold level, whether constant or variable. An example of applying a constant threshold level for different rivers flow regimes across the world can be found in Fleig et al. (2006). For perennial rivers, a relatively low threshold in the range Q_{70} to Q_{95} can be considered reasonable. For intermittent and ephemeral rivers having a majority of zero flow, Q_{70} could easily be zero (Table 5.3), and hence no drought events would be selected. Meigh et al. (2002) found Q_{70} or Q_{90} to be reasonable

threshold levels for catchments in southern Africa; however, for ephemeral rivers, the mean flow was used as threshold. Similarly, [Tate and Freeman \(2000\)](#) studied eight river flow records from the southern African region and applied threshold levels ranging from $Q_{12.5}$ to Q_{90} depending on the proportion of zero flow. It should be noted that when choosing ‘high’ constant thresholds, a river would be in a drought for very long periods as zero flow periods will be considered as drought periods. For example, using Q_{20} as an exceedance threshold implies being in a drought for 80% of the time ([Box 5.1](#)), that is, drought is no longer a deviation from normal.

In arid or semi-arid regions, one may prefer a seasonal or variable threshold level, as in [Kjeldsen et al. \(2000\)](#), which applied Q_{75} of the monthly FDC to select drought events from daily river flow records in Zimbabwe. Another option is to calculate percentiles based on the non-zero values only or analyse deviations from normal flow in the (high) flow period, as an index of lower than normal water availability. Alternatively, one can focus on characterising periods when the flow is considered as zero, using so-called no-flow indices ([Section 5.4.2](#)).

In a regional study, the lack of long series over larger areas may impose restrictions on the use of very low threshold levels due to the presence of too many non-drought years at some sites, that is, the flow never falls below the chosen threshold in a year. On the other hand, the chance of droughts lasting longer than a year (multi-year droughts) increases for increasing threshold levels, and care should be taken when selecting a relatively high threshold if the purpose is to analyse time series of seasonal drought events. If the objective is to study multi-year droughts, higher thresholds are sought. For example, the monthly mean flow was applied in a study on multi-year droughts and their termination in the UK, as these droughts were considered to pose the most severe consequences ([Parry et al., 2016b](#)).

[Van Huijgevoort et al. \(2012\)](#) developed a method combining the variable threshold level method with a consecutive dry-period method (CDPM) to be able to compare droughts across different climatic regions. By combining the two methods, one avoids that the threshold level method identifies droughts in arid regions when the river runs dry for a long period. For each time series, the daily flow values are assigned to a percentile value (based on daily exceedances) resulting in a time series of percentiles rather than discharge. If less than 5% of a time series contains no-flow days ($X_5 > 0$) ([Section 5.4.2](#)), the variable threshold level method is followed only. For stations or grid-cells where this does not hold, the variable threshold level method is combined with the CDPM, which builds on the duration of no-flow periods in the time series, that is, consecutive number of dry days, $N_{\text{dry}}(n)$, where n is the number of the no-flow event. The $N_{\text{dry}}(n)$ series is ranked and an exceedance frequency associated with each value (duration in this case). Next, a particular percentile is selected as a constant threshold. A site or region is assumed to experience a drought if the consecutive number of no-flow days (spells) at a given time step exceeds this threshold, or if the flow is lower than the variable flow threshold. For further details, the reader is referred to [Van Huijgevoort et al. \(2012\)](#).

One example of a varying threshold level approach used operationally is the Low-Flow Index (LFI) developed by [Cammalleri et al. \(2017\)](#). The LFI is implemented within the Copernicus European Drought Observatory (EDO) for operational, near real-time monitoring of streamflow drought ([Boxes 13.2 and 13.3](#)). The LFI is based on simulated daily discharge from the LISFLOOD hydrological model ([Section 9.4.2](#)) and compares the water deficit during drought periods with the historical climatological conditions to derive the severity of the events. To use the index as a measure of drought severity, the 10-day cumulative deficits below the daily Q_{95} threshold (estimated by means of a 31-day moving window from a historical period), are fitted to the Exponential distribution. The cumulative distribution function ([Section 6.2.2](#)) is then used as a standardised measure ([Section 5.5](#)) of the severity

of the drought and, subsequently used to classify observed droughts into mild, moderate, severe and extreme events. The index has the advantage of being useful in a daily operational drought monitoring system.

5.4.1.2 Time resolution

Many factors affect the choice of time resolution of the time series to be studied. Whether to apply series of annual, monthly or daily data (if available), depends on the hydrological regime under study (Section 2.2.2), the specific problem to be solved and the variable analysed. In a temperate climate, a given year may include both severe droughts (seasonal droughts) and months with abundant water, implying that annual data may not reveal severe seasonal droughts. Dry regions, such as B- and Cs-climates (Sections 2.2 and 3.3), are more likely to experience droughts lasting for several years, that is, multi-year droughts, which supports the use of a monthly or even an annual time step. Hence, different time resolutions (annual, monthly and daily) may lead to different results depending on the drought event selection approach, as demonstrated by Beyene et al. (2014).

The threshold level method introduced by Yevjevich (1967) was originally based on analysing sequential time series with a time resolution of 1 month or longer. The approach has also been used for analysing streamflow droughts from a daily-recorded hydrograph (e.g., Heudorfer and Stahl, 2017; Fleig et al., 2006; Meigh et al., 2002; Hisdal et al., 2001; Kjeldsen et al., 2000; Tallaksen et al., 1997; Woo and Tarhule, 1994; Zelenhasić and Salvai, 1987). These studies demonstrate the potential of this method using a daily time step for a complete description of the stochastic process of seasonal (within-year) droughts. However, the use of a daily time resolution introduces two special problems, namely, dependency among droughts and the presence of minor droughts. During a prolonged dry period, it is often observed that the flow exceeds the threshold level for a short period of time, and thereby, a large drought is divided into a number of minor droughts that are mutually dependent (Fig. 5.10). To avoid these problems, which could distort an extreme value modelling, a consistent definition of drought events should include some kind of pooling in order to define an independent sequence of drought events (Box 5.2, Worked Example 5.4).

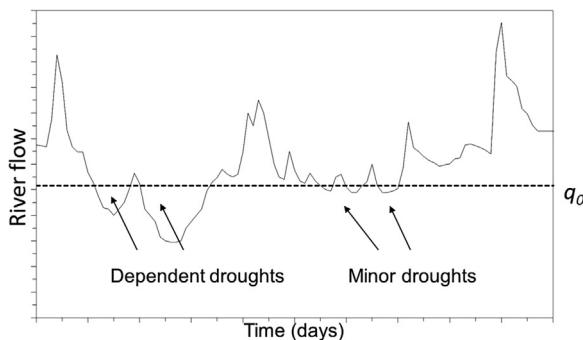


FIGURE 5.10

Daily time series of river flow illustrating the problem of mutual dependence and minor droughts, here using a constant threshold, q_0 .

Modified from Tallaksen (2000).

The question of mutually dependent droughts is also of importance when considering drought termination, even for a monthly time resolution. This requires the user to think about what constitutes a recovery in their system of interest. A drought can be temporarily interrupted by a high flow event before returning to low flow conditions. As such, this may not indicate a lasting recovery, but the degree to which this is the case must be determined by the specific application. The user must specify parameters in the drought termination methodology that allow for short duration interruptions of the droughts above the threshold and specify above threshold flow criteria (e.g., in terms of duration or magnitude) required for recovery. Some degree of subjectivity in parameter selection is unavoidable, though sensitivity analyses can be undertaken to determine the robustness of the parameters chosen (e.g., Parry et al., 2016b).

Box 5.2 Pooling procedures

Tallaksen et al. (1997) compared three different pooling procedures for dependent droughts for two contrasting Danish catchments: the moving average procedure (MA), the sequent peak algorithm (SPA) and the inter-event time and volume criterion (IC) for both Annual Maximum Series (AMS) and Partial Duration Series (PDS) (Section 6.3.2). MA simply smooths the time series applying a moving average filter and it was recommended to apply a moving average window of 10 days. The IC is used to pool two subsequent events with characteristics (d_i, v_i) and (d_{i+1}, v_{i+1}) (Fig. 5.7) if (a) the inter-event time, t_i , between two droughts is less than or equal to a critical duration, t_{\min} , and (b) the ratio between the inter-event excess volume, z_i , and the preceding deficit volume v_i is less than a critical value p_c . The pooled drought is then again pooled with the next drought if (a) and (b) are fulfilled and so on. The pooled drought deficit characteristics (i.e., duration, d_{pool} and volume, v_{pool}) are calculated as follows:

$$d_{\text{pool}} = d_i + d_{i+1} + t_i \quad (\text{B5.1a})$$

$$v_{\text{pool}} = v_i + v_{i+1} - z_i \quad (\text{B5.1b})$$

where d_{pool} is referred to as the full duration, whereas the term real duration is used when the inter-event time, t_i , is not included in the sum (Worked Example 6.2).

The SPA is a method for selecting drought events that implicitly pools events and is described in a separate section (Section 5.4.3). The study by Tallaksen et al. (1997) showed that the problem of minor droughts in PDS is implicitly reduced using MA and SPA, and in this respect, these procedures have an important advantage as compared to the IC method. In either case, minor droughts can be removed from the sample by introducing a volume- or time-based criterion (or a combination) as demonstrated in Worked Example 5.4 (Step 4).

Overall, the SPA method differed significantly from the other two pooling methods for high thresholds due to the presence of multi-year droughts. This restricts the use of the SPA method for analysis of seasonal (within-year) droughts to low threshold levels. A very low threshold, on the other hand, may result in a high number of zero-drought years (the flow is never below the threshold in a given year), in which case the PDS model is superior to AMS (Tallaksen et al., 1997). Kjeldsen et al. (2000) show that the SPA generally extracts larger extreme events than MA using a PDS approach. The advantage of the SPA method is that no parameters need to be determined prior to its use as compared to the choice of averaging window in the MA method and two parameters in the IC method. Kjeldsen et al. (2000) further suggest removing the smallest droughts according to a frequency factor because these small events disturb the frequency distribution modelling, notable in a PDS approach. The choice of frequency factor is subjective and must be regarded as a parameter of the method. The main advantage of the MA method is that it reduces the problem of minor droughts at the same time as mutually dependent droughts are pooled. However, it may well introduce dependency between the drought events, especially if the averaging interval is large. The SPA method, on the other hand, has a more straightforward interpretation as no modification is done on the observed data. The threshold can be interpreted as the desired yield from a reservoir, and the drought deficit volume defines the required storage in each period (Section 5.4.3).

Worked Example 5.4 Threshold level method

<https://github.com/hydrodrought/hydrodroughtbook>

The threshold level method can be used to select drought events from time series of river flow if there are not too many missing values in the dataset and a meaningful threshold, Q_0 , is chosen. Data from River Ngaruroro at Kuripapango (NZ) are used to demonstrate the procedure in the this worked example.

1. Loading the data

Fifty-six years of daily flow (20 September 1963 to 8 October 2019) are downloaded from the International Dataset (Section 4.5.1). In this river, the low flow season occurs at the turn of the calendar year. To avoid problems with allocating droughts to a specific calendar year because of drought events starting in one year and ending in another, the start of the hydrological year is set to 1 September. An event is attributed to the start of the hydrological year it occurs (i.e., to the first of the two calendar years).

2. Filling in missing values

The time series for River Ngaruroro contains missing values. We do not know if a missing value (NA) represents a flow below the threshold or above the threshold, as the flow value itself is unknown. A single missing value will cause the function *drought_events()* to terminate a dry spell (drought event) or similar, a wet spell. Accordingly, most characteristics derived for this event (e.g., drought duration, drought termination, drought volume) will not be correctly estimated.

A conservative approach would be to eliminate years with missing values completely. Instead, to avoid losing too many years of observations, we infill periods of missing data by linear interpolation if they are of short duration. Here, short duration is defined as periods <15 days, whereas years containing long periods of missing values (≥ 15 days) have been removed. This results in 49 years of daily flow (1 September 1964 to 31 August 2019). In total 6 hydrological years are omitted from the series (1965–66, 1977–78, 1978–79, 1986–87, 1987–88, 2001–02). Table 5.7 displays information about the calendar years removed.

Table 5.7 Missing calendar years in the time series of river flow for River Ngaruroro at Kuripapango (NZ), showing: the removed year, total number of days in each year, number of days with flow observations, number of days with missing data and the fraction of days each year with observations.

No. 1	Removed year	Days in year	Days with flow observations	Days with missing data	Fraction with observations
1	1963	366	347	19	0.948
2	1965	365	294	71	0.805
3	1977	365	350	15	0.959
4	1978	365	305	60	0.836
5	1986	365	341	24	0.934
6	1987	366	336	30	0.918
7	2001	365	344	21	0.942
8	2019	366	38	328	0.104

3. Selecting threshold and drought events

A sequence of drought events is obtained from the river flow hydrograph by considering periods with flow below a threshold, Q_0 ; here Q_{90} , $4.95 \text{ m}^3 \text{ s}^{-1}$, is used. Drought characteristics are derived with the function *drought_events()*, and Table 5.8 depicts the related drought indices for the first 10 events, including:

- (a) first.day: the start date, defined as the first day below the threshold
- (b) last.day: the end date, defined as the last day below the threshold
- (c) duration: the drought duration (days), defined as last.day – first.day + 1
- (d) volume: the deficit volume (m^3), defined as the sum of the daily deficit flow times the duration (in seconds)
- (e) qmin: the minimum flow ($\text{m}^3 \text{ s}^{-1}$), defined as the minimum flow Q_{\min} within a drought event
- (f) tq_{\min} : the date of the minimum flow.

Table 5.8 Key drought deficit indices for River Ngaruroro at Kuripapango (NZ), listing the first 10 events in the time series.

Event	First day	Last day	Duration (days)	Deficit volume (m^3)	Q_{\min} ($\text{m}^3 \text{ s}^{-1}$)	Date Q_{\min}
1	1967–04–23	1967–04–23	1	6307.	4.88	1967–04–23
2	1967–04–26	1967–04–26	1	4579.	4.90	1967–04–26
3	1967–05–09	1967–05–10	2	17,453.	4.80	1967–05–10
4	1967–05–13	1967–05–14	2	18,835.	4.76	1967–05–14
5	1967–05–23	1967–05–23	1	3024.	4.91	1967–05–23
6	1968–02–07	1968–02–08	2	34,646.	4.69	1968–02–08
7	1968–02–17	1968–03–08	21	1,766,621.	3.44	1968–03–05
8	1968–03–11	1968–04–02	23	2,349,562.	3.23	1968–03–26
9	1968–04–06	1968–04–09	4	293,933.	3.76	1968–04–08
10	1969–03–25	1969–03–30	6	103,766.	4.68	1969–03–26

With 200 more rows

4. Removing minor droughts

Several minor droughts, lasting for a few days only, can be observed. To reduce the problem of minor droughts, two restrictions are imposed:

- (a) a minimum drought duration, d_{\min} , which removes droughts with duration less than a specified number of days
- (b) a minimum drought deficit volume, which removes droughts with a deficit volume less than a certain fraction, α , of the maximum drought deficit volume observed in the complete series of drought events.

In [Table 5.9](#), we append a logical column called Minor to [Table 5.8](#) of drought events. It is TRUE when drought duration is less than 5 days OR if the drought volume is less than 5% of the maximum drought deficit volume (i.e., 51133,25 m³). In total, 99 minor droughts were removed based on these criteria.

Table 5.9 Key drought deficit indices for River Ngaruroro at Kuripapango (NZ), listing the first 10 events in the time series. The last column (Minor) is TRUE/FALSE depending on whether the event is considered a minor drought or not.

Event	First day	Last day	Duration (days)	Deficit volume (m ³)	Q_{\min} (m ³ s ⁻¹)	Date Q_{\min}	Minor
1	1967-04-23	1967-04-23	1	6307.	4.88	1967-04-23	TRUE
2	1967-04-26	1967-04-26	1	4579.	4.90	1967-04-26	TRUE
3	1967-05-09	1967-05-10	2	17,453.	4.80	1967-05-10	TRUE
4	1967-05-13	1967-05-14	2	18,835.	4.76	1967-05-14	TRUE
5	1967-05-23	1967-05-23	1	3024.	4.91	1967-05-23	TRUE
6	1968-02-07	1968-02-08	2	34,646.	4.69	1968-02-08	TRUE
7	1968-02-17	1968-03-08	21	1,766,621.	3.44	1968-03-05	FALSE
8	1968-03-11	1968-04-02	23	2,349,562.	3.23	1968-03-26	FALSE
9	1968-04-06	1968-04-09	4	293,933.	3.76	1968-04-08	TRUE
10	1969-03-25	1969-03-30	6	103,766.	4.68	1969-03-26	FALSE

With 200 more rows

5. Pooling-dependent droughts

The inter-event time criterion (IC) is used to pool dependent droughts (i.e., droughts separated by a short period of flow above the threshold). If the time between two droughts is less than or equal to a critical duration, t_{\min} , the two events are pooled. In this example, t_{\min} is set equal to 2 days. If a drought event is pooled, two columns are added to the table:

- (a) dbt: the duration below the threshold, that is, the drought duration minus short period(s) above the threshold (note: the ‘full’ duration is derived from the start and end date of each pooled event)
- (b) pooled: the number of drought events that are pooled in each case.

The drought deficit characteristics of the 10 longest (pooled) drought events are listed in [Table 5.10](#). In total, there are 100 drought events, which equals an average of 2.04 events per year.

Key drought characteristics for all drought events occurring in the period (1 September 1964–31 August 2019), are summarised for different drought indices in [Table 5.11](#). For each year, the number of droughts in the year, the days below the threshold (summed over all events) in a year and the minimum flow in a year, are presented.

Histograms of drought duration for individual years are plotted in [Fig. 5.11](#). The longest drought durations (dbt) are found in 2014 with more than 60 days, followed by 1973, 2007, 1972, 1982 and 2008. A histogram of the drought duration for all years is seen in [Fig. 5.12](#), and a much skewed distribution is revealed. Short duration droughts dominate with 43 events lasting less than 11 days. Only nine events lasted more than 30 days.

Table 5.10 Key drought deficit indices for River Ngaruroro at Kuripapango (NZ), listing the 10 longest (d_{pool} , Eq. B5.1a) drought events (dbt is the number of days below the threshold). The last column (pooled) show whether these are pooled (1) or not (0).

No.	Event	First day	Last day	Duration (days)	Dbt (days)	Deficit volume (m^3)	Q_{min} ($m^3 s^{-1}$)	Date Q_{min}	Pooled
1	166	2015-01-06	2015-03-15	69	69	$1.02 \cdot 10^{-6}$	2.17	2015-03-04	0
2	37	1974-01-20	1974-03-17	57	56	$6.51 \cdot 10^{-6}$	2.88	1974-03-15	1
3	138	2008-01-10	2008-03-01	52	51	$6.41 \cdot 10^{-6}$	2.64	2008-02-28	1
4	30	1973-01-26	1973-03-12	46	46	$6.58 \cdot 10^{-6}$	2.66	1973-03-03	0
5	50	1983-02-16	1983-04-02	46	46	$7.38 \cdot 10^{-6}$	2.46	1983-03-30	0
6	148	2009-03-14	2009-04-26	44	43	$6.01 \cdot 10^{-6}$	2.53	2009-04-19	1
7	157	2013-02-07	2013-03-18	40	40	$7.09 \cdot 10^{-6}$	2.38	2013-03-15	0
8	124	2005-02-06	2005-03-16	39	38	$4.99 \cdot 10^{-6}$	2.68	2005-03-13	1
9	139	2008-03-09	2008-04-14	37	36	$5.22 \cdot 10^{-6}$	2.65	2008-04-06	1
10	59	1989-04-01	1989-04-29	29	29	$2.71 \cdot 10^{-6}$	3.3	1989-04-29	0

With 90 more rows

Table 5.11 Key drought deficit indices for River Ngaruroro at Kuripapango (NZ), listing the first 10 years containing drought events, i.e., the year, the number of droughts in the year, days below the threshold in the year (summed over all events) and the minimum flow in the year.

No.	Year	Number	Total days < threshold (days)	Q_{\min} ($\text{m}^3 \text{s}^{-1}$)
1	1967	2	44	3.23
2	1968	2	22	3.88
3	1969	3	37	3.89
4	1970	3	34	3.73
5	1972	7	114	2.66
6	1973	2	63	2.88
7	1974	2	10	4.31
8	1975	2	18	4.09
9	1977	1	25	3.46
10	1982	2	57	2.46

With 25 more rows

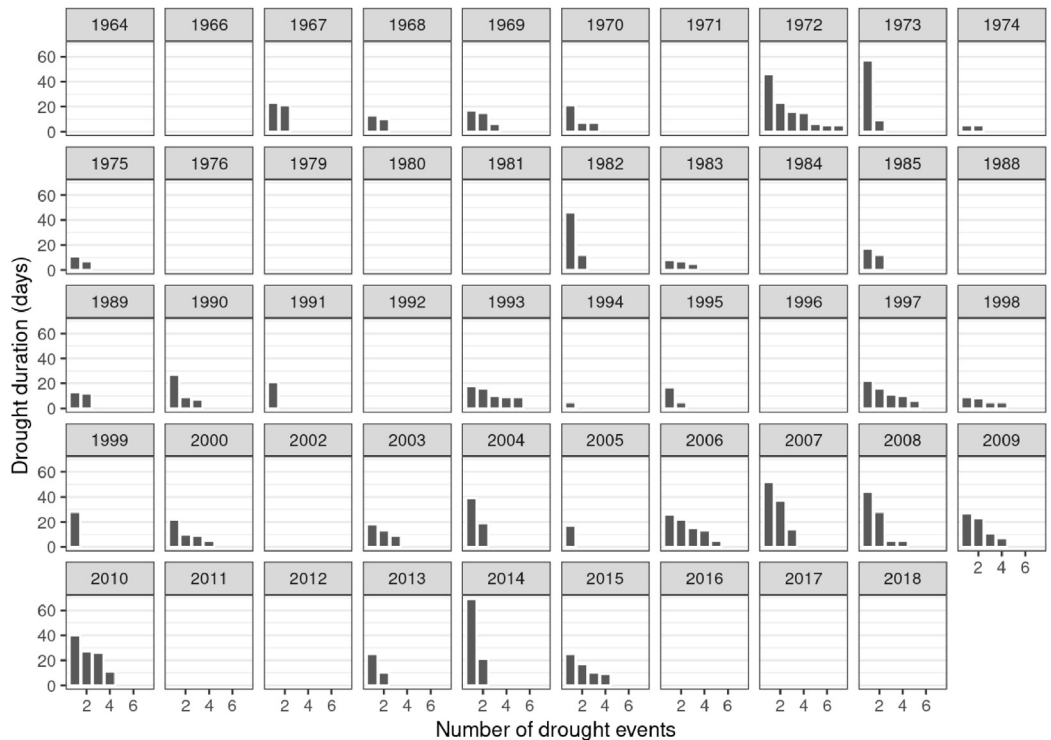


FIGURE 5.11

Histogram of drought duration for River Ngaruroro at Kuripapango (NZ) for each year in the period 1964–2018. Selection criteria: threshold level = Q_{90} , $d_{\min} = 5$ days, $\alpha = 0.005$ and $t_{\min} = 2$ days. Note, the year indicated is the first year of the hydrological year (e.g., 2014 represents the hydrological year 2014–15).

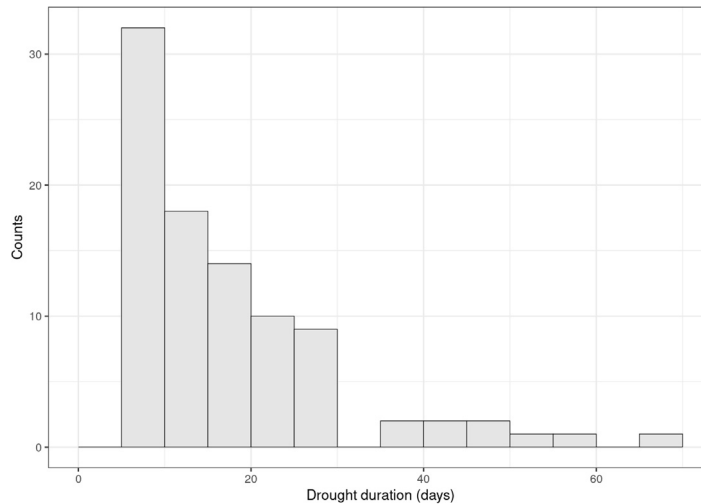


FIGURE 5.12

Histogram of drought duration for River Ngaruroro at Kuripapango (NZ) for the period 1964–65 to 2018–19. Selection criteria: Threshold level = Q_{90} , $d_{\min} = 5$ days, and pooling criteria $\alpha = 0.005$ and $t_{\min} = 2$ days.

5.4.2 Indices for intermittent and ephemeral rivers

As described and exemplified in [Sections 5.3.1 and 5.3.2](#), low flow indices derived from the flow duration curve and mean annual minimum flow may be zero for intermittent rivers and, in particular, ephemeral rivers ([Section 2.2.2](#)). To obtain relevant drought characteristics for rivers that frequently experience zero flow, that is, they run dry during a specific season (intermittent rivers), only experience flow following rainfall episodes (ephemeral rivers) or only experience zero flow during extreme dry years (perennial rivers), a series of so-called no-flow indices for daily river flow records have been proposed by [Datry et al. \(2017a; 2017b\)](#), [Sauquet et al. \(2020\)](#), and [URL 5.1](#). No-flow indices are useful to characterise flow intermittency and characteristics of ephemeral rivers when zero-flow periods are of particular interest; indices that are also more ecologically relevant.

Generally, a no-flow spell is defined as a period when river flow is less than or equal to a no-flow threshold. This could be zero or a small value below which the river flow is no longer measurable. A no-flow event is a contiguous period of days where the flow is below the no-flow threshold. Similar to the use of the threshold level method for perennial rivers, pooling of successive, dependent events can be applied to define a series of independent events ([Section 5.4.1](#)).

The no-flow indices include the proportion of no-flow years (NF FRAC) defined as the number of years with no-flow occurrence divided by the total number of years in the record. Other indices are related to the number of no-flow days, for example, the mean annual number of no-flow days (NF MAN), the coefficient of variation of no-flow days (NF CVAN) and the statistical distribution of the annual number of no-flow days. Similar, based on the duration of no-flow spells ([Section 5.4.1.1](#)), the mean annual maximum duration (NF MAMD), the Coefficient of Variance (CV, [Eq. 6.20](#)) of the annual maximum duration and the duration distribution can be estimated (either in a PDS or AMS approach). Indices based on the timing and seasonality of no-flows are also proposed, such as the mean onset of the first annual no-flow day, the variability of the onset, the mean termination of the first, last or annual maximum no-flow spell ([Worked Example 5.5](#)).

Worked Example 5.5 No-flow indices

<https://github.com/HydroDrought/hydrodroughtBook>

1. Loading the data

In this example, we download river flow data from catchments in the International Dataset that are classified as intermittent or ephemeral.

2. Identifying intermittent or ephemeral rivers

A river is here defined as intermittent or ephemeral if the river flow is below a threshold of $0.001 \text{ m}^3 \text{ s}^{-1}$ for at least 5 days each year. Six rivers fulfil the criteria: Sabar and Upper Guadiana in Spain, Dawib (Namibia), Elands (South Africa), Ray (UK) and Arroyo Seco (US). Only years without missing values are included in the analysis.

3. Computing no-flow indices

The following indices are calculated and included in Table 5.12:

- (a) NF FRAC: the proportion of no-flow years, defined as the number of years with no-flow occurrence divided by the total number of years in the time series
- (b) NF MAN: the mean annual number of no-flow days
- (c) NF CVAN: the coefficient of variation of no-flow days
- (d) no flow days: the number of days without flow for each year in the time series. This is a list of integer values where the number of values corresponds to the number of years in the record
- (e) NF MAMD: the mean annual maximum no-flow spell duration

Table 5.12 No-flow indices for Rivers Sabar and Upper Guadiana (Spain), Dawib (Namibia), Elands (South Africa), Ray (UK) and Arroyo Seco (USA).

River, country	No-flow indices, NF							
	NF FRAC	NF MAN (days)	NF CVAN	No flow days (days)	NF MAMD (days)	Onset	sd onset	Term
Sabar	1	185.	0.239	29	168	12 May	60.0	29 Nov
U.-Guadiana	0.116	8.12	3.26	40	8.12	12 Aug	25.8	14 Oct
Dawib	1	361.	0.0083	6	298.	1 Jan	0.	27 Jan
Elands	0.214	14.4	1.83	9	7.89	22 Aug	83.6	4 Sep
Ray	0.945	98.2	0.576	46	40.2	14 May	52.8	20 May
A. Seco	0.441	39.0	1.33	118	38.3	30 July	24.7	24 Oct

- (f) onset: arithmetic mean of the date when the first annual no-flow spell starts (using circular statistics, Fig. 8.1)
- (g) sd onset: standard deviation of the date when the first annual no-flow spell starts (using circular statistics)
- (h) term: arithmetic mean of the date when the first no-flow spell in a year ends (using circular statistics).

4. Visualising streamflow permanence

Streamflow permanence describes flow persistency, that is, the number of time steps (here months) that a river carries water over the years (each month is labelled flow, no-flow, or no data). Fig. 5.13 illustrates the duration of periods with flow (permanence) and no-flow (dry spells) of the six rivers: Sabar, Upper Guadiana, Dawib, Elands, Ray and Arroyo Seco. Sabar and Ray experience no-flow periods every year (NF FRAC = 1, Table 5.12), whereas

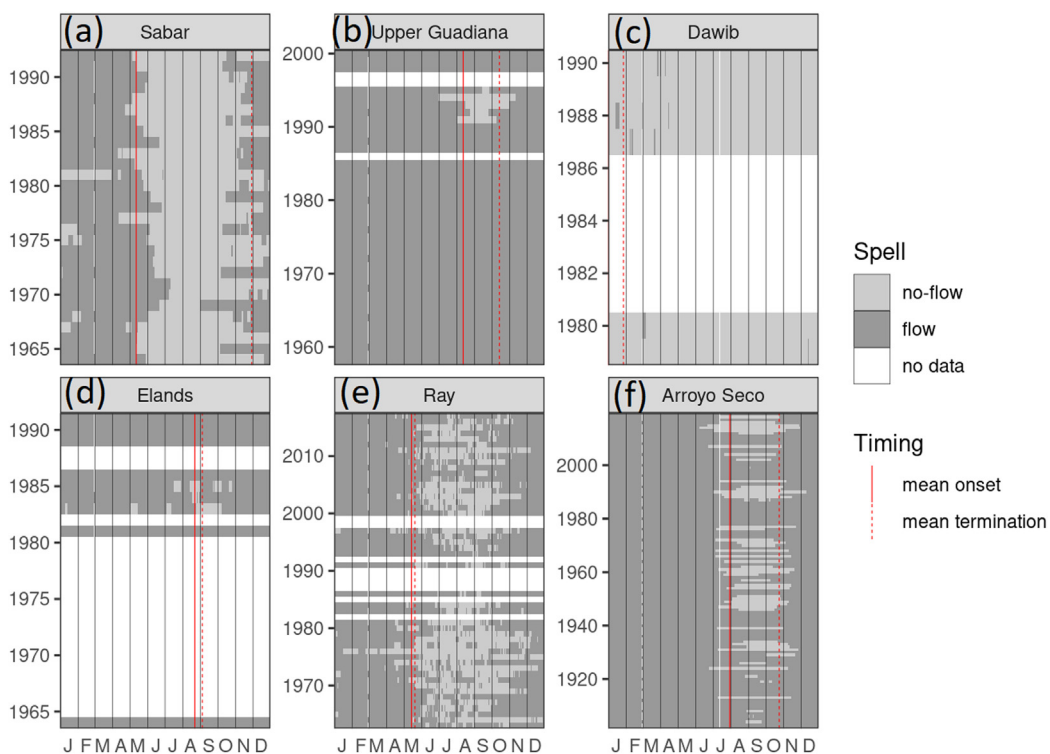


FIGURE 5.13

Periods of flow and no-flow spells (streamflow permanence) are illustrated for six intermittent or ephemeral rivers in the International Dataset: (a) Sabar (Spain), (b) Upper Guadiana (Spain), (c) Dawib (Namibia), (d) Elands (South Africa), (e) Ray (UK), and (f) Arroyo Seco (US). The horizontal axis shows the months in a year and the vertical axis the record years.

Elands and Arroyo Seco also have years without no-flow periods. Ray has many short no-flow periods in a year. Since the mean onset and termination date are calculated for the first no-flow event, the mean onset and termination almost coincide for this station (Table 5.12). Upper Guadiana was a perennial river until the 1990s when groundwater abstraction led to periods of no-flow during the summer (Sections 9.3.3 and 10.5.1.1). Dawib is clearly ephemeral and river flow is only observed occasionally, that is, the river can be dry for consecutive years. Since the whole year can be dry, the mean onset of the first annual no-flow period for the River Dawib is set to the beginning of the year, and, hence, the line is not visible in the figure.

5.4.3 The sequent peak algorithm

A procedure for preliminary design of reservoirs based on annual average river flow series is the mass curve or its equivalent, the Sequent Peak Algorithm (SPA) (e.g., Vogel and Stedinger, 1987). SPA can also be used for daily data to derive drought events. Let Q_t (m^3) denote the total daily inflow to a reservoir and Q_0 (m^3) the desired daily yield or any other predefined flow, then the storage S_t (m^3) required at the beginning of the period t , where t is a given day, reads (Tallaksen et al., 1997):

$$S_t = S_{t-1} + (Q_0 - Q_t) \quad \text{if } S_t > 0 \quad (5.5a)$$

$$S_t = 0 \quad \text{if } S_t \leq 0 \quad (5.5b)$$

An uninterrupted sequence of positive storage, S_t , $\{S_t, t = t_0, \dots, t_{end}\}$ defines a period with storage depletion and a subsequent filling up (Fig. 5.14). The required storage in that period, $\max\{S\}$, defines the drought deficit volume, v_i , and the time interval, d_i , from the beginning of the depletion period, τ_0 , to the time of the maximum depletion, t_{max} , defines the drought duration ($t_{max} - t_0 + 1 = d_i$).

This technique differs from the threshold level method in that periods when the flow exceeds the predefined flow (Q_0) do not necessarily negate the storage requirement, and several deficit periods may pass before sufficient inflow has occurred to refill the reservoir. Hence, based on this method, two droughts are pooled (Box 5.2) if the reservoir has not totally recovered from the first drought when the second drought begins ($S_t > 0$). The drought is not fully recovered until the required storage reaches zero ($S_t = 0$); hence, a sufficient recovery period is required with $Q_t > Q_0$. For further details about reservoir design and storage-yield analysis, the reader is referred to McMahan and Mein (1986) (Worked Example 5.6).

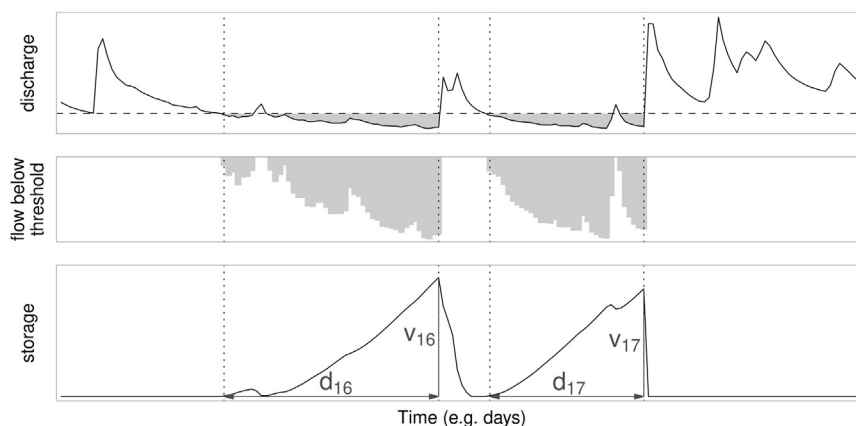


FIGURE 5.14

Defining drought events using the sequent peak algorithm (SPA), where d_i and v_i is the duration, respectively, the deficit volume, of the i^{th} event in the time series (here exemplified for event number 16 and 17).

Worked Example 5.6 Sequent peak algorithm

<https://github.com/HydroDrought/hydrodroughtBook>

1. Loading the data

Twelve years of daily data without missing values from River Ngaruroro at Kuripapango (NZ) are used as an example (01.09.1988–30.08.1999). The data are downloaded from the International Dataset (Section 4.5.1).

2. Calculating the required storage

- (a) Define the value of the desired yield (equals the threshold value); here Q_{90} is used
- (b) calculate the storage, S_t , according to Eq. 5.5. Storage is appended as a new column to Table 5.13 using the function `storage()` with discharge and the threshold (desired yield) as input values. As long as the discharge is above, or equal to, the threshold, the storage is zero as only flows below the Q_{90} contributes to the storage. This happens the first time on 14 March 1989 and only lasts 2 days (first entry in Table 5.13)
- (c) filtering for storage >0 and assigning new event numbers when the time increment in the (filtered) time series suddenly changes, allow us to identify a series of uninterrupted sequence of positive S_t .

3. Deriving drought deficit volume and duration

The deficit volume is the maximum value in an uninterrupted sequence of positive S_t , and the drought duration is the time from the beginning of the depletion period to the time of the maximum depletion (Table 5.13). The first two columns show the date and the corresponding flow value, Q . The duration of the first event starting on 14 March 1989 is only 1 day (equals the time to maximum depletion, which is on the first day). The date of the maximum depletion (i.e., $\max S_t$) is displayed in bold.

Table 5.13 Change in storage (S_t) calculated by the SPA from daily time series of river flow for River Ngaruroro at Kuripapango (NZ), listing selected periods in March 1989 when $S_t > 0$. The date of maximum depletion in a period is marked in bold, e.g., the first day (14 March 1989) in the first period selected.

Data, 10-year series		SPA
Date	River flow Q_t ($\text{m}^3 \text{s}^{-1}$)	Storage S_t ($\text{m}^3 \text{s}^{-1}$)
14 March 1989	5.08	0.0780
15 March 1989	5.20	0.0350
23 March 1989	5.05	0.115
24 March 1989	4.89	0.387
25 March 1989	4.88	0.669
26 March 1989	5.09	0.741
27 March 1989	4.80	1.10
28 March 1989	4.64	1.62
29 March 1989	4.55	2.24
30 March 1989	5.11	2.29

4. Results

An extract of the drought duration and deficit volume for the 12-year series is given in Table 5.14. Note that the time series starts with a flow value less than the threshold (not knowing the previous flow values), thus the first event should be omitted from the analysis. The most severe event starts in March 1989, lasts 38 days, and reaches its maximum deficit of $39.8 \text{ m}^3 \text{ s}^{-1}$ on 29 April 1989. Even though the SPA procedure is pooling minor and dependent droughts, the obtained time series of events still contains a number of minor drought events.

Table 5.14 Drought deficit volume, duration and date of maximum depletion calculated by the SPA for River Ngaruroro at Kuripapango (NZ), listing the five first events.

Event i	Deficit volume v_i ($\text{m}^3 \text{s}^{-1}$)	Duration d_i (days)	Date of maximum depletion
1	0.078	1	14-03-1989
2	39.8	38	29-04-1989
3	2.72	7	24-05-1989
4	11.7	14	09-03-1990
5	8.26	13	24-04-1990

5.5 Standardised indices

Standardised river flow indices are normally understood as indices standardised in a way that allows comparison across seasons, catchments and hydroclimatic regimes. Commonly, time series of discharge is divided by catchment area (i.e., expressed as flow per unit of area) or by the mean annual flow (i.e., expressed as deviation from the mean) prior to the derivation of drought indices. Alternatively, the index itself (e.g., deficit volume) can be standardised (e.g., by the mean flow, Tallaksen et al., 1997). A time series can also be standardised by subtracting the mean and divide by the standard deviation as done in a drought analysis based on the theory of runs for monthly river flow (Sharma and Panu, 2008). Modelled indices, such as the Palmer Drought Severity Index (Box 5.4), can also be viewed as standardised indices, but their derivation is based on a different modelling approach (Section 5.6.1).

In this section, a family of standardised indices is presented that stem from time series that are standardised to the normal distribution (Section 7.2.1) by transforming the given (observed or simulated) series into probabilities (by distribution fitting) or empirical frequencies (by ranking). They are commonly referred to as anomaly indices as they express both dry and wet anomalies in time series of hydrometeorological variables. Standardised indices are also suitable when gaining insight on the propagation of drought from meteorological, soil moisture to hydrological drought (Zhang et al., 2015; Barker et al., 2016; WMO and GWP, 2016) as the values are comparable across the different time series.

In addition to extreme values obtained directly from the standardised time series (given as standard deviations from the mean), drought characteristics, such as drought duration, average deficit and areal extent, can be derived by applying a threshold to the standardised time series. Barker et al. (2016) used a value of -0.84 , which corresponds to the commonly used 20th percentile (non-exceedance) threshold (equivalent to Q_{80} commonly used in hydrology, Box 5.1). It is important to bear in mind that the average or cumulative deficit ($-$) can be derived from standardised time series, however, not deficit volume in absolute terms (L^3 or L).

5.5.1 Empirical quantiles

Empirical ranking methods convert data that are ranked according to their magnitude into an estimate of: (a) the associated cumulative probability using plotting positions (parametric approach), or (b) the cumulative frequency using simple ranks, i/N , commonly referred to as river flow quantiles or percentiles (non-parametric approach) (Section 6.2.1). River flow percentiles from the empirical cumulative distribution function (ecdf) are referred to as the flow duration curve in hydrology (Section 5.3.1). In (a), the values are assumed independent and homogeneous allowing return levels to be estimated based on non-exceedance probabilities, whereas in (b), one may speak of a historical likelihood (i.e., a non-exceedance frequency) for a particular observation. It is important to keep in mind that the uncertainty associated with the estimate of the (non-)exceedance frequency of the smallest, respectively largest event is large, and similar to the uncertainty in the extreme end of a fitted distribution (Section 6.2.2). Empirical ranking can also be applied to time series of lake or groundwater level (Worked Example 5.7).

5.5.2 Standardised (to the normal distribution) indices

The Standardised Precipitation Index (SPI) and the later developed Standardised Precipitation-Evapotranspiration Index (SPEI) are among the most commonly used meteorological drought indices (Box 5.3). The SPI was developed by McKee et al. (1993) and measures the anomaly in precipitation (dry and wet) at a given location for different accumulation intervals by transforming the historical record to the normal distribution. Staudinger et al. (2014) later suggested an extension to the

Box 5.3 Standardised meteorological indices (SPI and SPEI)

The Standardised Precipitation Index (SPI), outlined by [McKee et al. \(1993\)](#) and [Guttman \(1999\)](#), measures standardised anomalies in precipitation and is commonly used to quantify and compare dry (or wet) anomalies. SPI is recommended as a key meteorological drought index by the World Meteorological Organization ([WMO and GWP, 2016](#)) and the Lincoln Declaration on Drought ([Hayes et al., 2011](#)). The index is computed by summing precipitation over k months, termed accumulation periods, and fitting these accumulated precipitation values to a parametric statistical distribution from which non-exceedance probabilities are transformed into a standard normal distribution with a mean of zero and standard deviation of one ($\mu = 0, \sigma = 1$). Accordingly, SPI gives the actual precipitation as a standardised deviation from the normalised probability distribution function for various accumulation periods. Negative standard normal values indicate drier than normal conditions, whereas positive values indicate wetter than normal conditions. In this way, accumulated precipitation can be compared across locations with different climatology and highly non-normal precipitation distributions. Commonly used accumulation periods are 1, 2, 3, 6, 9, 12 and 24 months. For example, SPI-6 for June a given year is a normalised measure of accumulated precipitation during the previous 6 months (January to June) that year as compared to a benchmark period. [McKee et al. \(1993\)](#) also arbitrarily classified drought severity and denoted $\text{SPI} \leq -2$ as extreme drought, $-1.5 \geq \text{SPI} > -2$ as severe drought, $-1.0 \geq \text{SPI} > -1.5$ as moderate drought, $0 \geq \text{SPI} > -1$ as minor drought and $\text{SPI} > 0$ corresponding to no drought. An anomaly value of 1.65, 2.0 or 3.0 is equivalent to the value exceeded or equalled for 95, 98 respective 99.87% of the time (ref. the Normal distribution).

The Standardised Precipitation-Evapotranspiration Index (SPEI; [Vicente-Serrano et al., 2010](#)) is an extension of SPI derived from time series of precipitation less potential evapotranspiration (P - PET) rather than merely precipitation. In this book, SPI and SPEI are used as supporting drought indices to help understand the development of hydrological drought. SPEI was introduced to account for additional meteorological variables, such as temperature and wind speed, which affect evaporation, while maintaining the same statistical methodology as the SPI. Thus, SPEI can be considered a meteorological water balance index ([Section 2.2.2](#)) as well as a multivariate, modelled index ([Section 5.6.1](#)). It is generally recommended to use the Penman-Monteith (P-M) formulation ([Section 3.3](#)) to calculate PET . [Stagge et al. \(2014\)](#) recommend using the Hargreaves equation ([Hargreaves and Samani, 1985](#)) or P-M with the Hargreaves radiation term if radiation data are not available, retaining the physical foundation of the P-M equation. The inclusion of PET makes SPEI a significant different drought index than the SPI as demonstrated in a study of drought likelihood across Europe ([Stagge et al., 2017](#)).

SPI and SPEI values are easily statistically interpretable, representing the number of standard deviations from accumulated precipitation (P), or meteorological water balance (P - PET), for a given accumulation period, location and time of year. The SPI and SPEI can be used to identify both periods of below and above normal precipitation (P), respective meteorological water balance (P - PET). SPI and SPEI are commonly calculated for a monthly temporal resolution, but can also be derived using a daily resolution, for example, an SPI-3 can be derived for all days in a year, where one at each daily time step looks 3 months back ([Stagge et al., 2015](#)). Selection of a common benchmark period allows for consistency and provides a baseline (or reference) to compare against as new data become available.

SPI is commonly normalised using the 2-parameter Gamma distribution ([Section 6.4.3](#)), which is bounded by zero and has a relatively flexible shape parameter. This makes it well suited for a range of precipitation regimes. Unlike distributions for SPI, candidate probability distributions for SPEI generally require a location parameter because meteorological water balance may take on negative values (if $PET > P$). Distributions considered for SPEI normalisation include the Generalised logistic, Generalised Extreme Value (GEV), Normal, log-Normal and Pearson type 3 distributions ([Section 6.4](#); [Appendix 6.1](#)). [Stagge et al. \(2015\)](#) recommend the GEV distribution for SPEI for Europe based an extensive statistical testing (using gridded climate data). SPI and SPEI values may be limited to a given range, for example $[-3, 3]$ corresponding to a return level of 741 years, to ensure reasonableness given the high uncertainty in the extreme end of the distribution.

SPI separating between rainfall and snow melt deficits, the Standardised Snow Melt and Rain Index (SMRI). The concept of deriving standardised indices by converting to the standard normal distribution (mean of zero and standard deviation of one), has later been adopted to a wide range of other hydrometeorological variables covering all components of the hydrological cycle. In the Handbook of Drought Indicators ([WMO and GWP, 2016](#)), the different indices are classified into five groups: ‘meteorological’, ‘soil moisture’, ‘hydrology’, ‘remote sensing’ and ‘composite or modelled’. SPI and SPEI are examples of the first type, whereas, for example, the Standardised Soil Moisture Index (SSMI; e.g., [Kwon et al., 2019](#)) and the Empirical Standardised Soil Moisture Index (ESSMI; [Carrão et al., 2016](#)) are examples of soil moisture anomaly indices. Many of these fall into the category of multivariate, modelled indices as they are derived based on more than one variable ([Section 5.6.1](#)).

Note that ESSMI is computed by fitting a non-parametric empirical probability density function rather than a parametric distribution to the data.

Zaidman et al. (2002), which to our knowledge was the first drought study to express river flow as a standardised flow anomaly using a daily time resolution, measured the flow anomaly in standard deviations from the mean flow. A log-normal distribution was fitted to 365 sub-series covering the period 1960–95 (one for each day in the year), and the flow value on a given day was compared to the mean flow that day. A flow anomaly index was then introduced using a varying threshold approach, in which an anomaly of two standard deviations represented the onset of drought conditions. Related indices were developed to describe the time-varying extent and areal severity (cumulative deficit) of both streamflow and precipitation drought across Europe.

Standardised flow indices using the same theoretical background for characterising anomalies in time series of monthly data as the SPI, include the Standardised Streamflow Index (SSI, Modarres 2007) and the Streamflow Drought Index (SDI, Nalbantis and Tsakiris, 2009), the latter being similar to the SSI, but just named differently. Modarres (2007) fitted different distributions to monthly river flow for a catchment in Iran and the two-parameter gamma distribution was found superior for all months apart from July, in which case, the Generalised Pareto gave the best fit. The SDI uses the two-parameter log-normal distribution for normalisation, and hydrological drought is defined using the same five classes as for SPI (from non-drought to extreme drought). Svensson et al. (2017) tested a range of distributions for a UK dataset of observed monthly river flow and found that the rejection rate was generally lower for three- and four-parameter distributions. However, some distributions not bounded by zero, such as the GEV distribution, occasionally resulted in negative streamflow values. To limit this problem, they suggested using the Tweedie distribution, which is bounded below by zero. The SSI is used operationally in some drought monitoring and early warning systems (Bachmair et al., 2016). The Standardised Runoff Index (SRI; Shukla and Wood, 2008), is used to reflect deviations in modelled runoff per unit area and is suitable for analysing gridded runoff across space. In the original paper, the Gamma and the two-parameter log-Normal (LN) distributions are fitted to simulated monthly runoff for a catchment in the United States, with the Gamma distribution proving slightly better fit for low runoff values. It is further hypothesised that the 3-parameter LN and GEV distributions may have even better general applicability for runoff over widely varying hydro-climatic regimes (Shukla and Wood, 2008).

The Standardised Groundwater level Index (SGI) was introduced by Bloomfield and Marchant (2013) to compare features of groundwater droughts using groundwater level data from different boreholes. The SGI uses the normal scores transform (Everitt, 2002), a non-parametric normalisation method, which assigns a value to ranked observations of groundwater levels for a given month. A non-parametric approach to standardisation was favoured by Bloomfield and Marchant (2013). They showed that no consistent parametric models could be fitted to a wide range of groundwater hydrographs, and that even when a hydrograph for a single site was considered, no consistent parametric model could be fitted for all months of the year. Unlike SPI, the SGI, which is derived from groundwater levels, represents an aggregate of what happened in the previous months and thus, requires no accumulation period. Bloomfield and Marchant (2013) identified the SPI accumulation period (in months) that gave a maximum correlation between SPI and SGI for a given site.

There is no commonly agreed definition of groundwater drought status (severity) based on SGI. However, Bloomfield et al. (2019) defined any month with a SGI of -1 or less, as being a groundwater drought month and periods of continuously negative SGI reaching a monthly value of -1 or less, as an episode of groundwater drought similar to the World Meteorological Organisation definition of a SPI drought (Hayes et al., 2011).

The indices described in this section can be calculated for different temporal resolutions (e.g., daily or monthly) and different, user-preferred, accumulation periods, normally given in months. Stage

et al. (2015) derived daily SPI and SPEI time series, but still used a monthly accumulation period (i.e., 1, 2 or more months). In addition, a distinction can be made between the period over which the time series are standardised and the period that serves as reference for this standardisation (benchmark or reference period), which does not necessarily equal the period studied. This would be the case, for example, if the standardisation was done based on the full record and one later wants to extend this period using the same transformation to the new, updated data for consistency.

The accumulation period should be chosen in accordance with the variable, the hydroclimatological regime and the purpose of the study. For standardised meteorological indices, such as the SPI, accumulation periods longer than 1 month are often used as a proxy to reflect longer term memory within the hydrological cycle. Time series of soil moisture, river flow or groundwater implicitly incorporate such time lags (in precipitation) as the data reflect what happened in a certain time prior to the time of observation, representing the memory of the system. For example, soil moisture deficits, important among others for agriculture and ecosystems, may be related to meteorological deficits of a few months (or shorter), whereas river flow deficits in catchments with large storages, for example, groundwater dominated catchments, are related to long-term meteorological deficits of typically 12 months or more (Sections 3.4 and 3.5). However, if focus is on short-term drought in fast responding catchments, a shorter (e.g., SPI-3), accumulation period is likely better suited.

In Europe, a 6-month accumulation period for precipitation (SPI-6) is commonly chosen as a reasonable representation of medium-duration, seasonal streamflow drought (e.g., Kingston et al., 2015; Van Loon and Van Lanen, 2012). It also correlates well with streamflow drought in both headwaters and downstream reaches (López-Moreno et al., 2013). In terms of spatially aggregated values, such as river flow or groundwater, it is common to limit the accumulation period to the unit used in its calculation, normally 1 month.

There exist several software packages for calculating standardised indices by transforming the time series to the standard Normal distribution. Their calculation involves several steps, notable the choice of probability distribution to be fitted to the sample data (Section 6.4). This requires caution as one cannot simply apply a given software (e.g., for SPI) to another variable or region, without considering how well a given distribution fits the data at hand, it being a single time series or a regional dataset. Different variables possess different distribution properties (e.g., bounded by zero or not, degree of skewness), and the distribution function must be chosen accordingly. Contradictory to the SPI (Box 5.3), there is no consensus regarding which distribution to use for the Standardised Streamflow Index (SSI) and whether to use parametric or non-parametric approaches. Tjrdeman et al. (2020) compared time series of SSI for more than 300 rivers in Europe computed with different probability distributions and (parameter) fitting methods as well as different non-parametric methods. Although the Tweedie distribution — being bounded by zero — is highlighted as performing well having a low rejection rate, the key message is that the sensitivity of the various approaches to properties of the sample (both low and high flow), and associated uncertainties should be carefully considered prior to any drought analysis.

Standardised drought indices can be calculated for catchments or grid cells and as such, used to describe the drought extent, that is, spatial drought characteristics (Section 5.7). A catchment or grid cell can be considered to be in drought when the value at the site or grid cell in question is below a given threshold, for example, the 20th percentile (non-exceedance) threshold (equivalent to the 80% exceedance frequency commonly used in hydrology, Box 5.1), corresponding to a standardised value of 0.842. The drought extent can then be calculated as the percent area with an index value below the threshold.

For a further discussion about non-parametric methods to derive standardised drought indices, such as the transformation of plotting positions (Section 6.2.2) to the standard Normal distribution, the reader is referred to Tjrdeman et al. (2020). In case of a regional study, it is important to choose the same reference period, distribution and fitting method to allow comparison across catchments.

Worked Example 5.7 Standardised Groundwater level Index (SGI)

<https://github.com/HydroDrought/hydrodroughtBook>

Here, we illustrate how to estimate the SGI from a groundwater level time series using data from a well at Stonor Park, UK (Table 5.15). The Stonor Park well (described in Sections 3.4.1 and 4.5.3), measures the groundwater level in a typical permeable aquifer in a region with a temperate oceanic climate with no dry season and a warm summer. There are no major abstractions in its neighbourhood. It is recommended that standardisation is applied to data from a period of at least 30 years. If the purpose is to compare SGI across sites, standardisation should be done for a common (benchmark) period.

No.	Time	Level (m aSL)
1	1969-12-28	75.0
2	1970-01-04	74.6
3	1970-01-11	74.2
4	1970-01-18	73.9
5	1970-01-25	73.6
6	1970-02-01	73.5
7	1970-02-08	73.7
8	1970-02-15	74.0
9	1970-02-22	74.2
10	1970-03-01	74.5

With 2014 more rows

1. Loading data

Groundwater level data for Stonor Park are available for a 40-year period (1970–2010) with a weekly time resolution. The data are downloaded from the Local dataset (Section 4.5.3.2)

2. Creating a regular times series of monthly data

The estimation of SGI requires data to be on a regular time step, so values may need to be interpolated or, if you have frequent observations, such as those produced by data logging systems, a sub-set can be used. For this example, we will use a monthly time step. The level data (recorded as metres above sea level, m aSL) from Stonor Park are already approximately monthly, so we linearly interpolate the levels to the first day of each month (Table 5.16). Use your interpolation method of choice, but be careful not to ‘over’ interpolate if the data have longer gaps (e.g. Marchant et al., 2022).

Table 5.16 Groundwater level from a well at Stonor Park (UK) interpolated to the first day of each month.

No.	Time	Level (m aSL)	Month
1	1970-01-01	74.8	January
2	1970-02-01	73.5	February
3	1970-03-01	74.5	March
4	1970-04-01	76.1	April
5	1970-05-01	77.1	May
6	1970-06-01	77.6	June
7	1970-07-01	77.3	July
8	1970-08-01	76.1	August
9	1970-09-01	74.4	September
10	1970-10-01	72.8	October

With 470 more rows

3. Calculating SGI values

- (a) Extract the level data for an individual month from the full groundwater level time series
- (b) order the groundwater level data for a given month from lowest to highest and estimate the standardised rank for each level, that is, rank divided by the number of observations in a given month, plus one, that is, $(N + 1)$
- (c) estimate the inverse standardised normal cumulative value ($\mu = 0, \sigma = 1$) from the standardised rank for each level (Bloomfield and Marchant, 2013). This value is the SGI value
- (d) repeat Steps (a) to (c) for each calendar month separately. You will end up with 12 sets of monthly level data with associated inverse standardised normal cumulative values or SGI values
- (e) combine SGI values with associated dates estimated in Steps (c) and (d) and re-order oldest to most recent to get a monthly time series of SGI values for the site of interest.

4. Ordering SGI values

Table 5.17 displays the month, the groundwater level, the name of the month, the rank of the value, the standardised rank and the Standardised Groundwater Index (SGI). In Fig. 5.15, the time series of the monthly groundwater levels (Fig. 5.15a) and SGI (Fig. 5.15b) for the period 1970–2010 at Stonor Park are plotted. The three most severe droughts can be observed in 1976, 1992 and 1997.

Table 5.17 Groundwater data from a well at Stonor Park (UK), including calculated SGI value using the inverse standardised normal cumulative value from the standardised rank for the first 10 events in the record.

No.	Time	Level (m aSL)	Month	Rank	Standardised rank	SGI
1	1970-01-01	74.8	January	26	0.634	0.343
2	1970-02-01	73.5	February	19	0.463	0.0918
3	1970-03-01	74.5	March	16	0.390	0.279
4	1970-04-01	76.1	April	14	0.341	0.408
5	1970-05-01	77.1	May	16	0.390	0.279
6	1970-06-01	77.6	June	18	0.439	0.153
7	1970-07-01	77.3	July	19	0.463	0.0918
8	1970-08-01	76.1	August	18	0.439	0.153
9	1970-09-01	74.4	September	16	0.390	0.279
10	1970-10-01	72.8	October	15	0.366	0.343

With 470 more rows

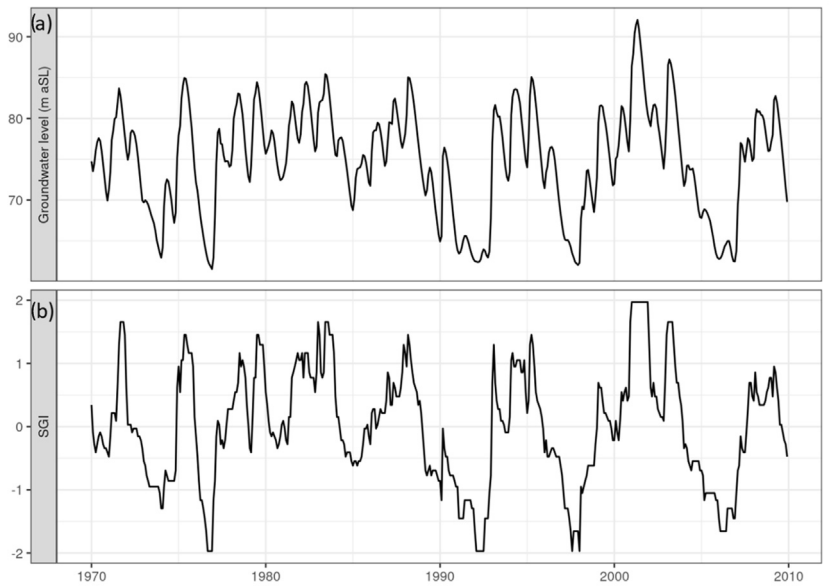


FIGURE 5.15

Groundwater level time series from a well at Stonor Park (UK) for the period 1970–2010: (a) monthly groundwater levels, and (b) the Standardised Groundwater Index (SGI).

5.6 Multivariate indices

The demand for indices that better reflect specific users' needs has led to the development of drought indices that include different components of the hydrological cycle (i.e., multivariate indices). Multivariate drought indices are numerical representations of drought characteristics merging inputs from two or more components of the hydrological cycle (climatic or hydrological) as opposed to single drought indices (Sections 5.3, 5.4 and 5.5). As such they commonly include one subsurface component (e.g., soil water or groundwater). Multivariate drought indices are here separated into modelled indices and combined indices.

Modelled drought indices (Section 5.6.1) are multivariate drought indices merging two or more hydrometeorological variables into one index, often including several (observed or simulated) components of the hydrological cycle, for example, a combination of meteorological variables (e.g., precipitation, evaporation) and hydrological variables (e.g., river flow, reservoir levels). A candid example of a modelled index is the Palmer Drought Severity Index (Box 5.4), which is derived from a soil water balance accounting routine. The SPEI (Box 5.3) can also be considered a modelled index. Some other well-known modelled indices are presented in Section 5.6.1. Combined drought indices (Section 5.6.2) are multivariate drought indices that consider jointly two or more stand alone drought indices, often including both climatic and hydrological drought indices. Combined drought indices are not modelled, although the underlying drought indices may be modelled.

Hayes et al. (2012) and WMO and GWP (2016) provide an overview of indices that are based on several variables, discuss their strengths and weaknesses and refer to studies where these indices are applied. Note that in the book, the term composite indices as introduced by WMO and GWP (2016) has been avoided, rather multivariate indices are used, encompassing modelled and combined.

5.6.1 Modelled indices

A range of drought indices have been developed based on observed or simulated hydrological variables, often including a combination of meteorological variables, such as precipitation and evaporation, used as input to simple or advanced water balance models. Commonly, these indices are not purely drought indices, rather they describe the whole spectre of moisture conditions from wet to dry. One of the first and most frequently applied such index, especially across the United States, is the Palmer Drought Severity Index, PDSI (Palmer, 1965) (Box 5.4). Although the PDSI is sometimes used as an index of hydrological drought, it is more correctly referred to as a meteorological (or soil moisture) drought index following a disciplinary perspective (Section 1.2) and is also the term used by Palmer (1965).

The PDSI has commonly been criticised for not being comparable across locations. Wells et al. (2004) suggest a so-called Self-Calibrating Palmer Drought Severity Index (SC-PDSI), which automatically calibrates the index at any location by replacing empirical constants in the calculation with site specific values derived based on local climate variability. By using the SC-PDSI across the United States, they demonstrate that the spatial comparability is improved compared to the original PDSI.

The water balance accounting model that forms the basis of the PDSI has facilitated the development of several related indices representing different response time and thus drought types (Jacobi et al., 2013). Examples are the monthly moisture anomaly index (ZINX) (Soulé, 1992), the Palmer Drought Hydrological Index (PDHI) (Palmer, 1965; Soulé, 1992) and the Crop Moisture Index (CMI) (Palmer, 1968). PDHI modifies the original PDSI by accounting for longer-term dryness that potentially will affect water resources (e.g., reservoir storage, river flow, groundwater). Similar to the PDSI, it needs information on monthly temperature and precipitation, and the water holding capacity of the soil. As it does not require specific information about groundwater and river flow, it is generally not considered a hydrological drought index.

The Surface Water Supply Index, SWSI, is a predictive indicator of total surface water availability within a catchment for spring and summer water use compared to historic supply (Shafer and Dezman, 1982). This index falls in the category of empirical hydrological drought indices and was developed to complement the PDSI in snow-dominated regions. It was originally applied for major river basins in Colorado (Hayes et al., 2012) and later modified and applied in other western states in the United States (Heim, 2002). The SWSI is computed from snowpack, precipitation, and reservoir storage data, and each component has a monthly weight assigned to it depending on its typical contribution to the surface water within a given catchment. The weighted components are summed to determine a catchment representative SWSI value. Similar to the PDSI, the SWSI is standardised and centred on zero and with a similar range. An advantage of the SWSI is that it gives a representative measure of surface water availability across a region, including the influence of snow and reservoirs. However, several aspects limit its application. Changes in the water management within a catchment, such as flow diversions or new reservoirs, imply that the entire SWSI algorithm needs recalculation to account for changes in the weight of each component. Thus, it is difficult to obtain a homogeneous time series of the index (Heddinghaus and Sabol, 1991). The weights may also vary across regions. Two versions of the SWSI are in use in the United States, one is an 'outlook' requiring river flow forecasts for its calculation, whereas the other provide a current assessment of the available water resources and does not need forecast information.

The Aggregate Dryness Index (ADI) (Keyantash and Dracup, 2004) considers the total available water in a region, addressing different types of drought (meteorological, agricultural and hydrological). It accounts for the basic elements of the hydrologic cycle, including stored water, that is, monthly time series of precipitation, evaporation, streamflow, reservoir storage, soil moisture content and snow water content (if applicable). Groundwater data are not included. Principle Component Analysis (PCA, Section 7.5.3) is used to extract dominant hydrologic signals from correlations among the observed time series. The ADI is the first principal component, normalised by the standard deviation of the monthly series and constructed separately for each month and region (test regions in the United States). Based on ADI time series, drought indices, such as drought severity, magnitude and duration, can be derived similar to other (standardised) drought indices (Section 5.5). An advantage of the approach is that new data can easily be added to the procedure.

Box 5.4 Palmer Drought Severity Index

The Palmer Drought Severity Index (PDSI) is one of the first efforts to account for more than just precipitation in the assessment of drought in agriculture (Palmer, 1965). The index is based on the supply and demand concept of the soil water balance equation taking into consideration monthly mean precipitation and temperature as well as the local available water content of the soil. It is most relevant for impacts on sectors sensitive to soil moisture conditions, such as agriculture (Willeke et al., 1994). The soil moisture accounting zone contains parameters that are empirically derived based on climatic conditions at nine sites in the USA. Evaporation is estimated using Thornthwaite's equation (Thornthwaite, 1948) and all water balance components estimated, including runoff, depend heavily on the water capacity of the soil. The index is not well adapted to snow or frozen soil conditions.

This standardised index is centred on zero with a typical range from -4 to $+4$. Negative values denote dry conditions, and positive values denote wet conditions (with $\text{PDSI} < -3$ representing severe to extreme drought). The PDSI has proved useful as a soil moisture drought monitoring tool and has been used to trigger actions associated with drought contingency plans (Willeke et al., 1994). It is typically calculated on a monthly basis, and a long-term archive of monthly PDSI values for every Climate Division (URL 5.2) in the United States is available at the National Climatic Data Center, from 1895 to date (URL 5.3). In addition, weekly PDSI values are calculated for each Climate Division during the growing season and are available in the US Department of Commerce Weekly Weather and Crop Bulletin (URL 5.4). These weekly Palmer Index maps are also available on the World Wide Web (URL 5.5).

5.6.2 Combined indices

Here, two so-called combined indices are described, that is, indices that are a combination of different stand alone indices, either weighted or not, including multiple types of data. Commonly, an n -entry table (n : number of single drought indices) is used to derive the overall severity as represented by the combined drought index. Such indices are also named composite, joint, multivariate, aggregated, blended or hybrid. Combined indices are often applied in drought monitoring and early warning systems as they aim to track and deliver relevant information about drought impacts to improve drought management for various sectors (Section 13.2).

One of the earliest examples of combined indices is the US Drought Monitor (USDM) (Svoboda et al., 2002). It combines several indices, including the SPI, the PDSI, and percentiles of soil moisture and river flow (Section 13.3.3.1). It also includes subjective expert knowledge on possible impacts. Finally, droughts are classified into abnormally dry (D0), moderate (D1), severe (D2), extreme (D3), and exceptional drought (D4) based on threshold values for each of the individual indices.

The second example is the Combined Drought Indicator (CDI) (Sepulcre-Cantó et al., 2012) developed as part of the European Drought Observatory (EDO). EDO is an integrated component of the Copernicus Emergency Management Service (URL 5.6) and monitors the evolution of the drought using the CDI (Box 13.3). CDI considers the evolution of a drought event as a three-stage cascading process from rainfall, to soil moisture and finally, vegetation state. It was designed for detecting and monitoring areas that either are affected or have the potential to be affected by agricultural drought. Fig. 5.16 shows a schematic presentation of the CDI. The CDI is based on monitoring three drought characteristics, each representing a different drought development stage: (a) precipitation, described by the Standardised Precipitation Index accumulated over 3 months (SPI-3, Section 5.5) using observed gridded precipitation derived from in-situ data, (b) soil moisture described by modelled soil suction (pF) related to plant water stress and calculated using a distributed hydrological model (i.e., LISFLOOD, Section 9.4.2) forced by gridded weather observations, and (c) vegetation state, described by the fraction of Absorbed Photosynthetically Active Radiation (fAPAR) derived from satellite measurements. Details on the

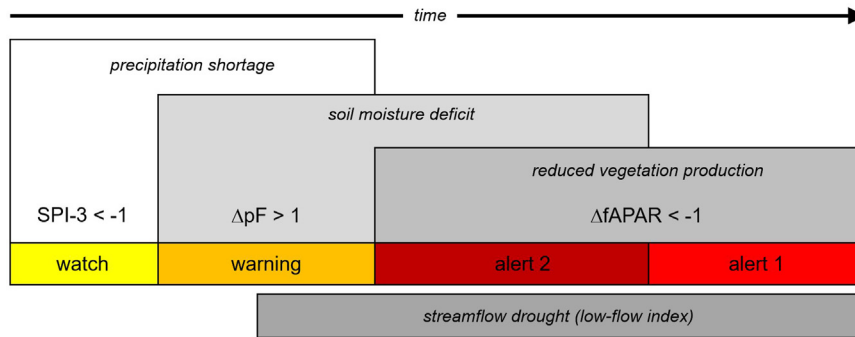


FIGURE 5.16

Combined drought indicator (CDI). Conceptual description of the propagation of a drought event according to the CDI and its different elements: Precipitation shortage (deficit) as described by the Standard Precipitation Index accumulated over 3 months, SPI-3; soil moisture deficit as described by the anomaly in modelled soil suction ΔpF ; reduced vegetation production as described by the anomaly in fraction of absorbed photosynthetically active radiation ($\Delta fAPAR$); corresponding hazard category (coloured boxes); and temporal collocation of streamflow drought (as represented by the Low-Flow Index, LFI).

Modified from Sepulcre-Cantó et al. (2012).

computation of these characteristics can be found in Sepulcre-Cantó et al. (2012). The CDI modelling framework defines three trigger levels of drought status, all based on anomalies: a watch status (yellow) when only precipitation is in deficit ($SPI-3 < -1$); a warning status (orange) when both precipitation and soil moisture are in deficit ($SPI-3 < -1$ and $\Delta pF > 1$) and an alert status (red) when also vegetation is affected ($\Delta fAPAR < -1$) regardless of precipitation or soil moisture deficit severity. When both soil moisture and vegetation anomaly thresholds are crossed, the trigger reaches alert level 2 (dark red), indicating a more severe drought condition. In addition, a partial recovery and full recovery in terms of vegetation stage are identified based on the same three indices. In addition to the CDI, EDO also presents a Low-Flow Index (LFI, Section 5.4.1). Box 13.2 gives an example of the application of the CDI to monitor the evolution of a drought at a site in Italy.

In addition to WMO and GWP (2016), Hao and Singh (2015) reviewed different combined indices and discuss their strengths and weaknesses. Bachmair et al. (2016) reviewed drought indices used in operational drought early warning systems and conclude that there is still a need for improvement of such indices to better reflect the wider impacts of drought on the environment and society.

5.7 Spatial drought characteristics

Droughts tend to show strong spatial coherence over wide areas, and it is of key interest to include the spatial aspect in drought studies. This may be the proportion of a catchment in drought, but will frequently refer to a regional, continental or global context. The spatial aspects include an assessment of the area in drought, its severity and development over time. More specifically for a given drought affected region, it may include the distribution of contiguous drought clusters and tracking of these clusters.

Independent of the spatial scale that is studied, spatial drought characteristics can be derived following two approaches, the non-contiguous drought area approach (NCDA) and the contiguous drought area approach (CDA). The NCDA does not require that the areal units (e.g., catchments or grid cells) in drought are connected. It straightforwardly counts the number of areal units in drought in the study area. Accordingly, spatial drought indices, such as the proportion of a region experiencing drought, the total area covered by drought and the total deficit over the drought area, can be obtained. The CDA on the other hand identifies spatial drought clusters, which are connected areal units (i.e., neighbouring units) in drought (e.g., [Andreadis et al., 2005](#); [Sheffield et al., 2009](#); [Corzo Perez et al., 2011](#); [Tallaksen and Stahl, 2014](#); [Diaz Mercado, 2021](#)). Commonly, an areal threshold, that is, minimum area (e.g., in km²) or number of connected areal units in drought is imposed before these are considered a cluster. Example studies of both approaches are presented in the following.

Spatial drought patterns can be studied by merely plotting drought indices (catchments or grids cells) on a map, independent of the type of approach ([Figs. 8.16, 10.12 and 11.4](#)). [Fig. 5.17](#) illustrates the groundwater drought duration on 28 July in central and southern Norway during the severe summer drought in 2018. The drought duration is calculated as the number of continuous days up to 28 July with subsurface storage below the 90th percentile (exceedance frequency), S_{90} ([Box 5.1](#)), based on the benchmark period 1981–2010. The estimates are based on a semi-distributed (1 × 1 km) version of the process-based hydrological model HBV ([Section 9.3.2.1](#)), forced with gridded observed precipitation and temperature.

[Tase \(1976\)](#) quantified spatial drought characteristics by generating monthly precipitation at a systematic grid. The threshold level method was then applied to each grid cell to derive so called Area-Deficit-Intensity characteristics. For a given threshold level and number of grid cells, the following deficit characteristics were defined for each time step, deficit area (number of grid cells with precipitation below a certain threshold level), total areal deficit (sum of drought deficit volumes (L³) in the drought-affected grid cells) and maximum deficit intensity (maximum deficit volume in one grid cell). The derivation of these spatial drought characteristics is detailed in [Box 5.5](#) and [Hisdal et al. \(2004\)](#).

Quantitative, spatial drought characteristics for precipitation were for the first time reviewed by [Rossi et al. \(1992\)](#). Assessments with focus on hydrological drought are given in [Hisdal \(2002\)](#), [Corzo Perez et al. \(2011\)](#), [Wong et al. \(2011\)](#), [Hao et al. \(2017\)](#) and [Diaz Mercado \(2021\)](#). Most studies define drought locally (at a grid cell) by an anomaly percentile or standardised value, and successively derive spatial drought indices. For example, drought indices plotted on a map, such as [Fig. 5.17](#) can serve as a basis for the NCDA or CDA (e.g., to determine the total area with a given drought duration, for example >60 days).

A similar approach can be adopted for river flow data if disaggregated to a gridded (or some other area unit) scale. However, whereas precipitation can be regarded as a point process, and gridded precipitation as an average over the grid cell, river flow represents integrated values over the catchment. Hydrological variables also show higher temporal consistency than precipitation. These properties must be accounted for if spatial interpolation is required. How to estimate gridded runoff from observed discharge is discussed on a general basis in [Gottschalk and Krasovskaia \(1998\)](#).

With climate change, a key question is whether one can detect a trend in drought occurrence and area affected on the national, regional or global scale. Often diverging conclusions are made depending among other on the type of variable studied and drought index used in the spatial analysis ([Section 11.4](#)).

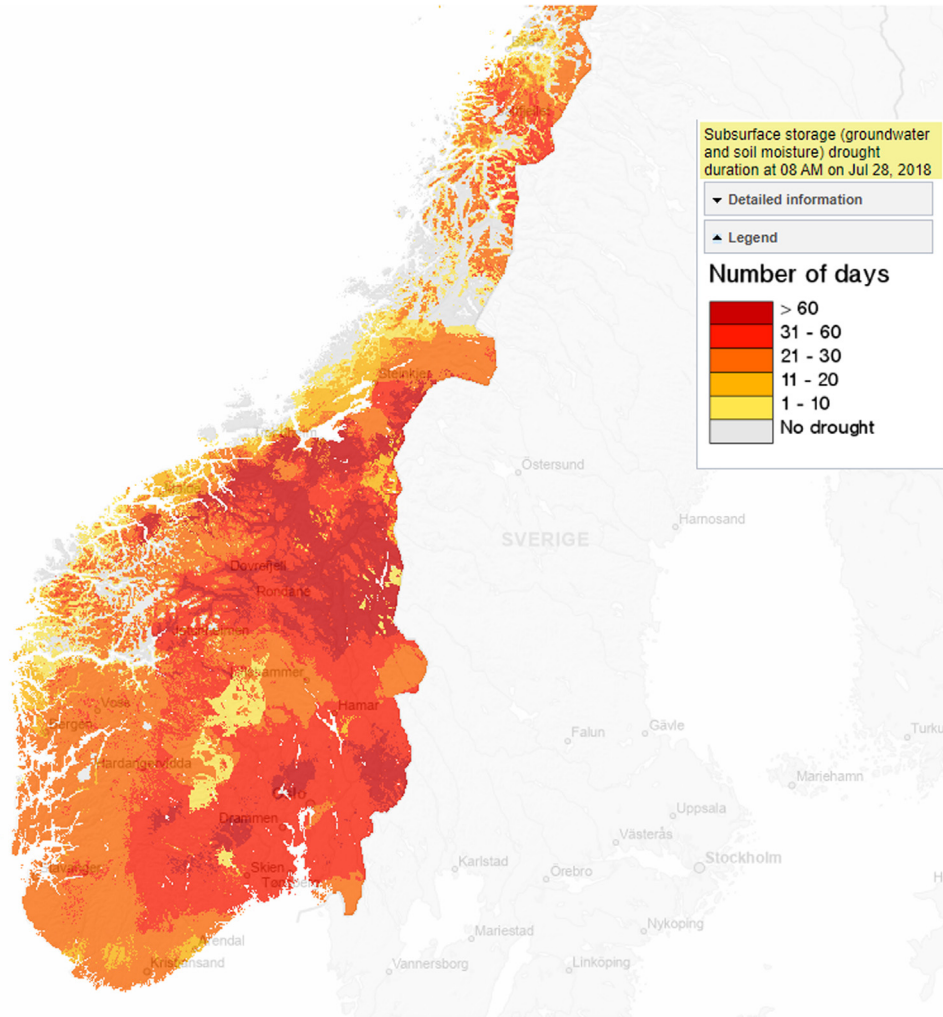


FIGURE 5.17

Snapshot of drought severity, in terms of the duration of simulated subsurface water storage (combined soil water and groundwater) below the S_{90} in central and southern Norway, 28 July 2018 ([URL 5.7](#)).

5.7.1 Examples of non-contiguous drought area approach

[Hisdal and Tallaksen \(2003\)](#) presented a case study, the first to our knowledge, which derived spatial hydrological drought characteristics based on observed time series of monthly precipitation and river flow. Denmark was divided into 260 grid-cells and river flow generated at a systematic grid. It was assumed that each catchment and river flow record could be assigned to one representative grid cell due to small catchment areas. Each time series were linearly transformed by the Empirical Orthogonal

Functions (EOF) method (Section 7.5.3), and the monthly mean and the EOF-weight coefficients subsequently interpolated by kriging. The frequency distributions of the first two (river flow) or three (precipitation) amplitude functions were then derived. By performing Monte Carlo simulations, amplitude functions corresponding to 1000 years of data were generated. Based on these simulated functions as well as interpolated mean and weight coefficients, long time series of precipitation and streamflow were simulated for each grid cell. Persistency (or autocorrelation, Box 6.3) between months was included in the river flow generation procedure. The droughts were allowed to develop over time and spatial drought characteristics, as developed by Tase (1976), were determined. Finally, drought severity-area-frequency curves were derived, which allowed an estimate of the probability of an area of a certain extent to experience a drought of a given severity. A comparison of drought characteristics showed that streamflow droughts were less homogeneous over the region, less frequent and lasted longer than precipitation droughts.

Tallaksen et al. (2009) examined drought propagation at the catchment scale. The analysis was conducted using monthly time series covering the period 1961–97 for the Pang catchment (170 km²) in the United Kingdom, with a particular focus on the average area in drought for different components of the hydrological cycle. The time series included observed rainfall and simulated groundwater recharge, head and discharge. Drought events were derived separately for each grid cell and variable using a time invariant, but spatially varying threshold level, combined to yield catchment-scale drought characteristics, such as the drought deficit area (Box 5.5). In addition, a critical minimum area was introduced as a second threshold to define a drought event, that is, a drought exists only if a certain percentage of the catchment area is experiencing a deficit. The study revealed notable differences in the spatial and temporal characteristics of drought for the different variables. Meteorological droughts covered frequently the whole catchment, were more numerous and lasted 1–2 months only. In comparison, droughts in recharge and hydraulic head covered typically a smaller area and lasted longer (4–5 months).

The Regional Deficiency Index (RDI), which counts the fraction of catchments or grid cells in drought in a region, was introduced by Stahl (2001) to investigate drought homogeneity in 19 European regions. If the river flow is equal or below the selected threshold, the catchment (or grid cell) is considered to be in drought ($DI(t) = 1$, otherwise 0, where t is the day number in the record). In this way, a daily time series of binary values DI_i can be generated for each catchment i (or grid cell i). The RDI time series, ranging from 0–1, is then calculated as follows:

$$RDI(t) = \frac{1}{K} \sum_{i=1}^K DI_i(t) \quad (5.6)$$

where K is the number of catchments (or grid cells) per region.

Prudhomme et al. (2011) applied the RDI to investigate the ability of gridded hydrological models to reproduce observed low flow events in 23 regions across Europe. The RDI was derived from observed river flow (standardised by catchments area) within a region and compared to RDI from simulated, gridded runoff in the same region. By plotting the RDI in a heat map where time of the year is plotted against year (e.g., Hannaford et al., 2011), one can get a good overview of drought development in time. A heat map can also be used to show drought development in space and time (Fig. 11.5).

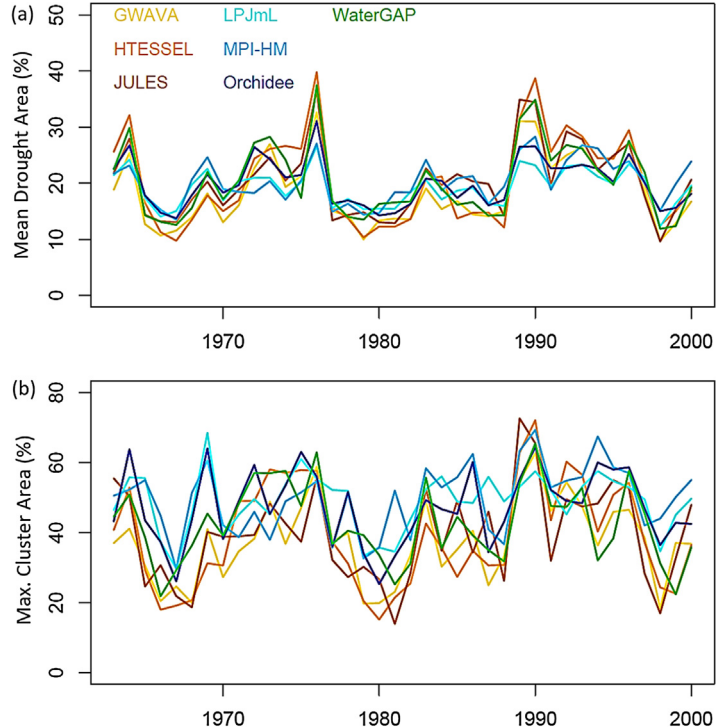
Examples of global scale studies include spatial analysis of soil moisture and runoff. [Sheffield et al. \(2009\)](#) applied Drought Severity-Area-Duration (SAD) curves to study drought in the different continents. The drought was derived from soil moisture simulated with a global land surface model using the threshold level approach. The SAD curves provided the drought severity against the area in drought for durations of 3, 6, 12 and 24 months. They also presented the severity and maximum spatial extent of selected major droughts for different continents. [Van Huijgevoort et al. \(2012\)](#) used modelled runoff from 10 off-line, global hydrological and land-surface models to investigate the area in drought in 20 regions covering the world using the threshold level approach. In addition to the description of major continental droughts (e.g., the 1980s drought in the Sahel), they investigated the synchronicity of the area in drought between the regions through a hierarchical cluster analysis. The synchronicity of the area in drought was highest in regions affected by El Niño-Southern Oscillation (ENSO) ([Section 2.2.3](#)), i.e., Australia, southeast Asia, Amazon and southern Asia, in strong El Niño years.

5.7.2 Examples of contiguous drought area approach

[Tallaksen and Stahl \(2014\)](#) compared the performance of seven off-line global hydrological and land-surface models in mapping spatial and temporal patterns of droughts (daily runoff) in Europe. The mean annual drought area was defined as the average of the daily total area in drought, whereas the annual maximum drought cluster area was the area of the largest cluster of spatially contiguous grid cells in drought within a year. [Fig. 5.18](#) shows the annual time series of the mean and maximum annual

FIGURE 5.18

Spatial drought characteristics in Europe derived from simulated runoff using seven large-scale models; time series of: (a) mean annual drought area, and (b) annual maximum drought cluster ([Tallaksen and Stahl, 2014](#)).



Box 5.5 Spatial drought characteristics

Tase (1976) introduced the spatial aspect in the definition of a drought by generating monthly precipitation at a systematic grid of points. Details of the indices and their derivations can be found in Hisdal et al. (2004), including their definitions. A similar procedure for deriving spatial indices of hydrological drought has been proposed for monthly or daily river flow or groundwater level time series by Tallaksen et al. (2009), from which the following elaboration is based.

A time invariant, but spatially varying threshold level, $Q_0(i)$, is applied to time series of a hydrological variable X for each spatial unit i (grid cell, sub-catchment) to detect drought events. An indicator function is introduced, which specifies whether a drought occurs ($=1$, below the threshold) or not ($=0$, above the threshold).

$$1_{\{X(i,t) < Q_0(i)\}} \quad \text{B5.5.1}$$

where $X(i,t)$ is the hydrological variable for unit i and time step t (flux: LT^{-1} and state variable: L), $Q_0(i)$ is the threshold for unit i (flux: LT^{-1} and state variable: L), i is unit ($-$), and t is time step ($-$).

The duration of a drought event j is defined as the number of uninterrupted time steps (days, months) with a flux or state variable (in any unit area) below the threshold for one or more units.

$$d_T(j) = \sum_{t=1}^{L(j)} \max\{1_{\{X(i,t) < Q_0(i)\}}, \quad i = 1, K\} \quad \text{B5.5.2}$$

where $d_T(j)$ is the duration of drought j (T), $L(j)$, the number of time steps in drought j ($-$), and K the number of units ($-$).

An important drought characteristic is the drought deficit area. Each unit represents a specific fraction $u(i)$ of the total area. The average area in drought during an event j is defined as the sum of unit areas (grid cells or polygons) in a drought over an uninterrupted number of time steps (days, months) with a flux or state variable below the threshold for one or more units, divided by the number of time steps in a drought.

$$A_T(j) = \frac{\sum_{t=1}^{L(j)} \sum_{i=1}^K u(i) (1_{\{X(i,t) < Q_0(i)\}})}{L(j)} \quad \text{B5.5.3}$$

where $A_T(j)$ is the fraction of total area in a drought for drought j ($-$), and $u(i)$ the fraction of the total area that is covered by a unit i ($-$).

Clearly, the sum of the area of all units K equals the whole area:

$$\sum_{i=1}^K u(i) = 1 \quad \text{B5.5.4}$$

The average deficit volume of a drought event j over the whole spatial domain (catchment, model area) is defined as the sum of the deficit volumes over an uninterrupted number of time steps (days, months) with a flux below the threshold for one or more units. It is averaged subsequently for the whole domain (catchment, model area) (and not the drought-affected area). Averaging is done implicitly by including $u(i)$ in Eq. B5.5.6.

$$v_T(j) = \sum_{t=1}^{L(j)} \sum_{i=1}^K v(i,t) \quad \text{B5.5.5}$$

$$v(i,t) = \begin{cases} u(i)(Q_0(i) - X(i,t))\Delta t & \text{for } X(i,t) < Q_0(i) \\ 0 & \text{for } X(i,t) \geq Q_0(i) \end{cases} \quad \text{B5.5.6}$$

where $v_T(j)$ is the deficit volume in a flux for the drought j (L), $v(i,t)$ is the deficit volume in a flux for unit i for time step t , and Δt is the time step length (T).

Eq. B5.5.5 cannot be used to calculate the total deficit in groundwater level, because head is a state variable, thus a measure of storage. Rather than summing up the deficit in each time step, the average deficit is calculated over all grid cells in drought and over each time step in drought (defined as the average deviation from the threshold over the affected area and over the duration of the drought event). Thus, the deficit volume in head for a drought event j is defined as the sum of deviations from the threshold over an uninterrupted number of time steps (days, months) with a head below the threshold

Continued

Box 5.5 Spatial drought characteristics—cont'd

for one or more units. Subsequently, it is averaged for the whole domain (catchment, model area) by including $u(i)$ in Eq. B5.5.8 and divided by the number of time steps in a drought.

$$v_T^*(j) = \sum_{i=1}^{L(j)} \sum_{t=1}^K v^*(i, t) \quad \text{B5.5.7}$$

$$v^*(i, t) = \begin{cases} u(i)(H_0(i) - X(i, t))\Delta t & \text{for } X(i, t) < Q_0(i) \\ 0 & \text{for } X(i, t) \geq Q_0(i) \end{cases} \quad \text{B5.5.8}$$

where $v_T^*(j)$ is the total deficit volume in a state variable for drought j (L), and $v^*(i, t)$ is the deficit volume in a state variable for unit i and for time step t (L).

drought area for runoff as estimated by the different models at a 0.5 degree spatial resolution. Consistent model behaviour was seen for the annual variability in mean drought area, whereas the annual maximum drought cluster showed high variability among models. Comparison with nearly 300 catchment-scale river flow observations showed an overall tendency to overestimate the number of drought events and hence underestimate drought duration, whereas persistence in drought-affected area (weekly mean) was underestimated by the models.

An example of a spatial drought analysis at the global scale using CDA is provided by [Corzo Perez et al. \(2011\)](#). They used a minimum areal threshold of two grid cells (approximately 5000 km²). Indices included were: (a) the number of drought clusters, mean area, duration, and deficit volume over all drought clusters, and (b) location of (large) drought clusters. As an example, they plotted the number of drought clusters in a heat map, where time of the year (day) is plotted against year for the period 1976–2001. The number of clusters varied from about 550 to 800 across the world. In addition, the maximum area, duration and deficit volume for a sample of clusters (e.g., Köppen-Geiger hydroclimatological regions) were derived at a given time step.

5.7.3 Drought tracking

Tracking drought in space and time simultaneously is a challenge. [Diaz et al. \(2020\)](#) proposed an approach to characterise spatio-temporal drought dynamics building on the CDA. They used gridded values of SPEI for an area to test the approach. The resultant estimate of drought tracks in space allowed for identification of drought paths delineated by an onset and an end in space and time. The information obtained was used to compute the following drought characteristics: the severity, the onset location, the end location, the direction and the rotation of the drought. The compass rose was used to track the direction of a drought spatial unit, and the rotation was defined depending on whether the pathway of the unit was mostly clockwise or counter-clockwise.

5.8 Application at large scale

Drought studies over large spatial domains (e.g., [Sections 10.5.4, 11.3.3.3, 11.4.3](#)) commonly encounter a challenge in the choice of drought index. As both the climate and catchment characteristics have a large influence on the runoff generating processes, the hydrological regime may differ

substantially over the region of study, notable across continents and globally. Accordingly, this implies large differences and variations in drought characteristics. Key challenges when assessing large-scale drought characteristics are intermittent or ephemeral river systems (Section 5.4.2) and regions with strong seasonality, such as snow regimes or monsoon dominated regimes. In case of intermittent or ephemeral rivers, the challenge of commonly used thresholds for perennial rivers (e.g., Q_{90} – Q_{70} , Section 5.4.1) being zero needs to be addressed. A set of no-flow indices have been developed to accommodate the presence of zero flow (Section 5.4.2).

Despite major differences across the study region, potentially including perennial, intermittent and ephemeral river systems, it is still preferred to apply only one drought index to identify drought if the purpose is to map regional or continental scale drought patterns. One such approach is the consecutive dry period method (Section 5.4.1), as introduced by van Huijgevoort et al. (2012), where a combination of the classical variable threshold level method and a novel dry period method was deployed. The combined method allows characterisation of drought events that continue from periods with river flow into periods without river flow and vice versa.

Alternatively, some more extreme (dry or cold) regions may be excluded from the analysis if unrealistic drought characteristics are obtained. For global drought analysis, often big deserts and glaciated areas that contain no flow or only occasionally flow (ephemeral rivers) are removed, that is, masking these regions, to allow for a meaningful global drought analysis. In general, it is advisable to be careful when identifying droughts in intermittent and ephemeral rivers to ensure that meaningful results are obtained.

It is important to be aware that some indices are affected not only by the regional climate, but also by the size of the catchment given that they are derived from the original time series and not standardised. For example, it is not meaningful to directly compare drought deficit volumes for a small versus a large catchment. If the original river flow time series is used, volumes come in a unit of m^3 , which will be orders of magnitude higher for the major river compared to the small stream. This lack of fair comparison can be circumvented by some form of standardisation:

- (a) standardisation of the original time series, for example, dividing by catchment area, the mean (or median) or subtract the mean and divide by the standard deviation (Section 5.5). The time series, can also be standardised to the Normal distribution (Section 5.5.2)
- (b) standardisation of the derived indices, for example, dividing the deficit volume by the mean flow or mean deficit for a given catchment (Section 5.5).

Still, it is important to be aware that larger catchments overall will have a slower response to water input due to longer transit times.

A disadvantage of standardisation is that the obtained droughts and drought characteristics may be difficult to relate to operational and physical limits that are present in the system (e.g., ecological minimum flow requirements) unless scaled back to the original units. Accordingly, non-standardised indices may be preferred for operational purposes in a given catchment.

5.9 Relationship between indices

As illustrated in the previous sections, there exists a wealth of indices for characterising hydrological drought. Adding the choice of parameter values, such as averaging intervals, exceedance frequencies (Section 5.3.2) or accumulation periods (Section 5.5) to define the various indices, the count easily exceeds 100, see for example the review by Smakhtin (2001) and the Handbook of Drought Indicators

and Indices by [WMO and GWP \(2016\)](#). The preceding sections describe the most common low flow and drought deficit indices.

The choice of index, or indices, for a specific study primarily depends on the purpose of the study, the data availability and the hydrological variable of interest, and there is no one definition or index that fits all purposes ([Lloyd-Hughes, 2014](#)). However, even after the purpose has been well defined, there often are several indices that qualify. The questions arise: How similar are these indices? Do they express different aspects of the drought, or are they just slightly different? How many indices are needed to describe the most important aspects of the drought? To help answering these questions one can look at the relationships between indices.

Close relationships between indices have been reported in several studies, for example, between percentiles from the FDC (e.g., Q_{75}) and values from the annual minimum flow (e.g., *MAM*(7-day), [Section 5.3.2](#)) ([Smakhtin and Toulouse, 1998](#)), between the recession constant and *MAM*(7-day) ([Tallaksen, 1989](#)), between the recession constant and drought deficit volume ([Kachroo, 1992](#)), between drought deficit duration and volumes ([Zelenhasić and Salvai, 1987](#); [Van Loon and Laaha, 2015](#)) and between drought deficit duration and volume and BFI ([Clausen and Pearson, 1995](#)). However, weak relationships were found between drought duration and percentiles from the FDC ([Smakhtin and Toulouse, 1998](#)). [Wanders et al. \(2017\)](#) compared 20 meteorological, soil moisture and hydrological drought indices and found that even drought indices that are designed to monitor the same drought type (e.g., hydrological drought) show large discrepancies in their anomalies and hence, drought detection, although streamflow and groundwater drought indices show the highest correlation ($r_P = 0.5–0.95$). It is clear, however, that the choice of the most suitable drought indices requires more attention ([Bachmair et al., 2016](#)). As the conclusions about drought can be significantly different based on the selected drought index, this is important to keep in mind when performing a drought analysis.

Depending on the strength of the correlation between indices, an index can be derived from other indices in cases when the index cannot be estimated from the data at hand. Knowledge of the relationship between indices is also useful if the purpose is to select indices that are not correlated, for example, if to be included as candidate predictors in a multivariate regression model ([Section 8.4](#)). In some cases, the conversion has been from a low flow index to the same type of index with a different averaging interval or exceedance frequency (e.g., [Gustard et al., 1992](#)). In other cases, a single index, for example, BFI ([Section 5.3.3](#)), has been used to calculate other low flow indices using regression equations ([Demuth and Young, 2004](#)).

5.9.1 Ranks and correlation coefficients

Most of the studies mentioned above used correlation coefficients ([Section 7.3.2](#)) to analyse the relationships between indices. This is the most direct and useful approach when just a few indices are to be compared. The Pearson correlation coefficient, r_P ([Eq. 7.25](#)), is a measure of the linear relationship between two variables. Alternatively, the Spearman rank correlation coefficient, r_S , is used rather than r_P . The r_S is a non-parametric statistic, calculated based on the rank rather than on the actual value of the variables (i.e., x and y in [Eq. 7.25](#) are the numbers 1, 2, ..., n , where n is the number of stations). In contrast to r_P , r_S is independent of the actual values of the variables and therefore more robust to extreme values (outliers) in the series. Another difference is that r_P assumes normally distributed data, which could lead to incorrect correlation values when the data are not normally distributed. The use of correlation coefficients to study the relationship between low flow indices is illustrated in [Worked Example 5.8](#).

Worked Example 5.8 Ranks and correlation coefficients

<https://github.com/HydroDrought/hydrodroughtBook>

1. Loading the data

Twenty-nine time series ranging between 35 and 65 years of daily river flow from the Regional Dataset of Eastern Austria (Section 4.5.2) are downloaded and analysed. Table 5.18 displays the station number (Id), river, station name and record length (in days) of the 10 first stations.

Table 5.18 Key information of the first 10 gauging stations included in the Regional Dataset of Eastern Austria.

No.	Id	River	Station	Record length (days)
1	210039	Rabnitz	Piringsdorf	16,436
2	210054	Rabnitz	Mannersdorf	18,262
3	210062	Stoob	Oberpullendorf	18,262
4	210088	Wulka	Wulkaprodersdorf	18,262
5	210211	Lafnitz	Dobersdorf	23,741
6	210237	Pinka	Woppendorf	23,741
7	210245	Tauchenbach	Altschlaining	18,262
8	210,252	Tauchenbach	Hannersdorf	23,741
9	210286	Strem	Güssing	14,610
10	210294	Strem	Heiligenbrunn	23,741

With 19 more rows

2. Calculating the low flow indices

Seven low flow indices and the mean (\bar{Q}) and median flow (Q_{50}) are calculated. The values are shown in Table 5.19. The recession constant *ALPHA* is equivalent to α as defined in Eq. 5.1b, where a high value of α implies a fast recession. Also calculated, but not included in Table 5.19 because of space concerns, are $MAM(1\text{-day})/Q_{50}$, $MAM(10\text{-day})/Q_{50}$, $MAM(30\text{-day})/Q_{50}$, Q_{95}/Q_{50} and Q_{90}/Q_{50} , all standardised indices characterising flow variability rather than absolute values. The median (Q_{50}) is used here for standardisation rather than the mean (\bar{Q}) as it is less sensitive to outliers, especially in the high range.

3. Determining the ranks

The flow indices in Table 5.19 and the additional five standardised indices (divided by Q_{50}) are ranked in ascending order according to their (flow) values at each station, so that the lowest value gets the highest rank (1) and the largest value gets a rank of 14 (where 14 is the number of indices included). In case of the recession coefficient, *ALPHA*, a fast recession (high value) gets a low rank. The results show that the mean (\bar{Q}), Q_{50} and $MAM(30\text{-day})/Q_{50}$ have low ranks (i.e., they are among the highest flow values) for most stations (Fig. 5.19). This is typical for daily flow data being positively skewed with a tail towards higher values. $MAM(1\text{-day})$ and Q_{95} have high ranks (i.e., among the lowest flow values) for many stations. *ALPHA* has very mixed ranks with the highest rank (1) for eight stations and the second lowest (13) for seven stations.

Table 5.19 Selected flow indices for 10 (out of 29) stations in the Regional Dataset of Eastern Austria. For details about the indices listed, see Sections 5.3.1, 5.3.2 and 5.3.4.

No.	Id	Mean ($\text{m}^3 \text{s}^{-1}$)	Q_{50} ($\text{m}^3 \text{s}^{-1}$)	<i>MAM</i> (1-day) ($\text{m}^3 \text{s}^{-1}$)	<i>MAM</i> (10-day) ($\text{m}^3 \text{s}^{-1}$)	<i>MAM</i> (30-day) ($\text{m}^3 \text{s}^{-1}$)	Q_{95} ($\text{m}^3 \text{s}^{-1}$)	Q_{90} ($\text{m}^3 \text{s}^{-1}$)	Q_{70} ($\text{m}^3 \text{s}^{-1}$)	Alpha
1	210039	0.615	0.443	0.144	0.179	0.220	0.132	0.178	0.31	0.248
2	210054	0.913	0.68	0.274	0.320	0.373	0.257	0.311	0.49	0.545
3	210062	0.613	0.429	0.129	0.164	0.216	0.14	0.179	0.305	0.472
4	210088	0.548	0.414	0.197	0.227	0.262	0.15	0.191	0.299	0.419
5	210211	6.47	4.91	2.43	2.75	3.08	2.44	2.83	3.86	0.261
6	210237	2.30	1.59	0.596	0.804	0.939	0.66	0.8	1.2	0.388
7	210245	0.409	0.348	0.166	0.183	0.201	0.124	0.159	0.255	0.196
8	210252	0.692	0.52	0.209	0.246	0.293	0.18	0.236	0.39	0.401
9	210286	1.08	0.513	0.168	0.199	0.263	0.167	0.216	0.368	0.748
10	210294	1.47	0.67	0.211	0.262	0.334	0.214	0.271	0.47	0.597

With 19 more rows, and five additional (standardised) variables: Q_{90}/Q_{50} , Q_{95}/Q_{50} , $MAM(30\text{-day})/Q_{50}$, $MAM(10\text{-day})/Q_{50}$ and $MAM(1\text{-day})/Q_{50}$.

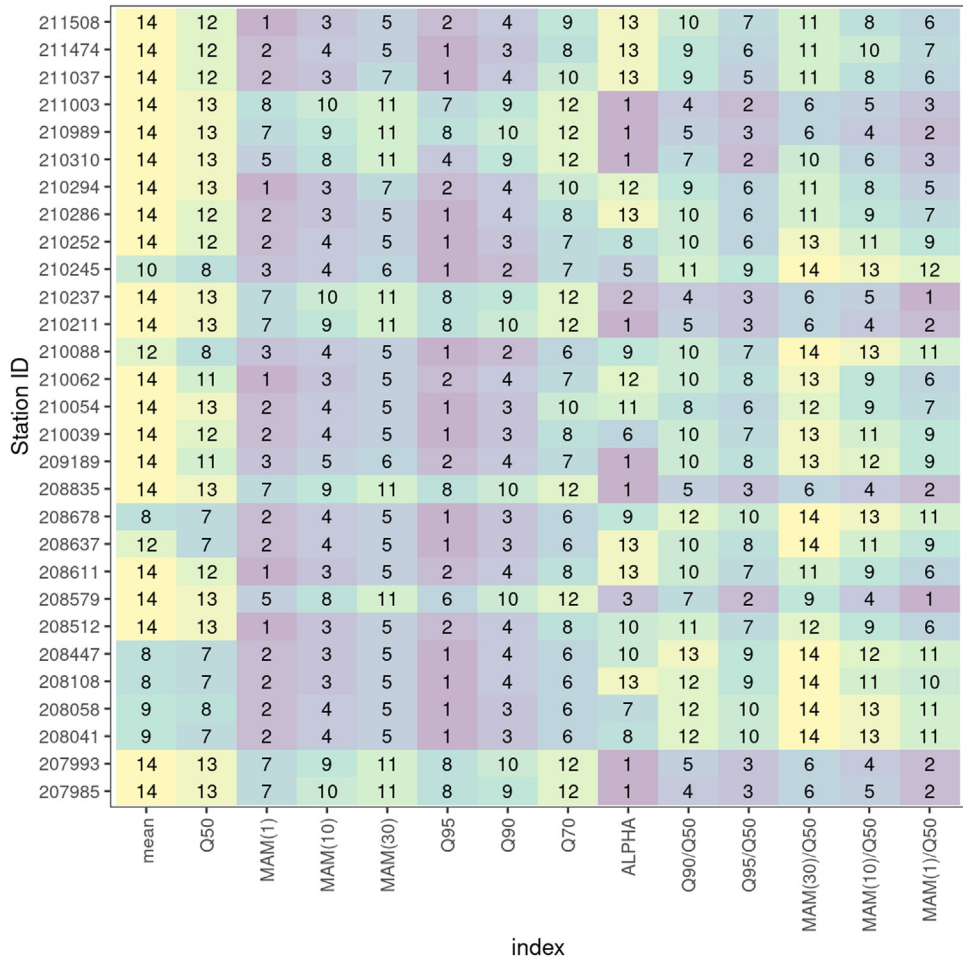


FIGURE 5.19

Ranks of low flow indices for the stations in Table 5.19, where 1 indicates the highest rank (i.e., the lowest flow and ALPHA value) and 14 the lowest rank (i.e., highest flow and ALPHA value) among the indices for a given station.

4. Calculating the Pearson correlation

The Pearson correlation coefficients are calculated for pairs of low flow indices (Fig. 5.20).

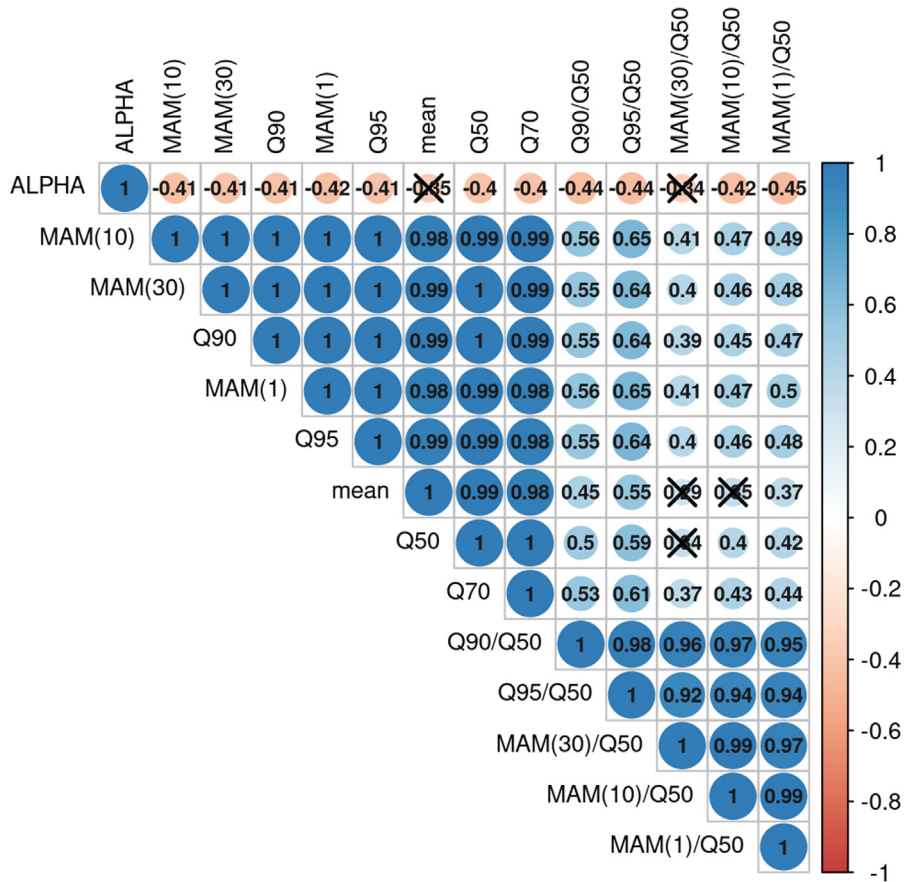


FIGURE 5.20

Pearson correlation coefficient matrix among the 14 low flow indices for the 29 gauging stations in the Regional Dataset of Eastern Austria (X shows a non-significant correlation).

5. Calculating the Spearman (rank) correlation

The Spearman (rank) correlation coefficients are calculated for pairs of low flow indices (Fig. 5.21).

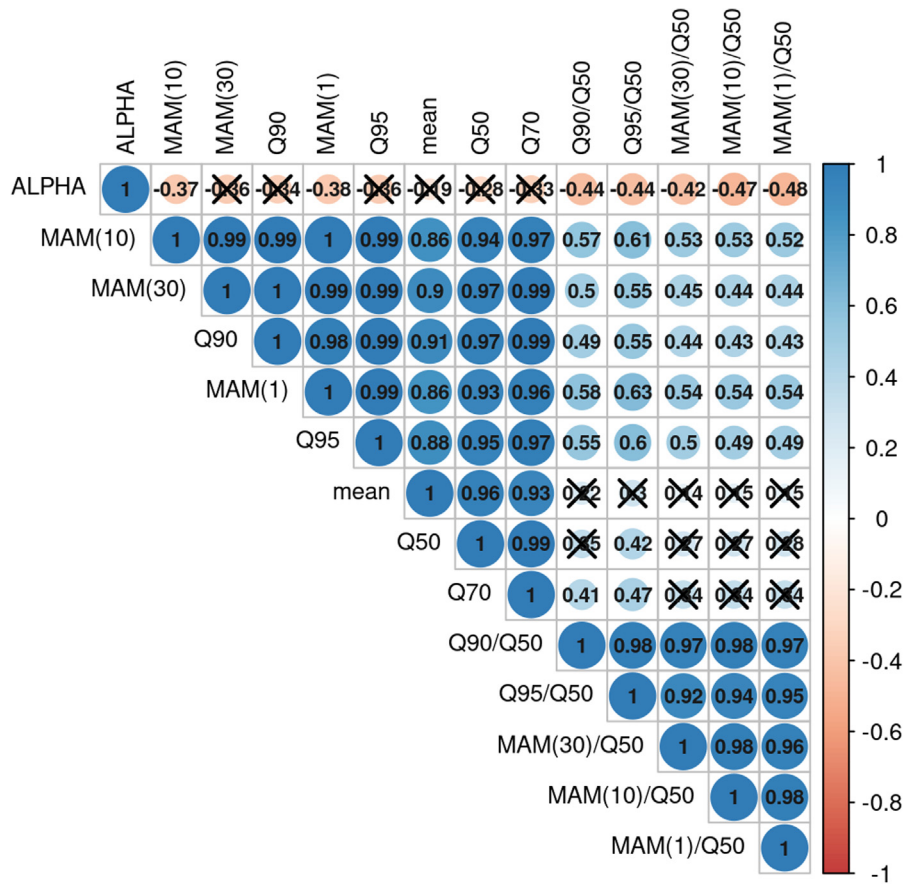


FIGURE 5.21

Spearman (rank) correlation coefficient matrix among the 14 low flow indices for the 29 gauging stations in the Regional Dataset of Eastern Austria (X shows a non-significant correlation).

6. Results

Figs. 5.20 and 5.21 show a positive correlation for all indices (i.e., when one index increases, so does the other) with the exception of *ALPHA* (the recession constant). The relationship between \bar{Q} and Q_{50} is, as expected, very strong ($r_P = .99$, $r_S = 0.96$). There are also strong relationships between these two central tendency measures and the ‘absolute’ low flow indices (*MAM(1-day)*, *MAM(10-day)*, *MAM(30-day)*, Q_{95} and Q_{90}) and among the standardised indices (*MAM(1-day)/Q₅₀*, *MAM(10-day)/Q₅₀*, *MAM(30-day)/Q₅₀*, Q_{95}/Q_{50} and Q_{90}/Q_{50}). *ALPHA* expresses the steepness of the recession and a high value of *ALPHA* (fast recession) correspond to a low ‘low flow value’, for example Q_{90} , implying a negative correlation. The standardised low flow indices are only weakly related to ‘absolute’ low flow indices with values of r_P and r_S around 0.4–0.6, and a coefficient of determination, R^2 (which in case of linear regression equals r_P^2) of around 0.4 (or less). Different relationship between these low flow indices may result for catchments in other climate regions, catchment size and catchment properties (e.g., hydrogeology, vegetation).

Figs. 5.20 and 5.21 show that r_S is smaller than r_P in many cases (but not all), which is commonly the case. The difference between the two coefficients is generally small, notable for indices without outliers and close to being normal distributed. In our case the dataset does hold a few relatively high values (for the large rivers), and r_P is affected by these, whereas r_S is not.

5.10 Summary

This chapter provides an overview of the derivation of the most commonly used hydrological drought characteristics. How to derive low flow and deficit characteristics both in terms of time series and single indices is explained and demonstrated using daily time series of river flow from the International Dataset. For operational applications, some examples are given in [Chapter 13](#). The methods described are applicable for observed or simulated time series of river flow or groundwater. It is also assumed that the series are stationary and undisturbed by human influence; hence there should be no trends or sudden jumps in the records caused by non-natural changes in the catchment. Further, a certain record length is required to obtain stable and reliable results. Although most examples are made for river flow (a flux), the derivation of groundwater drought characteristics, including groundwater level (a state variable) is also discussed. It is important to be aware of the difference in type of variable when estimating the indices. It should also be remembered that when comparing drought characteristics across catchments, the use of standardised series or indices is required.

A key point to be noted, is that there is no universal hydrological drought characteristic that fits all applications. The problem under study will influence the choice as will the data availability and the hydrological regime(s). Different hydrological regimes, i.e., perennial, intermittent or ephemeral rivers, have led to the development of both ‘flow’ and ‘no-flow’ indices. It is also important to be aware of how various ways of characterising a drought may lead to different conclusions regarding the drought hazard and its impacts.

A summary of the various approaches, related drought characteristics and indices ([Sections 5.3–5.8](#)) is given in [Table 5.20](#). [Section 5.9](#) uses the Regional Dataset of Eastern Austria ([Section 4.5.2](#)) to illustrate the relationship (correlation) between indices, and many indices express similar features of drought.

Table 5.20 Summary of low flow and drought deficit characteristics described in Chapter 5.

Method	Comments
Percentiles, FDC	Percentiles are used as low flow indices. They give information about the low flow regime of the river and are often used as threshold levels in the threshold level method. The FDC can be based on daily, monthly or some other time interval of river flow data. For perennial streams the percentiles will never be zero. For intermittent and ephemeral streams even Q_{50} can be zero.
$MAM(n\text{-day})$	$MAM(n\text{-day})$ are low flow indices. They give information about the low flow regime of the river. Large averaging intervals might be required in intermittent and ephemeral rivers to obtain non-zero values. Time series of annual minimum values, $AM(n\text{-day})$ are often fitted to a probability distribution to obtain estimates of T -year events. Challenges related to AM -series with many zero values is addressed in Chapter 6 .
Base flow indices	Base flow indices are derived from river flow and groundwater data. Commonly a hydrograph separation procedure is imposed to calculate the base flow proportion of the total river flow. An index that gives the ratio of base flow to total river flow is considered a measure of the flow that derives from stored sources. Accordingly, it can reflect the catchment’s ability to store and release water during dry periods. The base flow index (BFI) is one well known example.
Recession indices	The recession curve expresses the rate of decay of the hydrograph during periods with little or no precipitation. It describes in an integrated manner how different factors in the catchment influence the outflow process. Parameters of the recession model, also referred to as low flow indices, represent the recession rate; fast in flashy catchments with little storage and slow in catchments with large storages, such as a groundwater-dominated catchment.

Table 5.20 Summary of low flow and drought deficit characteristics described in Chapter 5. —cont'd

Method	Comments
The threshold level method	Drought event definition method. Derives time series of drought deficit event characteristics, such as the duration, the deficit volume and the termination of a drought based on a predefined threshold, constant or variable. Can be based on daily, monthly or some other time interval of river flow data. The time interval and the threshold level are decided by the purpose of the study and the hydrological regime of the river. Drought indices can be derived from the time series of drought events, for example, average drought duration.
Indices for intermittent and ephemeral rivers	To obtain relevant characteristics for rivers that frequently have zero flow, i.e., run dry during a specific season or during extreme dry years, 'no-flow' indices can be applied. They describe, for example, the start, end, frequency and duration of zero flow periods.
Sequent peak algorithm	Drought event definition method. Derives time series of drought characteristics, such as the duration of a drought and the deficit volume of a drought based on a predefined yield (threshold). Can be based on daily, monthly or some other time interval of streamflow data. The time interval and the yield will depend on the purpose of the study and the hydrological regime of the river. Drought indices can be derived from the time series of drought events, for example, average drought duration.
Standardised indices	Standardised indices are anomaly indices that are used to express dry and wet anomalies in time series of hydrometeorological variables. A standardised series transforms the given (observed or simulated) time series into probabilities (by distribution fitting) or empirical frequencies (by ranking), and hence, such indices are convenient to compare anomalies across space and for different variables. Examples of standardised hydrological drought indices are the Standardised Streamflow Index (SSI) and the Standardised Groundwater level Index (SGI).
Multivariate indices	Indices that include different components of the hydrological cycle are here separated into modelled indices and combined indices. Modelled indices are the merge of two or more hydrometeorological variables into one index, often based on using a water balance model (but not limited to), for example the Surface Water Supply Index (SWSI) computed from snowpack, precipitation, and reservoir storage data. Combined indices are multivariate drought indices that consider jointly different 'stand alone' indices, including multiple types of data, to better reflect drought impacts. Examples are the Combined Drought Indicator (CDI) used by the European Drought Observatory (EDO), and the US Drought Monitor (USDM).
Spatial drought characteristics	At-site drought indices derived for spatial units (catchments or grid cells) allow derivation of spatial drought characteristics, such as area covered by drought or the total deficit over the drought-affected area. If larger regions are studied, interpolated observed or simulated streamflow or groundwater (often gridded) data for the whole region under study are required. Two approaches are available, the Non-Contiguous Drought Area approach (NCDA) and the Contiguous Drought Area approach (CDA). NCDA does not require that the areal units in drought are connected, whereas the CDA identifies spatial drought clusters, i.e., connected neighbouring units in drought.
Large-scale studies	Drought studies covering large spatial domains commonly pose a challenge in the choice of drought index, as both perennial, intermittent, and ephemeral rivers may be included. A combination of the variable threshold level method and the consecutive dry period method is described as one option as is the use of no-flow indices in combination with more traditional flow indices for perennial rivers.

5.11 Further reading

- Bachmair, S., Stahl, K., Collins, K., Hannaford, J., Acreman, M., Svoboda, M., Knutson, C., Smith, K.H., Wall, N., Fuchs, B., Crossman, N.D., Overton, C., 2016. Drought indicators revisited: the need for a wider consideration for environment and society. *Wires Wat.* 3, 516–536, <https://doi.org/10.1002/wat2.1154>.
- Smakhtin, V.Y., 2001. Low flow hydrology: a review. *J. Hydrol.* 240, 147–186, [https://doi.org/10.1016/S0022-1694\(00\)00340-1](https://doi.org/10.1016/S0022-1694(00)00340-1).
- Tijdeman, E., Stahl, K., Tallaksen, L.M., 2020. Drought Characteristics Derived Based on the Standardised Streamflow Index: A Large Sample Comparison for Parametric and Nonparametric Methods. *Water Resour. Res.* 56(10), 1–25, <https://doi.org/10.1029/2019WR026315>.
- WMO and GWP, 2016. Handbook of Drought Indicators and indices, in: Svoboda, M., Fuchs, B.A. (Eds), Integrated drought management programme (IDMP), Integrated Drought Management Tools and Guidelines Series 2. World Meteorological Organization (WMO) and Global Water Partnership (GWP), Geneva, Switzerland, https://www.droughtmanagement.info/literature/GWP_Handbook_of_Drought_Indicators_and_Indices_2016.pdf.

References

- Andreadis, K., Clark, E., Wood, A., Hamlet, A., Lettenmaier, D., 2005. Twentieth-century drought in the conterminous United States. *J. Hydrometeorol.* 6, 985–1001. <https://doi.org/10.1175/JHM450.1>.
- Arciniega-Esparza, S., Breña-Naranjo, J.A., Pedrozo-Acuña, A., Appendini, C.M., 2017. HYDRORECESSION: a Matlab toolbox for streamflow recession analysis. *Comput. Geosci.* 98, 87–92. <https://doi.org/10.1016/j.cageo.2016.10.005>.
- Bachmair, S., Stahl, K., Collins, K., Hannaford, J., Acreman, M., Svoboda, M., Knutson, C., Smith, K.H., Wall, N., Fuchs, B., Crossman, N.D., Overton, C., 2016. Drought indicators revisited: the need for a wider consideration for environment and society. *Wires Wat.* 3, 516–536. <https://doi.org/10.1002/wat2.1154>.
- Barker, L.J., Hannaford, J., Chiverton, A., Svensson, C., 2016. From meteorological to hydrological drought using standardised indicators. *Hydrol. Earth. Syst. Sci.* 20, 2483–2505. <https://doi.org/10.5194/hess-20-2483-2016>.
- Beyene, B.S., Van Loon, A.F., Van Lanen, H.A.J., Torfs, P.J.J.F., 2014. Investigation of variable threshold level approaches for hydrological drought identification. *Hydrol. Earth Syst. Sci. Discuss.* 11, 12765–12797. <https://doi.org/10.5194/hessd-11-12765-2014>.
- Bloomfield, J.P., Marchant, B.P., 2013. Analysis of groundwater drought building on the standardised precipitation index approach. *Hydrol. Earth Syst. Sci.* 17, 4769–4787. <https://doi.org/10.5194/hess-17-4769-2013>.
- Bloomfield, J.P., Marchant, B.P., McKenzie, A.A., 2019. Changes in groundwater drought associated with anthropogenic warming. *Hydrol. Earth Syst. Sci.* 23, 1393–1408. <https://doi.org/10.5194/hess-23-1393-2019>.
- Bonsal, B.R., Wheaton, E.E., Meinert, A., Siemens, E., 2011. Characterizing the surface features of the 1999–2005 Canadian prairie drought in relation to previous severe twentieth century events. *Atmos.-Ocean* 49 (4), 320–338. <https://doi.org/10.1080/07055900.2011.594024>.
- Brodie, R.S., Hostetler, S., 2005. A review of techniques for analysing baseflow from stream hydrographs. In: Proceedings of the NZHS-IAH-NZSSS Conference, 28 November – 2 December 2005, Auckland, New Zealand. http://data.daff.gov.au/brs/brsShop/data/iah05_baseflow_final.pdf.
- Brutsaert, W., Nieber, J.L., 1977. Regionalized drought flow hydrographs from a mature glaciated plateau. *Water Resour. Res.* 13 (3), 637–643. <https://doi.org/10.1029/WR013i003p00637>.

- Cammalleri, C., Vogt, J., Salamon, P., 2017. Development of an operational low-flow index for hydrological drought monitoring over Europe. *Hydrol. Sci. J.* 62 (3), 346–358. <https://doi.org/10.1080/02626667.2016.1240869>.
- Carlotto, T., Chaffe, P.L.B., 2019. Master recession curve parameterization tool (MRCptool): different approaches to recession curve analysis. *Comput. Geosci.* 132, 1–8. <https://doi.org/10.1016/j.cageo.2019.06.016>.
- Carrão, H., Russo, S., Sepulcre- Cantó, G., Barbosa, P., 2016. An empirical standardised soil moisture index for agricultural drought assessment from remotely sensed data. *Int. J. Appl. Earth Obs.* 48, 74–84. <https://doi.org/10.1016/j.jag.2015.06.011>.
- Chapman, T.G., 1999. A comparison of algorithms for stream flow recession and base flow separation. *Hydrol. Process.* 13 (5), 701–714.
- Clausen, B., Pearson, C.P., 1995. Regional frequency analysis of annual maximum streamflow drought. *J. Hydrol.* 173, 111–130. [https://doi.org/10.1016/0022-1694\(95\)02713-Y](https://doi.org/10.1016/0022-1694(95)02713-Y).
- Corzo Perez, G.A., van Huijgevoort, M.H.J., Voss, F., Van Lanen, H.A.J., 2011. On the spatio-temporal analysis of hydrological droughts from global hydrological models. *Hydrol. Earth Syst. Sci.* 15, 2963–2978. <https://doi.org/10.5194/hess-15-2963-2011>.
- Crocker, K.M., Young, A.R., Zaidman, M.D., Rees, G., 2003. Flow duration curve estimation in ephemeral catchments in Portugal. *Hydrol. Sci. J.* 48 (3), 427–439. <https://doi.org/10.1623/hysj.48.3.427.45287>.
- Datry, T., Singer, G., Sauquet, E., Jorda-Capdevilla, D., Von Schiller, D., Stubbington, R., Magand, C., Pařil, P., Miliša, M., Acuña, V., Alves, M., Augeard, B., Brunke, M., Cid, N., Csabai, Z., England, J., Froebrich, J., Koundouri, P., Lamouroux, N., Martí, E., Morais, M., Munné, A., Mutz, M., Pesic, V., Previšić, A., Reynaud, A., Robinson, C., Sadler, J., Skoulikidis, N., Terrier, B., Tockner, K., Vesely, D., Zoppini, A., 2017a. Science and management of intermittent rivers and ephemeral streams (SMIRES). *Res. Ideas Outcomes* 3, e21774. <https://doi.org/10.3897/rio.3.e21774>.
- Datry, T., Bonada, N., Boulton, A. (Eds.), 2017b. *Intermittent Rivers and Ephemeral Streams Ecology and Management*. Academic Press, Elsevier, London, UK. <https://doi.org/10.1016/C2015-0-00459-2>.
- Demuth, S., Young, A.R., 2004. Regionalization procedures. In: Tallaksen, L.M., Van Lanen, H.A.J. (Eds.), *Hydrological Drought – Processes and Estimation Methods for Streamflow and Groundwater*. Developments in Water Science, vol. 48. Elsevier, Amsterdam, the Netherlands, pp. 307–343. <http://europeandroughtcentre.com/hydrological-drought-1st-edition-file-18/>.
- Diaz, V., Corzo Perez, G.A., Van Lanen, H.A.J., Solomatine, D., Varouchakis, E.A., 2020. An approach to characterise spatio-temporal drought dynamics. *Adv. Water Resour.* 137, 103512. <https://doi.org/10.1016/j.advwatres.2020.103512>.
- Diaz Mercado, V., 2021. *Spatio-Temporal Characterisation of Drought: Data Analytics, Modelling, Tracking, Impact and Prediction*. PhD Thesis. Delft University of Technology, the Netherlands. <https://ihedelftrepository.contentdm.oclc.org/digital/collection/phd1/id/59289/rec/1>.
- Duncan, H.P., 2019. Baseflow separation – a practical approach. *J. Hydrol.* 575, 308–313. <https://doi.org/10.1016/j.jhydrol.2019.05.040>.
- Everitt, B.S., 2002. *The Cambridge Dictionary of Statistics*, second ed. Cambridge University Press, Cambridge, UK.
- Feyen, L., Dankers, R., 2009. Impact of global warming on streamflow drought in Europe. *J. Geophys. Res. Atmos.* 114, D17116. <https://doi.org/10.1029/2008JD011438>.
- Fleig, A.K., Tallaksen, L.M., Hisdal, H., Demuth, S., 2006. A global evaluation of streamflow drought characteristics. *Hydrol. Earth Syst. Sci.* 10, 535–552. <https://doi.org/10.5194/hess-10-535-2006>.
- Furey, P.R., Gupta, V.K., 2001. A physically based filter for separating base flow from streamflow time series. *Water Resour. Res.* 37 (11), 2709–2722. <https://doi.org/10.1029/2001WR000243>.

- Gottschalk, L., Krasovskaia, I., 1998. Grid Estimation of Runoff Data. Report of the WCP-Water Project B.3: Development of Grid-Related Estimates of Hydrological Variables. WCASP - 46, WMO/TD-No. 870. WMO, Geneva, Switzerland. https://library.wmo.int/doc_num.php?explnum_id=9692.
- Gudmundsson, L., Tallaksen, L.M., Stahl, K., 2011. Spatial cross-correlation patterns of European low, mean and high flows. *Hydrol. Process.* 25 (7), 1034–1045. <https://doi.org/10.1002/hyp.7807>.
- Gustard, A., Bullock, A., Dixon, J.M., 1992. Low Flow Estimation in the United Kingdom. Report no. 108. Institute of Hydrology, Wallingford, UK. <https://doi.org/10.1002/esp.3290190707>.
- Guttman, N.B., 1999. Accepting the standardised precipitation index: a calculation algorithm. *J. Am. Water Resour. Assoc.* 35 (2), 311–322. <https://doi.org/10.1111/j.1752-1688.1999.tb03592.x>.
- Hall, F.R., 1968. Base flow recessions – a review. *Water Resour. Res.* 4 (5), 973–983. <https://doi.org/10.1029/WR004i005p00973>.
- Hannaford, J., Lloyd-Hughes, B., Keef, C., Parry, S., Prudhomme, C., 2011. Examining the large-scale spatial coherence of European drought using regional indicators of precipitation and streamflow deficit. *Hydrol. Process.* 25, 1146–1162. <https://doi.org/10.1002/hyp.7725>.
- Hao, Z., Singh, V.P., 2015. Drought characterization from a multivariate perspective: a review. *J. Hydrol.* 527, 668–678. <https://doi.org/10.1016/j.jhydrol.2015.05.031>.
- Hao, Z., Yuan, X., Xia, Y., Hao, F., Singh, V.P., 2017. An overview of drought monitoring and prediction systems at regional and global scales. *Bull. Am. Meteorol. Soc.* 98 (9), 1879–1896. <https://doi.org/10.1175/BAMS-D-15-00149.1>.
- Hargreaves, G.H., Samani, Z.A., 1985. Reference crop evapotranspiration from temperature. *Appl. Eng. Agric.* 1 (2), 96–99. <https://doi.org/10.13031/2013.26773>.
- Hayes, M., Svoboda, M., Wall, N., Widhalm, M., 2011. The Lincoln declaration on drought indices: universal meteorological drought index recommended. *Bull. Am. Meteorol. Soc.* 92, 485–488. <https://doi.org/10.1175/2010BAMS3103.1>.
- Hayes, J.M., Svoboda, M.D., Wardlow, B.D., Anderson, M.C., Kogan, F., 2012. Drought monitoring: historical and current perspectives. In: Wardlow, B.D., Anderson, M.C., Verdin, J.P. (Eds.), *Remote Sensing of Drought: Innovative Monitoring Approaches*. CRC Press, Taylor & Francis, Boca Raton, Florida, USA, pp. 1–19. <http://digitalcommons.unl.edu/droughtfacpub/94>.
- Heddinghaus, T.R., Sabol, P., 1991. A review of the Palmer Drought Severity Index and where do we go from here?. In: *Seven Conference on Applied Climatology*, Salt Lake City, 10–13 September 1991. American Meteorological Society, Boston, pp. 242–246. <http://citeseerx.ist.psu.edu/viewdoc/download?doi=10.1.1.176.3020&rep=rep1&type=pdf>.
- Heim Jr., R.R., 2002. A review of twentieth-century drought indices used in the United States. *Bull. Am. Meteorol. Soc.* 83 (8), 1149–1166. <https://doi.org/10.1175/1520-0477-83.8.1149>.
- Hewlett, J.D., Hibbert, A.R., 1967. Factors affecting the response of small watersheds to precipitation in humid areas. In: *Sopper, W.E., Lull, H.W. (Eds.), International Symposium on Forest Hydrology*. Oxford, Pergamon, New York, pp. 275–290.
- Heudorfer, B., Stahl, K., 2017. Comparison of different threshold level methods for drought propagation analysis in Germany. *Nord. Hydrol.* 48 (5), 1311–1326. <https://doi.org/10.2166/nh.2016.258>.
- Hisdal, H., 2002. Regional Aspects of Drought. PhD thesis. Faculty of Mathematics and Natural Sciences, University of Oslo, no. 221, Oslo, Norway. https://www.geo.uio.no/edc/downloads/phd_thesis_hisdal_2002.pdf.
- Hisdal, H., Tallaksen, L.M., 2003. Estimation of regional meteorological and hydrological drought characteristics: a case study for Denmark. *J. Hydrol.* 281, 230–247. [https://doi.org/10.1016/S0022-1694\(03\)00233-6](https://doi.org/10.1016/S0022-1694(03)00233-6).
- Hisdal, H., Stahl, K., Tallaksen, L.M., Demuth, S., 2001. Have streamflow droughts in Europe become more severe or frequent? *Int. J. Climatol.* 21, 317–333. <https://doi.org/10.1002/joc.619>.

- Hisdal, H., Tallaksen, L.M., Clausen, B., Peters, E., Gustard, A., 2004. Hydrological drought characteristics. In: Tallaksen, L.M., Van Lanen, H.A.J. (Eds.), *Hydrological Drought – Processes and Estimation Methods for Streamflow and Groundwater*. Developments in Water Science, vol. 48. Elsevier, Amsterdam, the Netherlands, pp. 139–198. <http://europeandroughtcentre.com/hydrological-drought-1st-edition-file-15/>.
- Iñiguez, V., Morales, O., Cisneros, F., Bauwens, W., Wyseure, G., 2016. Analysis of the drought recovery of Andosols on southern Ecuadorian Andean páramos. *Hydrol. Earth Syst. Sci.* 20, 2421–2435. <https://doi.org/10.5194/hess-20-2421-2016>.
- Institute of Hydrology, 1980. *Low flow studies (1-4)*. Wallingford, UK.
- Jachens, E.R., Rupp, D.E., Roques, C., Selker, J.S., 2020. Recession analysis revisited: impacts of climate on parameter estimation. *Hydrol. Earth Syst. Sci.* 24 (3), 1159–1170. <https://doi.org/10.5194/hess-24-1159-2020>.
- Jacobi, J., Perrone, D., Duncan, L.L., Hornberger, G., 2013. A tool for calculating the Palmer drought indices. *Water Resour. Res.* 49, 6086–6089. <https://doi.org/10.1002/wrcr.20342>.
- Kachroo, R.K., 1992. Storage required to augment low flows: a regional study. *Hydrol. Sci. J.* 37, 247–261. <https://doi.org/10.1080/02626669209492585>.
- Keyantash, J.A., Dracup, J.A., 2004. An aggregated drought index: assessing drought severity based on fluctuations in the hydrological cycle and surface water storage. *Water Resour. Res.* 40 (9), 1–13. <https://doi.org/10.1029/2003WR002610>.
- Kingston, D.G., Stagge, J.H., Tallaksen, L.M., Hannah, D.M., 2015. European-scale drought: understanding connections between atmospheric circulation and meteorological drought indices. *J. Climate* 28 (2), 505–516. <https://doi.org/10.1175/JCLI-D-14-00001.1>.
- Kjeldsen, T.R., Lundorf, A., Rosbjerg, D., 2000. Use of a two-component exponential distribution in partial duration modelling of hydrological droughts in Zimbabwean rivers. *Hydrol. Sci. J.* 45 (2), 285–298. <https://doi.org/10.1080/02626660009492325>.
- Klaassen, B., Pilgrim, D.H., 1975. Hydrograph recession constants for new south wales streams. *Civ. Eng. Trans. Inst. Eng. Aust.* 17 (1), 43–49.
- Kwon, M., Kwon, H.-H., Han, D., 2019. Spatio-temporal drought patterns of multiple drought indices based on precipitation and soil moisture: a case study in South Korea. *Int. J. Climatol.* 39, 4669–4687. <https://doi.org/10.1002/joc.6094>.
- Lloyd-Hughes, B., 2014. The impracticality of a universal drought definition. *Theor. Appl. Climatol.* 117, 607–611. <https://doi.org/10.1007/s00704-013-1025-7>.
- Longobardi, A., Van Loon, A.F., 2018. Assessing baseflow index vulnerability to variation in dry spell length for a range of catchment and climate properties. *Hydrol. Process.* 32, 2496–2509. <https://onlinelibrary.wiley.com/doi/epdf/10.1002/hyp.13147>.
- López-Moreno, J.I., Vicente-Serrano, S.M., Zabalza, J., Beguería, S., Lorenzo-Lacruz, J., Azorin-Molina, C., Morán-Tejeda, E., 2013. Hydrological response to climate variability at different time scales: a study in the Ebro basin. *J. Hydrol.* 477, 175–188. <https://doi.org/10.1016/j.jhydrol.2012.11.028>.
- Marchant, B.P., Cuba, D., Brauns, B., Bloomfield, J.P., 2022. Temporal interpolation of groundwater level hydrographs for regional drought analysis using mixed models. *Hydrogeol. J.* 30, 1801–1817. <https://doi.org/10.1007/s10040-022-02528-y>.
- Margariti, J., Rangelcroft, S., Parry, S., Wendt, D.E., Van Loon, A.F., 2019. Anthropogenic activities alter drought termination. *Elementa* 7 (1), 27. <https://doi.org/10.1525/elementa.365>.
- McKee, T.B., Doesken, N.J., Kleist, J., 1993. The relationship of drought frequency and duration to time scales. In: *Eighth Conference on Applied Climatology*, Anaheim, CL, USA, 17–22 January 1993, pp. 179–183.
- McMahon, T.A., Mein, R.G., 1986. *River and Reservoir Yield*. Water Resources Publications, Littleton, Colorado, USA. <https://www.wrpllc.com/books/wry.html>.

- McMahon, T.A., Nathan, R.J., 2021. Baseflow and transmission loss: a review. *Wires Wat.* 8, e1527. <https://doi.org/10.1002/wat2.1527>.
- Meigh, J., Tate, E., McCartney, M., 2002. Methods for identifying and monitoring river flow drought in southern Africa. In: Van Lanen, H.A.J., Demuth, S. (Eds.), *FRIEND 2002 – Regional Hydrology: Bridging the Gap between Research and Practice*. IAHS Publ. no. 274, pp. 181–188.
- Modarres, R., 2007. Streamflow drought time series forecasting. *Stoch. Env. Res. Risk A* 21, 223–233. <https://doi.org/10.1007/s00477-006-0058-1>.
- Nalbantis, I., Tsakiris, G., 2009. Assessment of hydrological drought revisited. *Water Resour. Manag.* 23, 881–897. <https://doi.org/10.1007/s11269-008-9305-1>.
- Nathan, R.J., McMahon, T.A., 1990. Evaluation of automated techniques for base flow and recession analyses. *Water Resour. Res.* 26 (7), 1465–1473. <https://doi.org/10.1029/WR026i007p01465>.
- Palmer, W.C., 1965. Meteorological Drought. Office of Climatology. US Weather Bureau, Washington DC, USA. Research Paper No. 45. https://www.droughtmanagement.info/literature/USWB_Meteorological_Drought_1965.pdf.
- Palmer, W.C., 1968. Keeping track of crop moisture conditions, nationwide: the new crop moisture index. *Weatherwise* 21 (4), 156–161. <https://doi.org/10.1080/00431672.1968.9932814>.
- Parry, S., Prudhomme, C., Wilby, R.L., Wood, P.J., 2016a. Drought termination: concept and characterisation. *Prog. Phys. Geog. Earth Environ.* 40, 743–767. <https://doi.org/10.1177/0309133316652801>.
- Parry, S., Wilby, R.L., Prudhomme, C., Wood, P.J., 2016b. A systematic assessment of drought termination in the United Kingdom. *Hydrol. Earth Syst. Sci.* 20, 4265–4281. <https://doi.org/10.5194/hess-20-4265-2016>.
- Peters, E., Van Lanen, H.A.J., 2005. Separation of base flow from streamflow using groundwater levels – illustrated for the Pang catchment (UK). *Hydrol. Process.* 19, 921–936. <https://doi.org/10.1002/hyp.5548>.
- Peters, E., Bier, G., Van Lanen, H.A.J., Torfs, P.J.J.F., 2006. Propagation and spatial distribution of drought in a groundwater catchment. *J. Hydrol.* 321, 257–275. <https://doi.org/10.1016/j.jhydrol.2005.08.004>.
- Piggott, A.R., Moin, S., Southam, C., 2005. A revised approach to the UKIH method for the calculation of baseflow. *Hydrol. Sci. J.* 50 (5), 911–920. <https://doi.org/10.1623/hysj.2005.50.5.911>.
- Prudhomme, C., Parry, S., Hannaford, J., Clark, D.B., Hagemann, S., Voss, F., 2011. How well do large-scale models reproduce regional hydrological extremes in Europe? *J. Hydrometeorol.* 12 (6), 1181–1204. <https://doi.org/10.1175/2011jhm1387.1>.
- Riggs, H.C., Caffey, J.E., Orsborn, J.F., Schaake Jr., J.C., Singh, K.P., Wallace, J.R., 1980. Characteristics of low flows. Report of an ASCE task committee. *J. Hydraul. Eng. ASCE* 106 (5), 717–731. <https://doi.org/10.1061/JYCEAJ.0005420>.
- Rossi, G., Benedini, M., Tsakiris, G., Giakoumakis, S., 1992. On regional drought estimation and analysis. *Water Resour. Manag.* 6, 249–277. <https://doi.org/10.1007/BF00872280>.
- Santos, A.C., Portela, M.M., Rinaldo, A., Schaeffli, B., 2019. Estimation of streamflow recession parameters: new insights from an analytic streamflow distribution model. *Hydrol. Process.* 33 (11), 1595–1609. <https://doi.org/10.1002/hyp.13425>.
- Sarailidis, G., Vasiliades, L., Loukas, A., 2019. Analysis of streamflow droughts using fixed and variable thresholds. *Hydrol. Proc.* 33, 414–431. <https://doi.org/10.1002/hyp.13336>.
- Sauquet, E., van Meerveld, I., Gallart, F., Sefton, C., Parry, S., Gauster, T., Laaha, G., Alves, M.H., Arnaud, P., Banasik, K., Beaufort, A., Bezdan, A., Datry, T., De Girolarno, A., M., Dörfliinger, G., Elci, A., Engeland, K., Estrany, J., Fialho, A., Fortesa, J., Hakoun, V., Karagiozova, T., Kohnova, S., Kriauciuniene, J., Morais, M., Ninov, P., Osuch, M., Reis, E., Rutkowska, A., Stubbington, R., Tzoraki, O., Żelazny, M., 2020. A catalogue of European intermittent rivers and ephemeral streams. *Zenodo*. <https://doi.org/10.5281/zenodo.3763419>.
- Sawaske, S.R., Freyberg, D.L., 2014. An analysis of trends in baseflow recession and low-flows in rain-dominated coastal streams of the pacific coast. *J. Hydrol.* 519, 599–610. <https://doi.org/10.1016/j.jhydrol.2014.07.046>.

- Schwalm, C.R., Anderegg, W.R.L., Michalak, A.M., Fisher, J.B., Biondi, F., Koch, G., Litvak, M., Ogle, K., Shaw, J.D., Wolf, A., Huntzinger, D.N., Schaefer, K., Cook, R., Wei, Y., Fang, Y., Hayes, D., Huang, M., Jain, A., Tian, H., 2017. Global patterns of drought recovery. *Nature* 548, 202–205. <https://doi.org/10.1038/nature23021>.
- Sepulcre-Cantó, G., Horion, S., Singleton, A., Carrao, H., Vogt, J., 2012. Development of a combined drought indicator to detect agricultural drought in Europe. *Nat. Hazard Earth Sys.* 12, 3519–3531. <https://doi.org/10.5194/nhess-12-3519-2012>.
- Shafer, B.A., Dezman, L.E., 1982. Development of a Surface Water Supply Index (SWSI) to assess the severity of drought conditions in snowpack runoff areas. In: *Western Snow Conference*. USDA, Soil Conservation Service, Denver, USA, pp. 164–175.
- Sharma, T.C., Panu, U.S., 2008. Drought analysis of monthly hydrological sequences: a case study of Canadian rivers. *Hydrol. Sci. J.* 53 (3), 503–518. <https://doi.org/10.1623/hysj.53.3.503>.
- Sheffield, J., Andreadis, K.M., Wood, E.F., Lettenmaier, D.P., 2009. Global and continental drought in the second half of the twentieth century: severity-area-duration analysis and temporal variability of large-scale events. *J. Climate* 22, 1962–1981. <https://doi.org/10.1175/2008JCLI2722.1>.
- Shukla, S., Wood, A.W., 2008. Use of a standardised runoff index for characterizing hydrologic drought. *Geophys. Res. Lett.* 35, L02405. <https://doi.org/10.1029/2007GL032487>.
- Smakhtin, V.Y., 2001. Low flow hydrology: a review. *J. Hydrol.* 240, 147–186. [https://doi.org/10.1016/S0022-1694\(00\)00340-1](https://doi.org/10.1016/S0022-1694(00)00340-1).
- Smakhtin, V.Y., Toulouse, M., 1998. Relationships between low-flow characteristics of South African streams. *Water S. A.* 24 (2), 107–112. https://www.researchgate.net/publication/264957822_Relationships_between_low-flow_characteristics_of_South_African_streams.
- Soulé, P.T., 1992. Spatial patterns of drought frequency and duration in the contiguous USA based on multiple drought event definitions. *Int. J. Climatol.* 12, 11–24. <https://doi.org/10.1002/joc.3370120103>.
- Stagge, J.H., Kingston, D.G., Tallaksen, L.M., Hannah, D., 2017. Observed drought indices show increasing divergence across Europe. *Sci. Rep.* 7, 14045. <https://doi.org/10.1038/s41598-017-14283-2>.
- Stagge, J.H., Tallaksen, L.M., Gudmundsson, L., Van Loon, A.F., Stahl, K., 2015. Candidate distribution for climatological drought indices (SPI and SPEI). *Int. J. Climatol.* 35 (13), 4027–4040. <https://doi.org/10.1002/joc.4267>.
- Stagge, J.H., Tallaksen, L.M., Xu, C.-Y., Van Lanen, H.A.J., 2014. Standardised precipitation-evapotranspiration index (SPEI): sensitivity to potential evapotranspiration model and parameters. In: Daniell, T.M., Van Lanen, H.A.J., Demuth, S., Laaha, G., Servat, E., Mahe, G., Boyer, J.-F., Paturel, J.-E., Dezetter, A., Ruelland, D. (Eds.), *Hydrology in a Changing World: Environmental and Human Dimensions*. FRIEND-WATER 2014, Montpellier, France, October 2014, vol. 363. IAHS Publications, pp. 367–373.
- Stahl, K., 2001. *Hydrological Drought—A Study across Europe*. PhD thesis. Albert-Ludwig-Universität Freiburg, Germany. <http://www.freidok.uni-freiburg.de/volltexte/202/pdf/stahl-diss.pdf>.
- Stahl, K., Vidal, J.-P., Hannaford, J., Tjeldeman, E., Laaha, G., Gauster, T., Tallaksen, L.M., 2020. The challenges of hydrological drought definition, quantification and communication: an interdisciplinary perspective. In: Yu, Z., Lu, C., Yu, D., Cai, J., Mahe, G., Mishra, A., Cudennec, C., Van Lanen, H.A.J., Orange, D., Amani, A. (Eds.), *Hydrological Processes and Water Security in a Changing World*, Beijing, China, 6–9 November 2018. *Proc. IAHS*, vol. 383, pp. 291–295. <https://doi.org/10.5194/piahs-383-291-2020>.
- Staudinger, M., Stahl, K., Seibert, J., Clark, M.P., Tallaksen, L.M., 2011. Comparison of hydrological model structures based on recession and low flow simulations. *Hydrol. Earth Syst. Sci.* 15, 3447–3459. <https://doi.org/10.5194/hess-15-3447-2011>.
- Staudinger, M., Stahl, K., Seibert, J., 2014. A drought index accounting for snow. *Water Resour. Res.* 50, 7861–7872. <https://doi.org/10.1002/2013WR015143>.
- Stoelzle, M., Schuetz, T., Weiler, M., Stahl, K., Tallaksen, L.M., 2020. Beyond binary baseflow separation: a delayed-flow index for multiple streamflow contributions. *Hydrol. Earth Syst. Sci.* 24, 849–867. <https://doi.org/10.5194/hess-24-849-2020>.

- Svensson, C., Hannaford, J., Prosdocimi, I., 2017. Statistical distributions for monthly aggregations of precipitation and streamflow in drought indicator applications. *Water Resour. Res.* 53, 999–1018. <https://doi.org/10.1002/2016WR019276>.
- Svoboda, M., LeComte, D., Hayes, M., Hei, R., Gleason, K., Angel, J., Rippey, B., Tinker, R., Palecki, M., Stooksbury, D., Miskus, D., 2002. The drought monitor. *Bull. Am. Meteorol. Soc.* 83 (8), 1181–1190. <https://doi.org/10.1175/1520-0477-83.8.1181>.
- Tallaksen, L.M., 1987. An Evaluation of the Base Flow Index (BFI). Report No 16, Report Series in Hydrology. University of Oslo, Norway.
- Tallaksen, L.M., 1989. Analysis of time variability in recessions. In: Roald, L., Nordseth, K., Hassel, K.A. (Eds.), *Friends in Hydrology*. IAHS Publ. no. 187, pp. 85–96. [Analysis-of-time-variability-in-recessions.pdf](https://doi.org/10.1016/0022-1694(94)02540-R).
- Tallaksen, L.M., 1995. A review of baseflow recession analysis. *J. Hydrol.* 165, 349–370. [https://doi.org/10.1016/0022-1694\(94\)02540-R](https://doi.org/10.1016/0022-1694(94)02540-R).
- Tallaksen, L.M., 2000. Streamflow drought frequency analysis. In: Vogt, J.V., Somma, F. (Eds.), *Drought and Drought Mitigation in Europe*. Kluwer Academic Publishers, the Netherlands, pp. 103–117. <https://link.springer.com/content/pdf/10.1007%2F978-94-015-9472-1.pdf>.
- Tallaksen, L.M., Hisdal, H., Van Lanen, H.A.J., 2009. Space-time modelling of catchment scale drought characteristics. *J. Hydrol.* 375, 363–372. <https://doi.org/10.1016/j.jhydrol.2009.06.032>.
- Tallaksen, L.M., Madsen, H., Clausen, B., 1997. On the definition and modelling of streamflow drought duration and deficit volume. *Hydrol. Sci. J.* 42 (1), 15–33. <https://doi.org/10.1080/02626669709492003>.
- Tallaksen, L.M., Stahl, K., 2014. Spatial and temporal patterns of large-scale droughts in Europe: model dispersion and performance. *Geophys. Res. Lett.* 41, 429–434. <https://doi.org/10.1002/2013GL058573>.
- Tase, N., 1976. Area-Deficit-Intensity Characteristics of Droughts. Hydrology Papers 87. Colorado State University, Fort Collins, USA. [HydrologyPapers_n87.pdf\(mountainscholar.org\)](https://doi.org/10.1002/2013GL058573).
- Tate, E.L., Freeman, S., 2000. Three modelling approaches for seasonal streamflow droughts in southern Africa: the use of censored data. *Hydrol. Sci. J.* 45 (1), 27–42. <https://doi.org/10.1080/02626660009492304>.
- Thornthwaite, C.W., 1948. An approach toward a rational classification of climate. *Geogr. Rev.* 38, 55–94. <https://doi.org/10.2307/210739>.
- Tijdeman, E., Stahl, K., Tallaksen, L.M., 2020. Drought characteristics derived based on the standardised streamflow index: a large sample comparison for parametric and nonparametric methods. *Water Resour. Res.* 56 (10), 1–25. <https://doi.org/10.1029/2019WR026315>.
- Van der Sluijs, P., De Gruiter, J.J., 1985. Water table classes: a method to describe seasonal fluctuations and duration of water tables on Dutch soil maps. *Agric. Water Manage.* 10, 109–125. [https://doi.org/10.1016/0378-3774\(85\)90001-0](https://doi.org/10.1016/0378-3774(85)90001-0).
- Van Huijgevoort, M.H.J., Hazenberg, P., Van Lanen, H.A.J., Uijlenhoet, R., 2012. A generic method for hydrological drought identification across different climate regions. *Hydrol. Earth Syst. Sci.* 16, 2437–2451. <https://doi.org/10.5194/hess-16-2437-2012>.
- Van Lanen, H.A.J., Peters, E., 2000. Definition, effects and assessment of groundwater droughts. In: Vogt, J.V., Somma, F. (Eds.), *Drought and Drought Mitigation in Europe*. Kluwer Academic Publishers, the Netherlands, pp. 49–61. <https://link.springer.com/content/pdf/10.1007%2F978-94-015-9472-1.pdf>.
- Van Loon, A.F., Van Lanen, H.A.J., 2012. A process-based typology of hydrological drought. *Hydrol. Earth Syst. Sci.* 16, 1915–1946. <https://doi.org/10.5194/hess-16-1915-2012>.
- Van Loon, A.F., Laaha, G., 2015. Hydrological drought severity explained by climate and catchment characteristics. *J. Hydrol.* 526, 3–14. <https://doi.org/10.1016/j.jhydrol.2014.10.059>.
- Vincente-Serrano, S.M., Begueria, S., Lopez-Moreno, J.I., 2010. A multi-scalar drought index sensitive to global warming: the standardised precipitation evapotranspiration index. *J. Climate* 23, 1696–1718. <https://doi.org/10.1175/2009JCLI2909.1>.

- Vogel, R.M., Fennessey, N.M., 1994. Flow duration curves. I: new interpretation and confidence intervals. *J. Water Res. Plan. ASCE* 120 (4), 485–504. [https://doi.org/10.1061/\(ASCE\)0733-9496\(1994\)120:4\(485\)](https://doi.org/10.1061/(ASCE)0733-9496(1994)120:4(485)).
- Vogel, R.M., Stedinger, J.R., 1987. Generalized storage-reliability-yield relationships. *J. Hydrol.* 89, 303–327. [https://doi.org/10.1016/0022-1694\(87\)90184-3](https://doi.org/10.1016/0022-1694(87)90184-3).
- Wanders, N., Van Loon, A.F., Van Lanen, H.A.J., 2017. Frequently used drought indices reflect different drought conditions on global scale. *Hydrol. Earth Syst. Sci. Discuss.* 1–16. <https://doi.org/10.5194/hess-2017-512>.
- Wells, N., Goddard, S., Hayes, M.J., 2004. A self-calibrating palmer drought severity index. *J. Climate* 17 (12), 2335–2352. [https://doi.org/10.1175/1520-0442\(2004\)017<2335:ASPDSI>2.0.CO;2](https://doi.org/10.1175/1520-0442(2004)017<2335:ASPDSI>2.0.CO;2).
- Willeke, G., Hosking, J.R.M., Wallis, J.R., Guttman, N.B., 1994. The national drought atlas. *Eos* 75 (8), 89–90. <https://doi-org.ezproxy.library.wur.nl/10.1029/94EO00706>.
- WMO and GWP, 2016. Handbook of drought indicators and indices. In: Svoboda, M., Fuchs, B.A. (Eds.), *Integrated Drought Management Programme (IDMP), Integrated Drought Management Tools and Guidelines Series 2*. World Meteorological Organization (WMO) and Global Water Partnership (GWP), Geneva, Switzerland. https://www.droughtmanagement.info/literature/GWP_Handbook_of_Drought_Indicators_and_Indices_2016.pdf.
- WMO, 2008. Guide to Hydrological Practices. Vol. I: Management of Water Resources and Application of Hydrological Practices. WMO Report No 168. World Meteorological Organization, Geneva, Switzerland. https://library.wmo.int/doc_num.php?explnum_id=10473.
- Wong, W.K., Beldring, S., Engen-Skaugen, T., Haddeland, I., Hisdal, H., 2011. Climate change effects on spatiotemporal patterns of hydroclimatological summer droughts in Norway. *J. Hydrometeorol.* 12, 1205–1220. <https://doi.org/10.1175/2011JHM1357.1>.
- Woo, M.-K., Tarhule, A., 1994. Streamflow droughts of northern Nigerian rivers. *Hydrol. Sci. J.* 39 (1), 19–34. <https://doi.org/10.1080/02626669409492717>.
- Yevjevich, V., 1967. An Objective Approach to Definition and Investigations of Continental Hydrologic Droughts. Hydrology papers 23. Colorado State University, Fort Collins, USA.
- Zaidman, M., Rees, H.G., Young, A.R., 2002. Spatio-temporal development of streamflow droughts in north-west Europe. *Hydrol. Earth Syst. Sci.* 6 (4), 733–751. <https://doi.org/10.5194/hess-6-733-2002>.
- Zelenhasić, E., Salvai, A., 1987. A method of streamflow drought analysis. *Water Resour. Res.* 23 (1), 156–168. <https://doi.org/10.1029/WR023i001p00156>.
- Zhang, Z., Chen, X., Xu, C.-Y., Hong, Y., Hardy, J., Sun, Z., 2015. Examining the influence of river-lake interaction on the drought and water resources in the Poyang Lake basin. *J. Hydrol.* 522, 510–521. <https://doi.org/10.1016/j.jhydrol.2015.01.008>.

Web references

- URL 5.1. <https://hal.inrae.fr/hal-02607367/document> (Accessed: 24 January 2023).
- URL 5.2. <https://psl.noaa.gov/data/usclimdivs/data/map.html> (Accessed: 29 January 2022).
- URL 5.3. <https://www.ncei.noaa.gov/access/metadata/landing-page/bin/iso?id=gov.noaa.ncdc:C00005> (Accessed: 29 January 2022).
- URL 5.4. <https://usda.library.cornell.edu/concern/publications/cj82k728n?locale=en&page=3#release-items> (Accessed: 29 January 2022).
- URL 5.5. <https://www.ncdc.noaa.gov/temp-and-precip/drought/weekly-palmers/> (Accessed: 29 January 2022).
- URL 5.6. <https://edo.jrc.ec.europa.eu/> (Accessed: 31 January 2022).
- URL 5.7. <https://www.xgeo.no/> (Accessed 12 July 2023).